Rebecca, Muirhead (2011) *The optimization of image guided radiotherapy in lung cancer.* MD thesis

http://theses.gla.ac.uk/2711/

The Optimization of Image Guided Radiotherapy in Lung Cancer.

Dr Rebecca Muirhead MBChB, MRCP

A thesis submitted in partial fulfilment

of the requirements for the award of the degree of

Doctor of Medicine

awarded by

Faculty of Medicine, Glasgow University, February 2010

The research contained in this

document was performed at

The Beatson, West of Scotland Cancer Centre, Glasgow, UK

and VU Medical Centre, Amsterdam, The Netherlands

from

February 2008 until December 2010.

ABSTRACT

The hypothesis of this work was whether IGRT could be safely implemented for clinical use in a busy oncology centre. I aimed to study a number of questions that remain unresolved in the current literature regarding safe and optimised implementation of IGRT techniques.

The first study undertaken was the calculation of a local set up margin using two widely recognised margin recipes. This involved the assessment and analysis of multiple images belonging to 100 patients. This allowed progression onto the next project which was assessment of the optimal safe method of delineation of 4DCT. The most efficient method was compared to gold standard.

At this point a different aspect of the radiation process was assessed, namely verification. A feasibility study of a simple, efficient form of imaging for use in review of a particular error was performed. This also involved the use of a novel tool which required independent assessment. This progressed into a further study of a larger number of patients using this tool and the images assessed previously to verify a novel form of radiation delivery.

Lastly a planning study was performed to quantify the clinical benefit of another delivery system. This involved the delineation and planning of a large number of radical lung patients with standard radiation treatment and the novel radiation treatment and an assessment of the potential clinical benefits.

The work presented in this thesis has answered some specific questions in IGRT in lung cancer, and contributed both locally and in the wider lung cancer community to increasing the use of IGRT in lung cancer.

ACKNOWLEDGEMENTS

DECLARATION

I declare that all the work in this thesis was performed personally unless otherwise acknowledged.

TABLE OF CONTENTS

TABLE OF CONTENTS

1.   Introduction: LUNG CANCER AND LUNG CANCER RADIOTHERAPY

List of Tables

List of Figures

Abbreviations

4DCT	Four-dimensional computed tomography
AP	Anterior-posterior
BEV	Beams eye view
CHART	Continuous hyperfractionated accelerated radiotherapy
COM	Centre of mass
CT	Computed tomography
CTV	Clinical target volume
CITV	Clinical target volume throughout the respiratory cycle.
DRR	Digitally reconstructed radiograph
EPID	Electronic portal imaging device
FDG	Fluorodeoxyglucose
GTV	Gross target volume
GITV	Gross tumour throughout the whole respiratory cycle
GITV_MIP	GITV delineated using the MIP image alone.
GITV_10phase	GITV delineated by creating a composite of 10 individual GTVs delineated on the 10 bins representing 10 phases of the respiratory cycle.
IGRT	Image guided radiotherapy
IMRT	Intensity Modulated Radiation Therapy
ITV	Internal target volume
LinAC	Linear accelerator
MLD	Mean lung dose
NSCLC	Non-small cell lung cancer
OAR	Organs at risk
PET	Positron emission tomography
RGRT	Respiratory Gated Radiotherapy
SBRT	Stereotactic body radiotherapy
SCLC	Small cell lung cancer
SD	Standard deviation
V20 Lung	Volume of lung receiving at least 20Gy

1. INTRODUCTION TO LUNG CANCER AND LUNG CANCER RADIOTHERAPY

1.1 Introduction to Lung Cancer

1.1 Lung Cancer

Lung Cancer remains the UK's commonest cause of cancer death accounting for 1 in 5 deaths. In the UK, around 35,000 people die from lung cancer annually, with around 41,000 diagnoses. It is the second most common cancer in men after prostate and the third most common cancer in women after breast and bowel cancer [1]. Rates of lung cancer in Scotland are among the highest in the world, reflecting the high smoking prevalence [2]. Other factors such as poor diet, exposure to industrial carcinogens and air pollution may also contribute [3,4]. In addition, in the West of Scotland, about 6% of male lung cancers are attributed to asbestos exposure associated with the ship-building industry [5]. There is a large population of deprived patients with multiple co-morbidities making treatment more challenging and long term survival more difficult to achieve [6].

Treatment is dictated by the tumours pathology and staging. There are other factors such as performance status, co-morbidities, previous medical diagnosis, previous treatment and pulmonary function tests that are all taken into consideration in the treatment decisions; however these are individually assessed in each case as they can vary widely.

In terms of pathology, this work will concentrate on non-small cell lung cancer, the main types of which are squamous cell carcinoma, adenocarcinoma and large cell carcinoma. Although the pathology of a NSCLC tumour is increasingly being used to dictate systemic treatment options with chemotherapy and biological agents, in radiotherapy, all pathological sub-types are treated with the same radiotherapy techniques.

Staging is determined by diagnostic imaging with computed tomography (CT), positron emission tomography (PET) and histological sampling of lymph nodes where necessary

with either transbronchial approach or at mediastinoscopy [7,8]. Staging is reported according to the International Staging System, first published in 1986 by the American Joint Committee on Cancer (AJCC) and the Union Internationale Contre le Cancer (UICC) [9]. Table 1-1 shows the international staging system for lung cancer.

1.1.2 Management of NSCLC.

In NSCLC, only patients with Stage I-IIIB can receive treatment with curative intent. This study concentrates on this group. These patients have a primary tumour with or without local nodes all of which can be encompassed within a radiotherapy field.

The gold standard management of Stage I and II NSCLC is radical surgery, with 5-year survival in pathologically staged patients with Stage IA, IB, IIA and IIB patients reported as 74%, 58%, 46% and 36% [9]. Unfortunately due to a number of issues, particularly poor pulmonary function and co-morbidities, the British resection rate is only 11% [10]. For medically inoperable patients, conventionally conformal radiotherapy is the standard of care in the UK and produces 5-year survival rates of between 0-42% [11]. As these patients are often frail with multiple co-morbidities, a different endpoint is often used: local control rate. The local control rate is a measure of the number of patients who have no recurrent disease either in the area irradiated, the surrounding normal lung or the regional lymph nodes. The local control rate in Stage I/II NSCLC patients treated with conformal radiotherapy is 30-94% [11]. There is however international agreement that for small tumours with no lymph node involvement, stereotactic body radiotherapy (SBRT), which has local control rates of 91.8%, 95% and 93%, is the gold standard for medically inoperable patients in selected patients [12,13,14]. This will be discussed further in 4.1.1.

The management of Stage III NSCLC is much less clear cut; however there is consensus that multimodality treatment is required. A combination of chemotherapy and radiotherapy are used, either concurrently or sequentially occasionally with the

Table 1-1. The international staging system for NSCLC, 2009.

T1a	Tumours ≤ 2cm
T1b	Tumours > 2cm to ≤ 3cm
T2	Tumour involves the main bronchi; Tumour has caused partial collapse of a lobe;
	The tumour has grown into the inner lining of the visceral pleura;
	The primary tumour falls into the size categories below:
T2a	Tumours > 3cm to ≤ 5cm
T2b	Tumours > 5cm to ≤ 7cm
T3	Tumours > 7cm; Additional tumour nodules in primary lobe;
	Any tumour < 2cm from the carina.
T4	Additional tumour nodules in ipsilateral lung; Tumour invading mediastinal structures.
N0	No involved lymph nodes.
N1	Involved hilar lymph nodes.
N2	Involved mediastinal lymph nodes.
N3	Involved contralateral lymph nodes.
M1a	Additional tumour nodules in contralateral lung; Malignant effusions; Pleural nodules.
M1b	Distant metastatic disease outwith the lung / pleura.

Stage IA   T1a N0 M0; T1b N0 M0

Stage IB   T2a N0 M0

Stage IIA   T1a N1 M0; T1b N1 M0; T2a N1 M0; T2b N0 M0

Stage IIB   T3 N0 M0; T2b N1 M0

Stage IIIA   Any T N2 M0; T3 N1 M0; T4 N0 M0; T4 N1 M0

Stage IIIB   Any T N3 M0; T4 N2 M0

Stage IV   Any T Any N M1

addition of surgery on completion. In our centre and throughout the UK, radical chemo-radiotherapy is treatment of choice. For a selected group of fit patients, concurrent chemo-radiotherapy provides a 5-year overall survival benefit of 4.5% over sequential treatment [15], however for those patients with large tumour bulk or who are less fit, sequential treatment is delivered. Irrelevant to whether the patient receives sequential or concurrent chemo-radiotherapy, the radiotherapy remains the same.

The dose prescribed in our centre and most commonly in the UK for radical radiotherapy in all stages, is 55Gy in 20 fractions over 4 weeks which most oncologists believe is biologically equivalent to a dose of approximately 64Gy in 32 fractions over 6 ½ weeks. Most centres worldwide however, deliver 2Gy doses daily to 60-66Gy in node positive disease and significantly higher doses to Stage I tumours using SBRT which will be discussed in the next section. There have only been three, large, phase III, dose comparison trials ever conducted [16,17,18]. These can be interpreted in many ways, however the widely accepted conclusions are that in 2Gy fractions, the dose must be ≥60Gy.

1.2 Current Radiotherapy techniques

1.2.1 CT Simulation

The CT simulator is a conventional diagnostic CT scanner with special radiotherapy planning software and LASERS to aid patient set-up. To ensure what is delineated on the planning scan is as close to what is treated as possible, immobilization techniques are used. The patients are set up at every simulation and treatment session using Sinmed Posirest Thoracic Board (Sinmed BV, The Netherlands) and a knee support. Figure 1-1 shows the patient in treatment position with the thoracic board. During CT simulation, the patient is positioned for treatment and to reproduce the position, marks are drawn on skin (one anteriorly and 2 each side laterally) where lasers representing the treatment centre fall. At check simulation if everything lines up

correctly these marks are then tattooed to the patient so that during treatment, these tattoo's can be used to set the patient up using the lasers. In patients known to have mediastinal disease 50ml intravenous iodinated contrast is administered at CT image acquisition to enable easier visualisation of the lymph nodes [19].

1.2.2 Delineation

The objective of radical radiation treatment is to treat all of the disease to a therapeutic dose level. This is achieved by firstly defining a planning target volume (PTV) by following the principles of ICRU 50/62 [20,21]. The delineation of the planned target volume (PTV) is performed by the clinician. There are several steps in the process that are all in accordance with ICRU 50 and 62. The general steps for delineation in lung radiation oncology are as follows:

1) Initially the gross tumour volume (GTV) is delineated; this is the visible extent of the malignant tumour. In our centre different clinicians use different window levels however ideally a uniform window width and level is required to minimize interclinician variation. EORTC guidelines suggest window width = 1,600 and level = -600 for parenchyma and window width = 400 and level = 20 for mediastinum [22].

2) A margin for local subclinical spread of the disease is given to create the clinical target volume (CTV). Although this margin in lung cancer is usually 5mm, the most robust paper from Giraud et al. [23] suggests that the microscopic margin should be 6mm and 8mm for squamous and adenocarcinomas respectively.

3) A further margin to create the internal target volume (ITV) is to ensure that the tumour is covered throughout the fraction as tumours can change in size, shape and position due to internal structure motion. In lung cancer the largest movement is due to respiration induced tumour motion, and hence a larger margin is given craniocaudally than anteriorly, posteriorly and laterally as respiration induced tumour motion is maximal in the cranio-caudal direction.

4) Finally, a margin for set-up error encompassing both systematic errors, due to different set-up on the CT simulator, and random set-up errors that can occur on

a day to day basis during treatment, to create the planned target volume (PTV). This set-up margin can be calculated using equations by Van Herk et. al. [24] and McKenzie et. al. [25]. This calculation is explained and performed later on in this paper.

In routine clinical practice in our centre, it is normal to combine some of these margins. The GTV is delineated and then a single additional margin that encompasses CTV, ITV and PTV margins is added to create the PTV. Craniocaudally 20mm is used, anteriorly posteriorly and in both directions laterally 15mm is used. This creates the PTV, which is the volume that we attempt to irradiate with between 95 to 107% of the prescribed dose.

The technologists in the physics department delineate the organs at risk (OAR), which are those normal tissues that are sensitive to radiation. The dose to these organs must be restricted. This can usually be achieved by optimisation during planning. In lung cancer radiation the OAR are the normal lung, the spinal cord, the oesophagus and to a lesser extent the heart. In our centre, only the normal lung and spinal cord are delineated routinely and taken into consideration when choosing the best plan. It is not routine clinical practice to outline the oesophagus and heart in our centre as in the view of our clinicians we do not have a high rate of oesophageal or cardiac adverse effects. As radical treatment becomes more toxic with increased doses and concurrent chemotherapy, outlining of these organs will no doubt become standard as it will become increasingly important to alter plans to limit the dose to these organs. The measures that are reviewed for the lung are the V20 lung and the mean lung dose (MLD) [26]. The V20 lung is the volume of "normal" lung that receives ≥20Gy. The "normal" lung is calculated by combining the volumes of the left and right lung, then excluding any lung tissue that is covered by the PTV. This measure correlates with the likelihood of radiation pneumonitis and thereafter long term lung damage. The mean lung dose (MLD) is the mean dose to the left and right lung combined. The spinal cord has a maximum dose cut off; this is achieved by ensuring one of the beams misses the cord entirely.

Figure 1-1. The patient immobilised in treatment position with a Sinmed Posirest Thoracic Board.
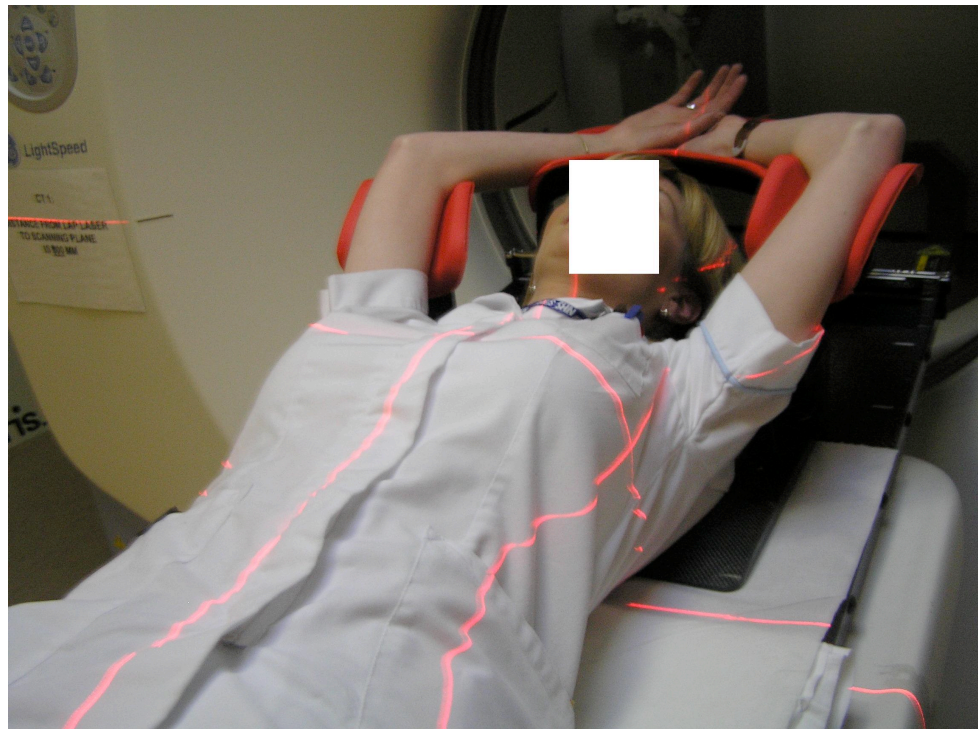
1.2.3 Planning and Plan calculation

Planning of 3D conformal radiotherapy lung cancer is usually performed with three to five photon beams and multi-leaf collimators that allow shaping of the beams. A typical radical plan involves one wedged anterior beam with an anterior oblique and further wedged posterior oblique both on the side of the tumour. Choice of gantry angle depends on the position of the spinal cord in relation to the tumour as one of the beams must miss the cord entirely to maintain an acceptable dose. Non-coplanar beams are rarely used.

Plan calculation in our centre is performed using the Varian Eclipse pencil beam algorithm (Version 8.6), however there are many other planning systems and different algorithms can be used. The plan is then optimised by adjustments to wedge angles, beam weights and gantry angles to cover the PTV with between 95-107% of the prescribed dose and limit the dose to organs at risk as much as possible. If following plan calculation the peripheries of the PTV are underdosed, boost fields to these areas can be added. The ability to create the best plan depends on the judgement, skill and experience of the operator. Occasionally there is no plan that maintains therapeutic dose within the PTV and has an acceptable OAR profile. In these cases, a number of possible plans with varying amounts of PTV covered or doses to OAR are created and it is the decision of the clinician where it is more clinically appropriate to compromise. Figure 1-2 shows a typical treatment plan in lung cancer radiotherapy.

As described above, the dose prescribed in our centre for a radical treatment is 55Gy in 20 fractions over 4 weeks or, if chemotherapy is being used concurrently, 66Gy in 33 fractions over 6 ½ weeks.

Figure 1-2. A standard, 3D conformal radiotherapy lung treatment plan.
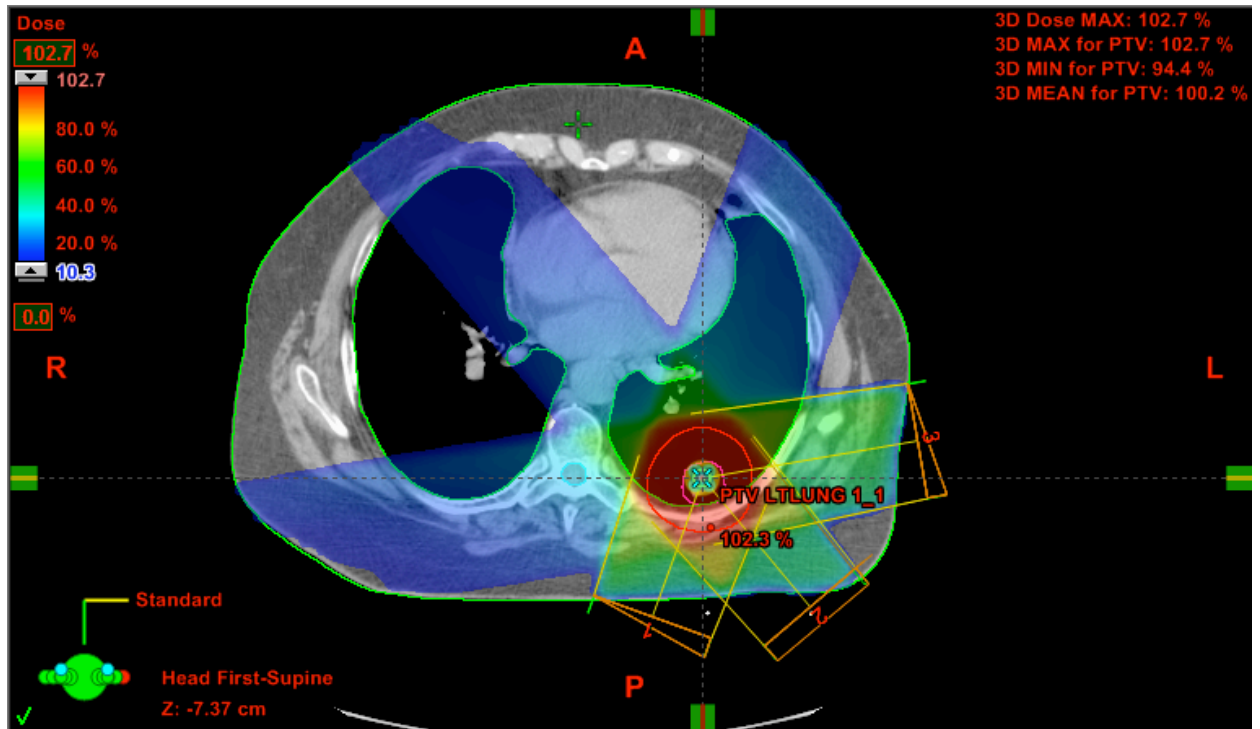
1.2.4 Check Simulation

There are three purposes of check simulation:

1) Verification of the patient's position at CT simulator is done by performing a bony match between a kV simulator image taken at check simulation, and the digitally reconstructed radiograph (DRR) created from the planning CT. Both orthogonal images for iso-centre verification and / or 'beams-eye view' of the actual treatment fields can be checked. If any shift is required this is performed. A number of radiotherapy departments are moving to eliminate this and move directly to pre-treatment verification on the linear accelerator (LinAC).

2) To check tumour motion, an anterior-posterior fluoroscopic image is produced on the check simulator, and provided the tumour can be visualised on kV image, this allows assessment of the respiration-induced tumour motion, if tumour appears to move out of the PTV, re-planning is required.

3) Finally, if all the previous checks are satisfactory, the tattoos are performed laterally and at midline as discussed above to allow set up with lasers during treatment.

1.2.5 Treatment and Verification

Patients are immobilised as on the CT simulator and aligned according to tattoos and lasers. The treatment is delivered on a daily basis.

Verification is required during treatment as any error in set-up may cause a failure to irradiate all of the disease or over-irradiation of normal/sensitive tissues. Verification is currently performed with images acquired using the treatment machine, taken on days 1, 2, 3, 8 and 15, which are matched to the DRR images using bony landmarks. Any deviation from the position at planning, is retrospectively considered and a shift is made if felt appropriate for future fractions.

Two different images are taken routinely, each preferred by different clinicians.

1) Orthogonal "iso-images" are single MV exposure images in both the anterior-posterior (AP) and lateral direction. These can be acquired for "on-line" or "off-line" review (the difference will be discussed below). These are compared to the same AP and lateral DRRs created from the planning CT, that were reviewed at check simulation, and any major errors in patient positioning can be identified. These images are preferred by some clinicians because they image the whole thorax in order to encompass rigid structures such as the spine that can be easily compared to the DRR. In addition, clinicians are more accustomed to viewing and identifying structures in AP and lateral fields rather than oblique fields. One exposure of the treatment machine for the acquisition of an iso-image delivers around 4mSv per exposure.

2) Another set of machine images, are "dual exposure images". They are created using a combination of; a fraction of the exit dose of the megavoltage (MV) treatment beam, during an actual treatment; and an additional exposure after treatment of the same field with an additional 20mm margin. This allows the more heavily exposed treatment field to be seen in the context of the adjacent normal tissue structures. Together these two images create a "double-exposure". The images can only be produced from the gantry angle of the beam, therefore are always beams eye view (BEV) images, as some of the image is obtained using the treatment beam. It is often difficult to identify structures in the double-exposure to compare to the DRR because fields can be small and the low differential absorption of MV X-rays in tissue gives them a similar appearance and hence makes it difficult to differentiate between structures. Furthermore clinicians are not accustomed to looking at oblique fields.

The majority of verification at present occurs "off-line", which is a term used when the images are reviewed after the radiation has been delivered. During off-line verification, the operator takes into account all shifts from CT planning position in all previous fractions and generates a decision (to correct or not and if so by how much) for the setup of subsequent fractions. The general guideline in our centre is that if the

bony landmarks are misaligned by less than 5mm no action is taken, if there is a consistent shift of 5mm in one direction a permanent shift is made. If there are continued concerns about patient set-up, further iso-images can be taken. If there is concern that the patient is moving position daily, "on-line" iso-images can be taken. On-line images are those taken prior to treatment, with a shift to the DRR position performed prior to treatment. Although iso-image can be performed on-line, the beams eye view double-exposure images cannot, as they are created using the treatment beam. This technique has many limitations and many discrepancies remain between what is planned and what is delivered [27]. More rational and objective off-line verification approaches are the "shrinking action-level" protocol [28] or the "no action-level" protocol [29] which have shown to reduce systematic errors more, with less imaging required. Figure 1-3 gives an example of a BEV EPID image, and some MV iso-images.

1.2.5 Potential Errors with current radiotherapy techniques

Errors are divided into systematic errors and random errors. A systematic error is an error that is not determined by chance but is introduced by an inaccuracy in the system. Systematic errors are consistent throughout the radiation treatment. A random error can happen during any treatment day as a result of an unforeseen difference to patient or treatment on that day. There are a number of potential systematic and random errors in lung cancer radiotherapy.

Figure 1-3. (a) - A BEV EPID image; (b) - An anterior iso-image; (c) - A lateral iso-image

(a)
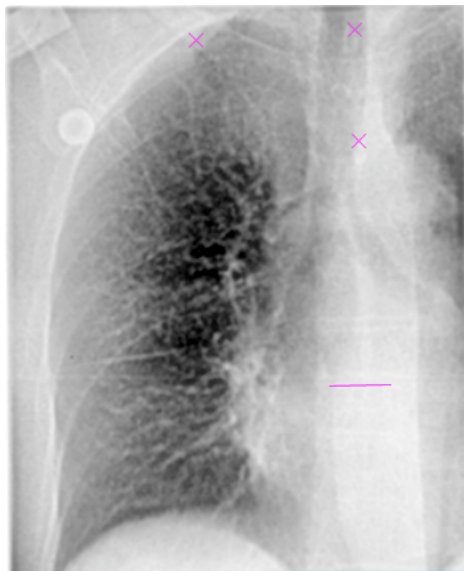
(b)
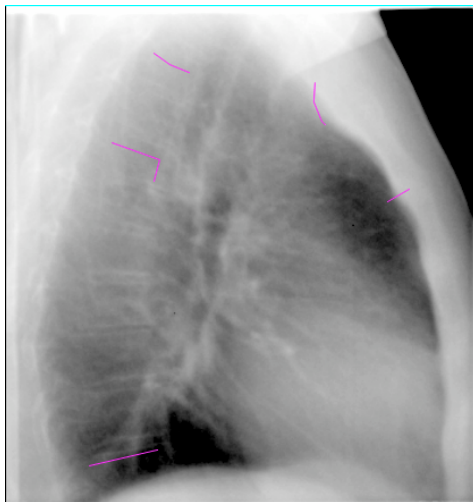
(c)

Potential systematic errors:

1) During the CT simulation, the main possible error is an error in set-up or tattooing which would result in consistent incorrect set-up during treatment eg. CT table sag, couch sag or LASER misalignment.

2) A number of possible errors arise from the delineation process. To understand these it is important to know how much of the composite margin (20mm cranio-caudal and 15mm lateral and anterio-posterior) is derived from each of the individual margins for, subclinical disease (CTV), internal movement (ITV) and set-up errors (PTV). I will hence discuss each margin individually with the possible errors:

- The GTV delineated by different clinicians can vary greatly and it has been shown that even experienced clinicians are capable of voluming areas where there is no gross tumour or omitting areas where there is gross tumour [30]. This would result in irradiation of normal tissue or missing tumour tissue. This classifies as a systematic error. It is very difficult to allow for this error as an addition to a margin, as although there are small differences in where to place a delineation line around a tumour, the larger differences in lung cancer arise from decisions on whether or not to include a lymph node that has not been biopsied. To include this in a margin is impossible as lymph nodes are in different positions and of different sizes. It is therefore not encompassed in any margin. Previously elective nodal irradiation dealt with this issue, however it is now thought superior to only include malignant nodes within the GTV. Usual practice has been to outline all nodes greater than 1cm. Local relapse alone in adjacent nodes following radiotherapy is rare [31,32], probably due to some of the surrounding nodes being partial irradiated in the entrance and exit beams [33].

- The GTV to CTV margin is currently 5mm. This margin is accepted as standard for ease and to allow a coherent approach. In reality, the most significant paper on microscopic disease in lung cancer has the margins being 6mm and 8mm for squamous and adenocarcinomas, respectively [21]. The majority of centres worldwide leave margins of 5mm, however it is

accepted that different patients have different degrees of microscopic invasion [34] and therefore as we cannot assess it in individual patients, it will inevitably be over or under estimated in many resulting in a systematic error.

- The CTV to ITV margin used in our centre, is currently a standard margin that is added to all tumours. It is well accepted however that respiration-induced tumour motion is unpredictable and varies enormously between patients [35,36,37]. Hence a standard margin will result in systematic error due to underestimation of movement or overestimation of movement for the majority that are at variance with the standard "population-based" margin allows.

- The ITV to PTV margin, or set-up margin, is a margin chosen by the radiation oncology team, based on experience and judgment drawn from observation and evaluation of the risk of failure and complications. This is currently what we use at the Beatson. It can also be calculated for an individual department using the McKenzie et al [23] or Van Herk et al [22] margin equations. There may be a systematic error introduced at this point if has been over or underestimated.

- In the ICRU 62 report, there is extensive discussion on how to add these margins together. If simple linear addition is used, it is recognised that the PTV may be inappropriately large. It is up to the local radiotherapy team to use their experience and judgement in deciding the method of addition of these margins.

3) During the plan calculation process, if an error occurred in creating the plan, or disseminating the information to check simulation or the treatment room a systematic error could occur.

4) During check simulation again if the patient is set-up incorrectly or tattooed incorrectly a systematic error would be introduced.

Potential random errors:

1) If the patient is set-up incorrectly on a particular day. This would result in a random error that fraction.

2) If the patient's tumour changes position over the course of four weeks of treatment due to re-inflation of a lung or inflammation of the surrounding normal lung, this is not consistently present from the beginning but could be consistently present towards the end of treatment therefore it could be considered both random or a systematic error.

3) If the patient loses weight or relaxes into the treatment couch, this could cause a variation from planning and hence a random error, however as with the tumour migration, if this error consistently becomes a problem, it could also be viewed as a systematic error.

Although our current technique of 3D conformal radiotherapy is relatively standard, section 1.2.5 highlights many limitations. The current verification technique of offline MV images can only reduce the systematic errors occurring due to a change in patient position. It does not deal with any other errors. Many of the potential errors highlighted above can be reduced with the use of other imaging techniques and thus the introduction of Image Guided Radiotherapy (IGRT).

1.3 Image Guided Radiotherapy

1.3.1 What is Image Guided Radiotherapy?

Image Guided Radiotherapy (IGRT) is the use of different imaging techniques to improve on the three main steps of radiotherapy: delineation, planning and verification. IGRT can improve target coverage, and facilitates a reduction in the large margins, that we traditionally use to allow for unknown or large errors, with a view to reducing dose to organs at risk (OAR). It can also facilitate alternative planning and

delivery techniques allowing us to escalate the dose and thereby improve the chance of local control.

A number of developments in radiotherapy have emphasised a need for improved IGRT:

> • Planning has become more conformal with the advent of intensity modulated radiotherapy (IMRT), arc therapy such as RapidArc (Varian Medical Systems, Palo Alto, Ca, USA) and tomotherapy (Tomotherapy Incorporated, Madison, WI, USA).

> • With increasing interest in dose escalation, accurate target coverage and sparing of organs at risk become more important, as inaccuracies have more consequences with bigger doses.

> • With some of the new delivery techniques, fall off doses around the PTV are becoming much steeper. As the risk of missing the target becomes greater there is a real need to use imaging techniques maximally to target the PTV better

1.3.2 Imaging techniques used in CT simulation and Delineation

1.   PET/CT

The role of positron emission tomography (PET/CT) for evaluation, treatment and follow up of lung cancer patients is rapidly increasing. PET/CT scans make use of the fact that most lung cancers have increased activity of glucose transporters and increased hexokinase activity compared with normal cells. A radioactive agent, fluorodeoxyglucose (FDG) is delivered to the patient. Due to the increased activity of glucose transporters and hexokinase activity, it accumulates at a higher rate in lung cancer cells than the normal tissues. Images taken after FDG administration allow easy localisation of gross tumour as most deposits of tumour measuring around >1cm show up as a "hot lesion" on the scan. FDG labelled with the positron-emitting isotope F-18, is the radiopharmaceutical of choice for imaging lung cancer. The intensity of a "hot lesion" on PET, represents the FDG uptake and can be quantified using the standardized uptake value (SUV). The SUV is derived by dividing the concentration of F-18 in the tumour, measured in Bq/gm, by the injected activity per unit body weight.

In NSCLC, PET/CT is increasingly used in a number of settings:

a) To evaluate undiagnosed pulmonary masses, with 96.8% and 77.8% specificity and sensitivity respectively [38].

b) To stage NSCLC in the mediastinum with a view to dictating therapy as there is 90% specificity and 85% sensitivity in the mediastinum [39].

c) To detect distant metastatic disease to prevent radical treatment when it is inappropriate, PET/CT can identify distant metastasis in an additional 12% of patients who have been staged with Stage I disease with all other standard imaging techniques [40].

d) To predict response following radical radiotherapy or chemoradiotherapy [41].

e) The SUV level can be used as a prognostic indicator [42].

f) For use in the delineation process, described in detail below.

The use of PET/CT in the delineation process is becoming more prevalent although there are a number of unresolved issues and significant potential for further development. In routine clinical practice, the majority of clinicians use it as a tool to localise areas of gross tumour. There is good evidence that the use of PET/CT for localisation can both increase and decrease volumes [43]. This is logical because PET/CT can both upstage and downstage mediastinal lymph nodes. In addition it can assist in deciding how much opacified lung is active tumour and how much is collapse or consolidation. Its use has also been reported to reduce interclinician variations in delineation [44] and a further paper compared PET/CT delineations to pathological specimens and found that using the additional information of a PET/CT improves target coverage from 75% to 89% [45]. There are three different ways that the PET/CT can be used for localisation:

a) PET/CT and planning CT can be co-registered so that they are portrayed simultaneously at the planning computer terminal however due to the concerns regarding image registration and spatial resolution this is not available in all centres.

b) A PET/CT scan can be used as a planning scan if the CT component is of an acceptable quality, however many patients in the UK continue to receive

sequential chemo-radiotherapy and it is not possible to perform a planning PET/CT after neo-adjuvant chemotherapy due to inhibition of SUV uptake by the tumour stunning.

c) Most centres have the PET/CT and the planning CT on adjacent computer screens and try to relate in information of the PET/CT onto the planning CT.

Another way in which PET/CT can be used for delineation is for automatically outlining the GTV using image segmentation methods that have primarily been based on either a threshold value (a percentage of SUV max) [46] or as an absolute SUV [47]. However consensus over an absolute ideal value has not been reached. A further limitation is that all image segmentation tools require clinical review and adjustment afterwards, reducing the time saving benefits offered by image segmentation.

Finally there is much interest in the possibility of "dose painting" [48]. NSCLC are heterogeneous and there is evidence confirming that areas of higher SUV uptake are the areas where local relapse is more likely [49]. Dose painting involves using a PET/CT during planning to deliver a bigger dose to those areas with higher SUV levels. An alternative approach uses data from a PET/CT scan towards the end of radiotherapy treatment and delivering a boost of radiotherapy to the areas with highest SUV levels [50].

In summary, there is little controversy regarding the use of PET/CT to aid gross tumour localisation and there is evidence confirming the benefits, however other uses of PET/CT in delineation continue to be research based and should not be used out with that setting.

2.   4DCT simulation

Four-dimensional CT (4DCT) or respiration-correlated CT scan is a single investigation generating spatial and temporal information on mobility [51,52]. It permits organ motion to be observed and quantified. Previously the CTV to ITV margin was a set, population based margin, added arbitrarily to all patients. However as discussed above,

it is well recognised that the intra-fraction tumour motion of each patients' tumour cannot be predicted. With a 4DCT, the intra-fraction tumour motion can be visualised and therefore an individualised margin, specific for each tumour, can be added. 4DCT has been shown to be a better method of assessing respiratory movement than previously used fluoroscopy [53] or the use of six, standard 3DCT's, in combination [54]. The use of 4DCT to individualise the CTV to ITV margins has been shown to improve tumour localisation and potentially decrease normal tissue irradiation [55]. It is therefore an imaging technique that can assist with delineation and an important tool in IGRT.

There are multiple commercial hardware and software packages available to perform a 4DCT. I will describe the Varian Medical Systems software that was used for this research as it is available in both centres where this research was undertaken.

To create a 4DCT scan, a respiratory trace is recorded throughout the scanning process and saved independently. This trace is the anterior-posterior movement of the chest wall captured by an infra-red marker box positioned on the xiphesternum. This infra-red marker box and its anterior-posterior motion is an external surrogate of the superior-inferior internal tumour motion. The CT scanner images a 20cm length of the thorax for the duration of a respiration cycle and takes 10 consecutive scans over one respiration cycle. The bed then moves and the next section of lung is scanned in exactly the same way. The different scans are divided into 10 "bins" relating to 10 sequential phases of the respiratory cycle. These are labelled 0%, 10%, …. , 90%. The 0% phase usually lies closest to maximum inhalation and maximum exhalation usually lies around 50%. In basic terms the respiratory trace is a sine wave. The clinically relevant parameters are the amplitude, which can increase or decrease depending of the depth of the patients breath; and the wavelength, which can increase or decrease depending on the rate of respiration. The ideal is to have regular breathing both in terms of wavelength and amplitude, unfortunately breathing patterns are seldom regular in patients with poor pulmonary function, thus there is interest in identifying the potential impact of coaching, on image quality and target coverage. There are

Figure 3-2. An illustration of the Varian RPM system.
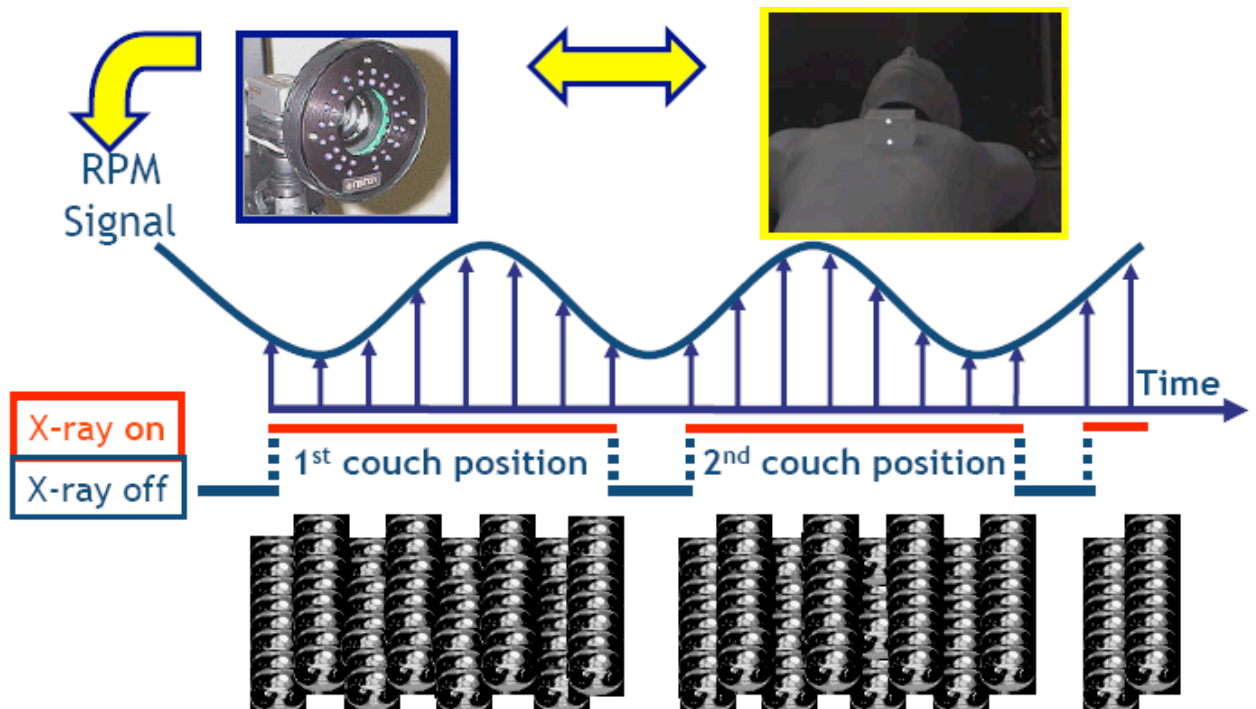
different methods of coaching a patient, for example, audio or visual or a combination of both. In addition, patients can undergo monophasic or biphasic coaching. During monophasic coaching only inspiration or expiration are prompted versus biphasic coaching where both inspiration and expiration are prompted. There are numerous papers looking at the benefits of coaching. All forms of coaching are shown to improve the regularity of the wavelength and the amplitude of the respiratory trace by varying degrees [56]. Whether it is the wavelength or the amplitude that are more consistent is important for different reasons.

During acquisition of the 4DCT planning scan, a consistent wavelength allows a better image. Improving the consistency of the amplitude of the respiratory trace, is not useful in improving image acquisition. However, if there is abnormally large movement amplitude during the recording of the respiratory trace in 4DCT, it may not represent the amplitude of tumour motion on treatment. If coaching is introduced during the planning scan in order to maintain constant wavelength, in theory coaching would have to happen during treatment in order to maintain the coaching amplitude. However introducing coaching for this theoretical risk, one has to be aware there are concerns coaching can increase the tumour amplitude which would translate into larger volumes and more toxicity [57]. This study suggested that a coached 4DCT could not be used when there is no coaching performed during treatment [54]. However on review of the study, it reported a mean increase in PTV of 10.2%, which from our own work, correlates with an increase in V20 of around 1-2%. This increase in V20 is extremely unlikely to be clinically relevant. The same paper suggests that there is a different centre of mass (COM) for the ITV delineated in coached and free breathing scans. The COM varies by a mean of 2.7mm. It is not described in which axes this movement occurs nor whether it is primarily in one direction or divided amongst the six directions. It is unlikely motion of this magnitude would result in any clinical consequence. As the evidence currently stands, there is no evidence that coaching at 4DCT to obtain a better image and not coaching on treatment will cause any clinical detriment to the patient.

It was hoped that coaching during treatment delivery would decrease the variability of the tumour amplitude and hence improve target coverage [58]. However the studies undertaken demonstrate a reduction in the variability of the external surrogate, not the internal tumour movement, and these do not necessarily correlate. It remains unproven whether coaching reduces the variability of the tumour amplitude. Respiratory gated radiotherapy is a different situation. This is when the radiation beam is switched on during one phase of the respiratory cycle. As the radiation beam requires a regular breathing cycle to switch on and off, a regular wavelength is a paramount therefore in respiratory gated radiotherapy, therefore coaching is recommended.

In summary, although coaching can improve consistency of wavelength and amplitude, and hence improve the image acquisition, there are concerns regarding its use and no evidence it results in improved target coverage outcome other in respiratory gated radiotherapy where it is recommended. Further investigation into the benefit of coaching in non-respiratory gated radiotherapy patients is required.

The 4D software is also used to create a Maximum Intensity Projection scan (MIP), an Average Intensity Projection (Ave-IP) and a Minimum Intensity Projection (Min IP) from the raw data. In these datasets, each pixel is assigned the highest (in the MIP), the average (in the Ave-IP) or the lowest (in the Min-IP) density value that occurred, taking account of all 10 scan phases. For a solid tumour moving within low density lung tissue, the MIP gives a good representation of the volume occupied by the tumour throughout the respiratory cycle, while the Ave-IP is the data-set appropriate for calculation as it represents the lung volume in its average position. Figure 1-4 demonstrates the difference between the different constructed image-sets.

There is great controversy regarding the best method of delineating from a 4D scan due to abundance of data-sets there are to deal with. This will be discussed further in Chapter 2.

Figure 1-4. Image demonstrating the different constructed image-sets: (a) demonstrates the different "bins" representing different phases of the respiratory cycle; (b) A Maximum Intensity Projection (MIP) which is where the highest density pixel is selected for the image-set; (c) A Minimum Intensity Projection (Min-IP) which is where the lowest density pixel is selected for the image-set; (d) An Average Intensity Projection (Ave-IP), where the average density pixel is selected for the image-set
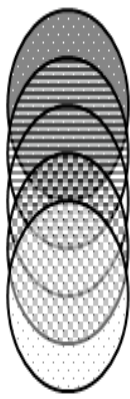
(a)   (b)   (c)   (d)

In 4DCT the traditional labels of GTV, which is enlarged to CTV, then ITV then PTV are no longer appropriate. On a 4DCT, there are a number of methods of delineating however the following volumes are commonly created using a 4DCT:

- The Gross Internal Tumour Volume (GITV) is the gross tumour in all phases of the respiratory cycle.

- The Clinical Internal Target Volume (CITV) encompasses the CTV in all phases of the respiratory cycle.

Whether the 5mm margin for microscopic invasion is added before or after the internal target motion will vary depending on the software available to the clinician, and clinician preference. The final margin applied is the set up margin from CITV to PTV. Figure 1-5 demonstrates the traditional labelling of structures, and the labelling of structures that will be used when there is discussion of 4DCT.

1.3.3 Imaging techniques used in Verification

There are 2 new radiotherapy verification developments in lung cancer.

1) The first is the development and use of novel image types to allow for easier verification of structures and better matching. These include kV imaging, fluoroscopy, CBCT, and MV-cine. Kilovoltage imaging and fluoroscopy have been traditionally been used in check simulation, but they can now be produced on the treatment machine using an imager which is attached to the linear accelerator. This treatment machine imager also allows the acquisition of cone-beam CT (CBCT) scans. These scans permit the 3-dimensional verification of the position of the tumour and surrounding organs at risk [59]. MV-cine are a number of BEV frames captured using the treatment beam run together to create a cine-image of the tumour during the treatment delivery [60].

2) The second is that there is now hardware and software to allow easy on-line image acquisition, review and set-up modification prior to treatment. Images of the patient, taken using treatment machine imagers attached to the radiation treatment machines are taken immediately prior to treatment. These are then

reviewed and matched to the planning DRR. Lastly immediately prior to treatment, a shift is made so that all systematic and random errors, in their traditional sense, are minimised. The patient is then treated.

In the current era of lung oncology, potential errors cannot be easily explained or understood using the traditional description of systematic and random errors, as explained above. Delivery errors are better divided into 4 categories which can have systematic or random components. They have been divided in this way so that the different imaging techniques, suitable for each error, can be discussed individually.

Figure 1-5. The image on the left demonstrates the terms dictated by ICRU 50 / 62 that are commonly used. The image on the right demonstrates the terms that will be used when discussing volumes delineated using a 4DCT.
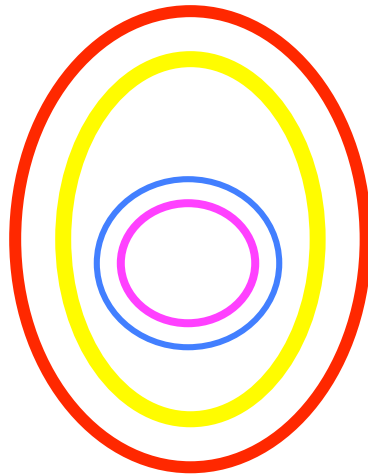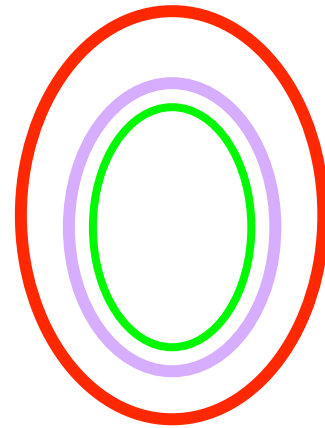
1.   Interfraction Patient Motion (set-up error)

Because immobilisation is imperfect, the patient will lie in a slightly different position every day. If this varies day to day during treatment, this is a random error whereas, if the patient lies in a consistently different position during planning and treatment this would result in a systematic error. More difficult to classify is if the patient begins to relax into the bed over the course of 4 weeks of radiation resulting in a consistently posterior set-up, this is probably best clarified as a newly acquired systematic error. Daily online matches to minimise interfraction patient set up error could be done with:

   1) A pre-verification MV iso-image, as discussed above, which delivers an additional dose of 4mSv.

   2) A CBCT which delivers a dose of 45mSv.

   3) A pair of static orthogonal kV images which deliver only 0.2mSv.

The newly acquired image can then be initially automatically matched using stable bony anatomy, such as the spine, to the planning DRR and then manually verified. The shift required to have the patient in the planning scan position is highlighted in the control room and when approved, the shift is made to the treatment bed. All corrections are limited by the image quality and the ability of the operator to perform/confirm the match. Figure 1-6 demonstrates a CBCT image and a pair of kV orthogonal images. Figure 1-3 is an example of MV images.

Prior to the introduction of treatment machine imagers, if on-line matching was required, MV images were traditionally used as it was only possible to create MV images using the LinAC. However MV radiation is absorbed via the Compton Effect and the uniform absorption makes it difficult to differentiate the stable bony structures such as the spine from the soft tissues. The harder it is to pick out the stable bony structures, the more difficult either an automatic or manual match is to make. There are now good comparative studies of MV images versus both CBCT and kV orthogonal images for set-up. These have consistently demonstrated inferiority of MV images and hence MV images do not have a role in interfraction patient motion [61].

When comparing kV orthogonal images to CBCT for on-line set up, they were found to be equally as good at matching to DRR in all planes, however correction of rotational errors remains superior with CBCT [62]. Rotational errors cannot be adjusted for on the

treatment unit, so if a rotational error of >2-5 degrees is noted, the patient would be repositioned and a further on-line image taken. As a result, other than with rotation that cannot be adjusted for, CBCT and kV orthogonal images are equally as good for reducing interfraction patient motion or set up. Due to the radiation dose of kV orthogonal imaging being lower, kV orthogonal images should be used for daily on-line set up as it delivers far less dose.

Daily on-line set up with kV images minimises the systematic and random errors present due to changed patient position, however many departments cannot image daily due to time constraints. Different imaging protocols include: on-line imaging daily for the 1st 5 days only, online imaging days 1-5 then weekly, online imaging weekly or on alternate days. An off-line protocol must then be implemented for the days that on-line imaging does not take place. An off-line protocol will reduce the systematic error however the random error will only be minimised the days an on-line image is performed. There is no consensus on which of these protocols is the best in reducing systematic set-up error. Higgins et al. recently published a paper comparing these off-line protocols. They compared daily online imaging, imaging the first 5 days, imaging weekly and imaging alternate days. They confirmed that daily online set-up can allow set up margins of 3-4mm and significantly reduces random set-up. Of the other imaging protocols, which only dealt with systematic error and do not make any difference to random error, an average of the 1st 5 days had unfavourable levels of geometric uncertainty in comparison to the weekly or alternate days protocol, which reduced systematic errors so that a set-up margin of 5mm could be used [63]. Further research is required to confirm the best imaging protocol.

In summary, kV orthogonal images are most suitable imaging technique for the interfraction patient motion error. As they deliver minimal radiation exposure it is possible to undertake online daily imaging which is effective at minimising both systematic and random set-up error.

2.   Interfraction Tumour Motion (tumour migration and volume change)

Tumour migration and volume change during the course of 4-6 weeks of radiation is a recognised phenomenon. This migration can be an increase in the volume, a decrease in the volume or a migration of the centre of mass as a result of many factors for example weight loss, inflammation or re-expansion of a lung. In terms of tumour migration: Sonke et al. report that the mean interfraction tumour migration of the volumes was 1.6mm (left-right), 3.9mm (cranio-caudal) and 2.8mm (anterior/posterior) [64]; Britton et al. results were not too dissimilar with migration of the tumour volume reported as 3mm (left-right), 5.4mm (cranio-caudal) and 4.5mm (anterior/ posterior) [65]. In terms of changes in tumour volume: Erridge et al. showed that in a population of 25 patients, tumour shrinkage of at least 20% occurred in 40% of the patients [66]; in Britton et al volume loss of at least 40% occurred in 50% of the patients; Bosmans et al report a 30% reduction in 13% of patients and a >30% increase in tumour size in 17% of patients [67]. There are other reports of volumes increasing over the course of radiotherapy, Underberg et al. reported an initial increase in tumour volume of 10cm3 in at least 2 of 40 patients [68], however the incidence of increase in tumour volume does appear to be less than the incidence of tumour volume reduction.

Another form of interfraction tumour motion is baseline shifts where end-inspiration and end-expiration position varies. Sonke et al. reported the largest study looking at this specific error in 56 patients. They found the systematic average baseline variations were 1.6, 3.9, 2.8mm and the random baseline variations 1.2, 2.4, 2.2mm in left-right, craniocaudal and anterior-posterior directions respectively [69]. The baseline shift is a difficult error to visualise and therefore monitor. As a result of this, Sonke et al. developed the 4D-CBCT, which is an online image which gives all the information of a CBCT with additional information on baseline shift and intrafraction tumour motion (respiration motion) [70]. It is currently unknown whether baseline shifts in an external structures correlate with baseline shifts in the internal tumour and this requires more investigation. This error becomes of more significance in respiratory gated radiotherapy where the aim is to irradiate in either end-expiration or end-inspiration.

Figure 1-6. (a) Three slices through a CBCT with the planning GTV superimposed, (b) A pair of orthogonal kV images with the structures from the planning DRR superimposed.

(a)

(b)
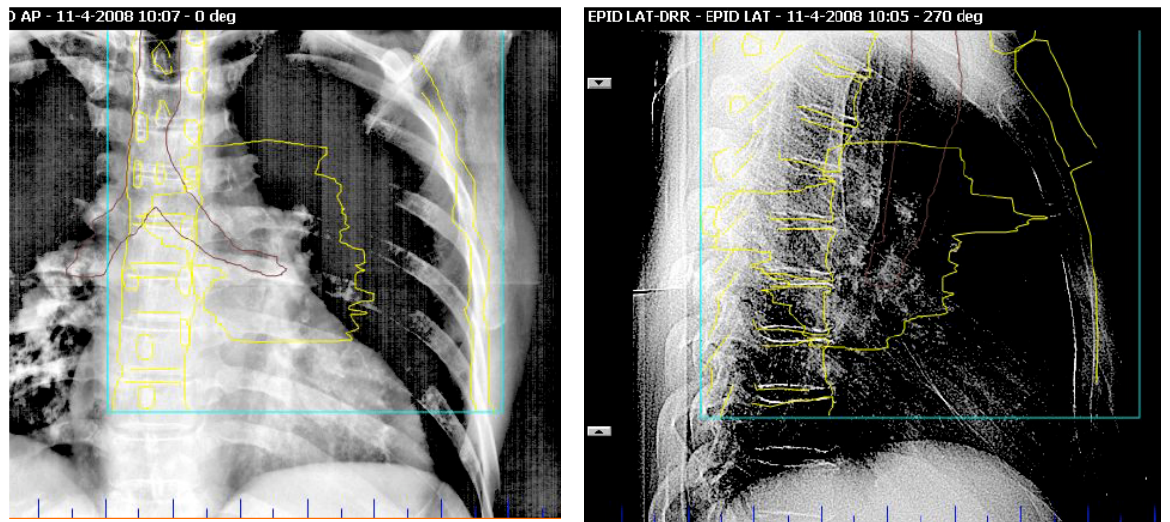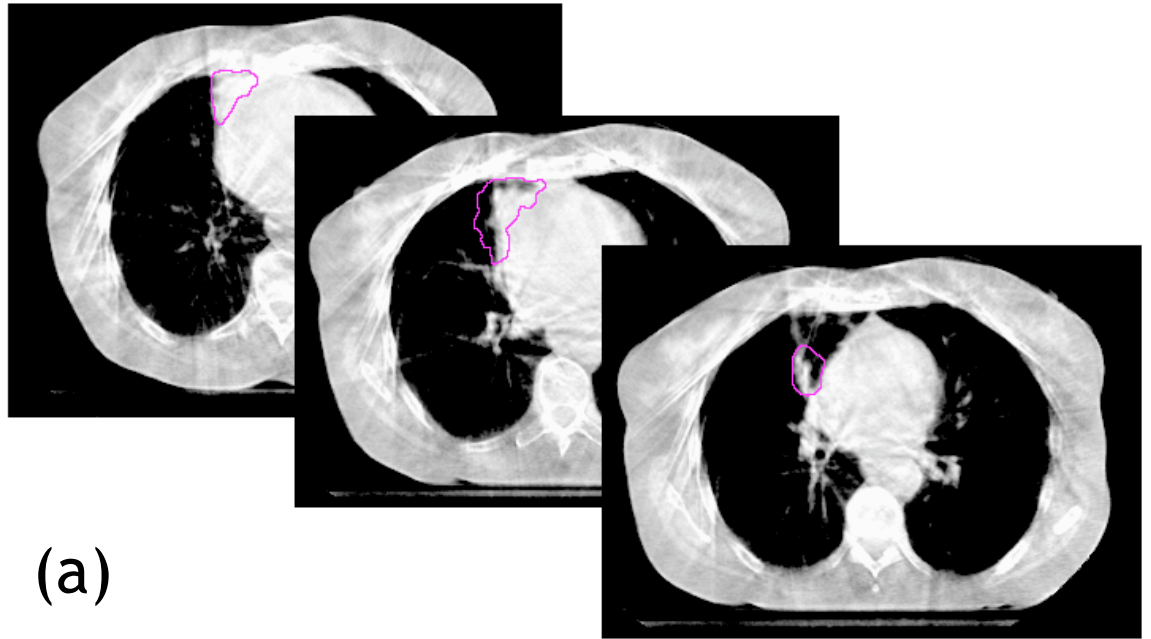
Each of these potential interfraction tumour motion errors can only be highlighted by CBCT. CBCT allows visualisation of the tumour bulk, and therefore enable a check to ensure there has not been significant alteration the tumour bulk or position from the planning scan. If either has occurred, the patient requires re-planning to prevent geographical miss. CBCT is the only imaging technique that gives an accurate position and size of the tumour and therefore should be incorporated into all verification protocols to check for interfraction tumour motion error. There is no evidence supporting daily imaging to identify interfraction tumour, the feeling is that CBCT can be used once or twice a week to identify any concerns however the ideal frequency of CBCT requires further investigation. A number of groups have suggested that in Stage I tumours doing a soft tissue match onto the tumour would reduce the errors that occur due to tumour migration [71,72], however on the other hand, in node-positive tumours, there are concerns that soft-tissue matching contribute further errors and hence are best avoided [73].

Using CBCT to identify patients where the tumour volume has altered or moved has raised the possibility of adaptive planning, i.e. altering the volume or plan to allow for these changes. Britton et al. repeated 4DCT planning scans on 10 patients undergoing radiotherapy and found that when the original plan was recalculated on the repeat 4DCT's, as a result of changes in tumour volume, mobility and patient set-up, occasionally there were dramatic dosimetric consequences [74]. There has been enthusiasm in some areas for reducing volumes in those patients whose tumours have shrunk, in order to spare normal lung by reducing the V20 during the radiation [75] however, there are some widely felt concerns regarding this. The reluctance to embrace this technique is because it has been shown that non-small cell lung cancer stem cells are radioresistent [76] and although the tumour bulk may have reduced, there may be a small number of radioresistant stem cells that cannot be visualised by the repeat imaging. By reducing the volume, these radioresistant cells may lie, unseen, outside the new gross tumour volume. By irradiating the most resistant cells to a lesser dose you increase the likelihood of local relapse. Consequently, replanning due to marked increase or migration of tumour volume, or patient set-up or body habitus may

reduce toxicity in the minority of patients who would suffer dosimetric consequences due to these events [70]. However adaptive planning following tumour shrinkage should be used with caution and only within clinical trials.

In summary, in node-positive tumours, once or twice weekly online CBCT with a bony match, can be used in to highlight those patients who have suffered a significant increase in tumour size, or tumour migration, so that a repeat 4DCT can occur for re-planning. If the tumour reduces in size, replanning would not be advised in these patients. In Stage I patients, online CBCT can be used for a soft tissue match.

3.   Intrafraction patient motion (patient moving during treatment)

While the patient lies on the treatment bed, there is some intrafraction patient movement. The intrafraction patient motion increases as the treatment time increases. Purdie et al suggested that any treatment taking more than 30 mins would require a further on-line image because after 34 mins, the intrafraction tumour position deviations changed from being 2.2mm, which was considered acceptable due to their 3mm action level, to >11mm which was considered unacceptable [68]. Hoogeman et al reported that the standard deviation (SD) of the intrafraction displacements increased linearly over time. The SD increased to 0.8, 1.2, 2.2mm respectively in a period of 15 mins [77]. As margins are getting smaller and especially in very conformal treatment such as stereotactic radiotherapy, these small errors become more important to quantify to ensure target coverage.

4.   Intrafraction tumour motion (respiration-induced tumour motion)

This is primarily the respiration-induced tumour motion during the radiation treatment. There is also a degree of intrafraction motion as a result of hysteresis and heart motion. Hysteresis is difference between the inhalation and exhalation trajectory of the tumour [78]. The challenge with intrafraction tumour motion is that it can vary from day to day, week to week. A single assessment of intrafraction motion is captured in a "snap-shot" 4DCT scan. This is described as a "snap-shot" because although 4DCT gives the additional dimension of time, the period of time it takes to scan the primary

tumour with motion is only for the duration of one respiratory cycle. However what is imaged on the 4DCT at simulation may or may not be the same respiration-induced movement and hysteresis that occurs during treatment. If the average movement and hysteresis is captured during the planning, and during any fraction of treatment there is slightly more or less movement than the average, this would be considered a random error and it is unknown if this would have clinical consequences. If during the 4DCT planning scan there is less or more tumour motion visualised than normal, the margin will consequently be either too big or too small, resulting in a systematic error. As a result the target would be consistently missed or normal tissue consistently irradiated, which is more likely to have a clinical consequence. There are a number of techniques that can be used to ensure that what is visualised during the CT planning scan is what is occurring on the treatment room.

1) Abdominal compression is designed to reduce the respiration induced motion so that it is kept at a minimum both during planning and subsequently during treatment. This compresses the abdomen, reducing the tidal volume and hence the intrafraction tumour motion [79,80]. However, the American Society for Therapeutic Radiology and Oncology state as a pre-requisite to immobilization in SBRT patients, that patients need to be able to lie comfortably despite their immobilization technique. It is recognised that patients feel less comfort with an abdominal compression frame in place. In addition, a recent paper has confirmed that although abdominal compression reduces motion, it increases the variation in the intrafraction tumour motion and therefore is not as suitable a method of managing intrafraction patient motion as previously thought [81].

2) CT scans undertaken during breath-hold have been mentioned in the literature [82]. This is used mainly in centres without 4DCT with the aim of capturing tumour in a stable position (a specific respiratory "gate"). This allows planning and treatment during breath hold with the aim of irradiating while the tumour is not moving thus removing the uncertainty of a population based margin or potentially decreasing the normal tissue irradiation. However as we have a 4DCT, the reproducibility of a breath-held CT on treatment is subject to a great deal of error

[83] and we have a population with significant co-morbidity who are not likely to tolerate breath hold, this is not something we plan to investigate.

3) The use of a single "snap-shot" 4DCT can produce random or systematic errors if the intra-fraction motion during treatment is different to that visualised at 4DCT planning. There are a number of papers that look at the likelihood of a systematic intrafraction tumour motion error. Michalski et al. reported tumour motion reproducibility of 87% and suggested rechecking the intrafraction tumour motion at some point after 4DCT to highlight the small proportion who had different amounts of movement [84], Bosmans et al. reported that although a small number of changes in tumour motion were seen over the course of treatment, in only 4% of patients this would have resulted in an increase of the internal margin [63], Guckenberger et al. found that the mean peak to peak tumour motion changed by only 0.9mm on two different scans [85], Sonke et al. reported that the mean variability of the tumour trajectory shape did not exceed 1mm (1 SD) [60]. These papers suggest that for the vast majority of patients it is safe to perform one 4DCT planning scan and treat without re-imaging the intrafraction motion. To identify the few patients who have a systematic error can be done by re-imaging the intrafraction tumour motion either prior to or during the first few fractions of treatment.

4) Fluoroscopy can be used to make a further assessment of the intra-fraction respiration induced motion; however tumours are not always seen on kV images. Fiducials can be implanted into the tumour percutaneously or transbronchially so that the intrafraction motion can be monitored easily on kV fluoroscopy. However this is not commonly performed, as insertion can be technically difficult, there is a significant risk of pneumothorax [86] and there are high drop-out rates after bronchoscopic placement [87].

5) Due to the fact a CBCT image is taken over a number of respiratory cycles, it gives a picture of the tumour over a number of respiratory cycles i.e. it gives an impression of intrafraction tumour motion. The CBCT image has the high density tumour in the average position of the tumour, however there is varying degrees of density around it that can be used to either subjectively assess the tumour motion

when comparing the image to the Ave-IP, or objectively quantify tumour motion using the complicated published technique [88]. This is a quick, subjective method that can be used to ensure the tumour motion does not differ widely from what was captured at 4DCT.

6) 4D-CBCT's allows online visualisation of intrafraction tumour motion [90]. Sonke et al. found that in Stage I tumours, the systematic intrafraction motion variability was 1.2, 1.2 and 1.8mm and the random variation was 1.3, 1.5 and 1.8mm (random) in left-right, craniocaudal and anterioposterior direction respectively [66]. These measurements confirm that in the majority of patients there is minimal variation in intrafraction tumour motion, however the 4D-CBCT offers an opportunity to identify any outliers with more variation which may result in geographical miss.

7) Many 4DCT planning scans require an external surrogate to be placed on the xiphisternum or the abdomen in order to create the scan. Amplitude Monitored Treatment Delivery (AMTD) is a novel technique developed in the VU Medical Centre, Amsterdam which uses the respiratory trace created using the external surrogate, as a surrogate for the internal tumour. AMTD is achieved by noting the maximum amplitude of the external surrogate cranio-caudal motion during the 4DCT scan as an estimation of the maximum intrafraction tumour motion. If the external surrogate cranio-caudal motion exceeds this threshold, the treatment machine is programmed to automatically turn off. The problem with this technique is that internal structures do not necessarily correlate with external surrogates. Correlation coefficients between tumour and external surrogate have been reported as 87% in the superior-inferior direction, but as little as 44% in the anterior-posterior position by Koch et al. [89] and 81% in all directions by Hoisak et al. [90]. The lack of correlation was also confirmed by a study examining the residual movement within one respiratory bin over a course of treatment and identified it to be as much as 6.2mm [91]. Implementing AMTD is a lengthy process, and as the machine is turned on and off treatment can take longer to deliver, increasing the intrafraction patient movement and potential consequent errors.

AMTD may offer assistance with target coverage that is otherwise missed due to intrafraction tumour motion, however this requires further investigation.

1.3.4 Different treatment delivery techniques available as a result of IGRT

1.3.4.1 Phase-Based and Amplitude-Based Respiratory Gated Radiotherapy

With the introduction of 4DCT, there has been a great deal of interest regarding the possibility of using the 4DCT to plan and deliver respiration gated radiotherapy (RGRT). This involves treatment delivery at selected phases of the respiratory cycle which can be achieved using different systems. Within our institution, the Varian RPM system (RPM; Varian Medical Systems, Palo Alto, CA) is used. The patient's respiration cycle is monitored continuously by an external surrogate; an infrared marker box placed on the xiphisternum. The movement of the marker box is picked up by a camera and a respiratory trace observed in the control room. This trace enables the selection of a respiratory phase or "gate" for treatment delivery and the treatment beam is switched on only during this interval. RGRT can be delivered in end-inspiration or end-expiration. There are two methods of RGRT, phase-based gating and amplitude based gating, each with advantages and limitations. Figure 1-7 illustrates phase-based and amplitude-based RGRT.

In Phase-based RGRT, the breathing cycle is divided into multiple time segments and radiation delivery is based on the same phase of the patient's respiratory cycle. The phases selected for irradiation are usually 90%, 0%, 10% or 40%, 50%, 60% in end-inspiration and end-expiration respectively. The main limitation of phase-gated RGRT is while there may be no baseline shift in the external surrogate baseline position; internally there may be a baseline shift. There is no information available as to whether or not there is any correlation between the external surrogate baseline shift and the internal tumour baseline shift. Hence the tumour position during the end-inspiration or end-expiration may differ from that captured on the 4DCT planning scan. Although the treatment beam is on at the correct time, end-inspiration or end-

expiration, the tumour position at this time could be different to that seen during planning. A further possible problem is the potential for a phase-shift between the external surrogate and the internal tumour. This would result in the extremes of motion of the tumour not coinciding with the extremes of position of the external surrogate. If this has occurred in the planning scan and continues throughout treatment, it is consistent so consequently will irradiate in the correct area. If a phase-shift occurs during treatment, but was not present at planning, in the beam would be switched on at the incorrect time. Spoelstra et al. used static MV images taken during RGRT treatment, during treatment at end-inspiration, to calculate the standard deviations of systematic (Σ) and random (σ) errors in tumour position and found them to be 1.8mm and 1.7mm respectively [92]. This study reassures us that baseline shifts and phase shifts are usually limited. The study also offers a quick verification method to ensure the tumour is in the field by taking an MV image.

In amplitude-based gating, treatment delivery is based on the absolute position of the marker block on the patient's thorax or abdomen, regardless of the phases in the patient's respiratory cycle. The limitation of amplitude-based RGRT is that if there is a baseline shift in the respiratory trace, and this does not correlate with a baseline shift in tumour position, the treatment beam will be switched on when the tumour is not in end-inspiration or end-expiration. Although there are studies looking at the dosimetric consequences of amplitude-based gating [93,94] there are no studies similar to the one mentioned above, confirming the residual motion within the treatment "gate".

RGRT has been shown to reduce the size of the PTV when compared to the standard 4D PTV [95], and there are some reports that toxicity parameters are reduced [96,97] with the use of RGRT although whether this represents a difference in clinical outcome and requires further investigation.

There are further concerns regarding both forms of RGRT.

1. One source of geometric uncertainty is the correlation between internal tumour motion and movement of the external surrogate when using the Varian RPM system, as occasionally it can be inconsistent [98]. Despite the Spoestra et al. confirming

minimal systematic and random residual motion, unease regarding disparities between external surrogate and internal tumour position remains.

2. Respiratory coaching is advised for RGRT. It is more important to reduce baseline shifts in RGRT and coaching has been shown to do this. In addition, the treatment beam requires a regular wavelength in the respiratory cycle to turn on. Coaching, especially auditory, increases the regularity of the wavelength therefore it is advised [99,100].

3. A further disadvantage of RGRT is that due to irradiation only proceeding during a specific respiratory 'gate' or 'phase', the radiotherapy beam spends around 80% of the respiration cycle switched off. Treatment delivery therefore takes longer which can in turn increase the risk of shifts in patient position [68].

4. As well as in continuous (non-gated) 4DCT treatment as discussed above, the use of a single 4DCT planning scan, for RGRT can also result in systematic errors in the treatment plan, and random errors during treatment when what is visualized on the planning 4DCT is not representative of intrafraction motion during treatment [101].

5. There remains differing ideas regarding whether the selected phase of respiration should lie in end-inspiration or end-expiration [102]. End-inspiration captures the lung at maximum expansion therefore potentially sparing more normal lung tissue [103] however the tumour remains in end-inspiration for significantly less time therefore there is a smaller treatment window [104] and the end-inspiration tumour position is more variable than the end-expiration tumour position. In end-expiration, there is a longer treatment window, the tumour position is more stable, but the lung is compressed therefore more lung is within the treatment field.

6. There also remains controversy concerning the threshold of craniocaudal tumour motion when RGRT should be considered. The AAPM recommended respiratory management for tumour movement greater than 5mm [105], Spoelstra et al. used 7.5mm, Starckschall et al. investigated if tumour motion could be used to predict those patients who would have the most clinical benefit however, they

only found a correlation between tumour motion and clinical benefit with RGRT in small tumours (GTV <100cm^3, [91]).

The theoretical advantages of RGRT are: reduction in toxicity; potential for dose escalation; and fewer patients having radical treatment withheld on account of large volumes or unacceptable toxicity parameters. It is an interesting concept; however the clinical benefit remains to be seen.

Figure 1-7. Illustration demonstrating the different forms of respiratory gated radiotherapy.
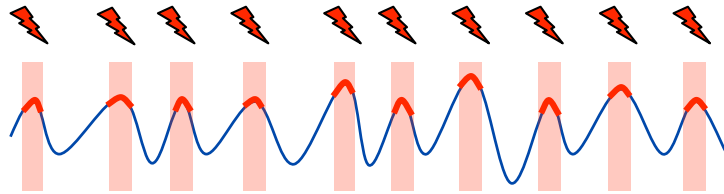
(a) End-inspiration Phase-Based Gated Radiotherapy

Position of external surrogate during maximum expiration at 4DCT.
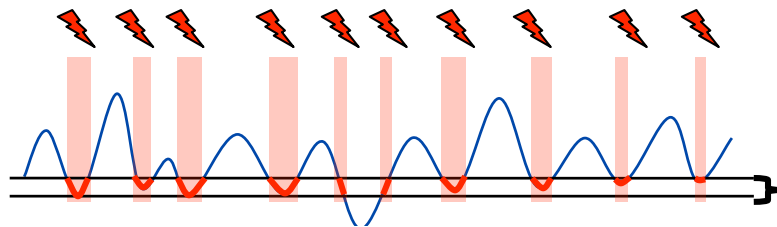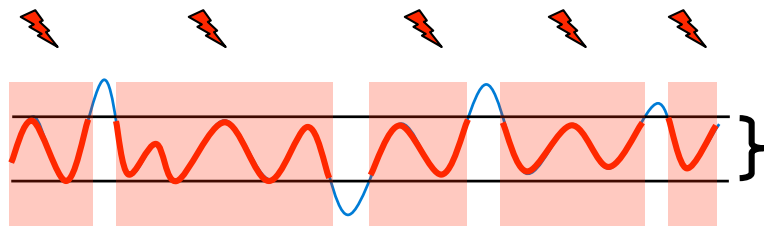
(b) End-expiration Amplitude-Based Gated Radiotherapy.

Amplitude observed at 4DCT

(c) Amplitude Monitored Treatment Delivery

1.3.4.2 Stereotactic Radiotherapy

Stereotactic body radiation therapy (SBRT) is a newly emerging radiotherapy treatment, aimed to deliver a high dose of radiation to the tumour, a biological dose equivalent of around 180Gy, utilizing either a single dose or a small number of fractions with a high degree of precision [106].

A combination of factors enables SBRT to deliver these large doses to the tumour. One such factor is to keep the planned target volume as small as possible, which is achieved by only treating tumours of <50mm in diameter and using very small, 3-5mm GTV to PTV margins. Another factor enabling the delivery of such high doses is the use of multiple fixed beams, usually 10-12 coplanar beams, with a linear accelerator so that the incidental dose to organs at risk in the beam projectory are not unacceptably high. The large numbers of beams make the isodose lines very conformal to the PTV and also results in very steep fall off dose gradients. The combination of a requirement of small margins and the steep fall off dose gradients require the high degree of precision required in SBRT. This precision is achieved by the use of IGRT. Due to the minimal margins and high doses, SBRT requires much more stringent constraints and minimisation of the effects of potential geometrical errors, with appropriate audit and QA. An awareness and calculation of the four errors discussed in detail in section 1.3.3. There is no fool-proof method for infallible management or prevention or of any of the four errors. They are potential errors that can be managed adequately with the techniques discussed below. Once a centre has decided how they hope to managed these errors and SBRT has been implemented, they must evaluate and audit their errors to ensure their method is adequate.

1) Methods to Manage Intrafraction Tumour Motion

These are discussed in more detail in section 1.3.3. All of these methods have limitations but used in combination, consistent local control rates of >90%, confirm that these are adequate.

- There was a great deal of interest in the Stereotactic Body Frame (Elekta Oncology Systems, Crawley, UK) that allows abdominal compression which has been proven to reduce intrafraction tumour motion. However a recent paper has demonstrated that the Stereotactic Body Frame with abdominal

compression can increase the variability in the intrafraction tumour motion and therefore this may not be as suitable a method of managing intra-fraction patient motion as previously thought [76].

- A 4DCT to assess the normal intrafraction tumour motion and encompass the movement in its entirety.

- CBCT or 4D-CBCT during online set up, where the intrafraction tumour motion can be assessed and the plan changed or adjusted only if the motion is different from what was seen at planning.

- The RPM system which can be used to monitor the external marker as a surrogate of intrafraction tumour motion so that the treatment beam can be stopped if the surrogate demonstrates different motion than seen at planning. As discussed above, the correlation is not always consistent; however this may be used in combination with other methods.

2) Methods to Manage Interfraction Tumour Motion

This motion is limited because a treatment course lasts no more than two weeks and tumours are less likely to migrate over this period of time. In SBRT, the CBCT that is used for set up is matched to tumour, rather than bone, so unless there has been a large change in position, so much so that the dosimetry is likely to be different, a tumour match will usually remove any error relating to interfraction tumour motion. If the tumour has increased in size between planning and any fraction, the patient will undoubtedly require re-planning to prevent under-dosing areas of the periphery of the tumour.

3) Methods to Manage Intrafraction Patient Motion

Increased treatment times result in increased intrafraction patient motion. Hoogeman et al. demonstrated that the SD of the intrafraction patient motion increased in 15 minute intervals from 0.8mm to 1.2mm to 2.2mm [73]. Purdie et al. confirmed this relationship by showing that the mean intrafraction patient motion increased from 2.2mm to 5.3mm when the treatment took over 34mins [68]. As a result of these studies, during SBRT where the patients are immobilized as they are in standard conformal radical radiotherapy, with the thoracic board and knee

support which is described as "frameless" SBRT, the CBCT should be repeated every 30 minutes. As treatments take on average 45 minutes, after about 25 minutes of treatment it should be paused in order to acquire a further CBCT. With this CBCT a further online set up with shift is performed prior to continuing the treatment. There are some other tools produced by different manufacturers to limit this error which can be used. The ExacTrac System (BrainLAB, Germany) continuously monitors around six infrared markers on the patient's chest wall during treatment, and cuts off the radiation beam if the markers move outwith the movement encompassed in the margin. This is thought to reduce the intrafraction patient motion, but at the expense of prolonging treatment. The second tool produced with an aim of reducing intrafraction patient motion was the Stereotactic Body Frame, but as discussed above reduces intrafraction tumour motion at the cost of increased variability. Therefore other methods which do not increase variation are preferable.

4) Methods to Manage Interfraction Patient Motion

Patient set up is of prime importance in SBRT in order to maintain the small GTV to PTV margins that are required. CBCT matching to tumour rather than to bony anatomy is required in all cases of SBRT. There has been a plethora of papers discussing the use of CBCT for tumour matching in SBRT and all have suggested that the remaining systematic errors are all within the 3-5mm margin applied [107,108].

There were three original Phase II trials of SBRT in early-stage medically inoperable NSCLC patients [12,13,14]. Since their publication SBRT has been implemented worldwide and there are now numerous Phase II trials reported. All three seminal trials used slightly different techniques. Timmerman et al. used abdominal compression with a Stereotactic Body Frame with the theoretical view at the time that this would reduce intrafraction tumour motion and intrafraction patient motion. To limit interfraction patient motion and interfraction tumour motion, this group used CBCT. Senan et al. used 4DCT for assessing and incorporating intrafraction tumour motion, CBCT for interfraction tumour and interfraction patient motion and the Exactrac system

intrafraction patient motion. The Japanese trial was a combination of many different immobilization and verification techniques.

The doses used in the three papers also differ, which may have resulted in the slightly different toxicity outcomes. Timmerman et al. used 60-66Gy in 3 fractions, Senan et al. used a variety of fractionation regimens depending on the likelihood of toxicity, but both of these papers had a biological effective dose of up to 180Gy. The Japanese paper used a wide range of doses (range 57Gy - 180 Gy) and found that there was a statistically significant outcome if doses were >100 Gy. As there is now significant literature on the tolerance and quality of life after a biological effective dose of around 180 Gy, this is usually what is used.

Despite different techniques, the outcomes in the three trials are similar. Timmerman recently published extended follow up of his prospective Phase II trial quoting 2-year local control rates of 95%. The Senan group had a median follow up of 12 months and reported a local control rate of 93%. Onishi et al. had a median follow up of 24 months and showed a local control rate of 92.9%, 3-year lung cancer specific survival was 88.4%. These outcome data are so good that there is a division in the radiation oncology community as to the next step. Some feel a Phase III randomised controlled trial of SBRT versus standard conformal radiotherapy is required and there is such a trial ongoing in Scandinavia, a similar trial from the Netherlands had to close due to poor accrual therefore it is unknown whether a trial of this nature will ever be successful. The other group feel the outcomes are comparable to those of surgery (outcomes of which are discussed in section 1.1.4) and Phase III randomised controlled trials of surgical resection versus SBRT are underway. Unfortunately the UK is lagging behind and certain centres have only just begun to implement SBRT into clinical practice.

1.4 Aims

The hypothesis of this work was whether IGRT could be safely implemented for clinical use in a busy oncology centre. The Beatson, West of Scotland Cancer Centre, as many centres in the UK are extremely busy and any development must be safe, of proven clinical benefit and optimised to minimise additional resource. The projects undertaken were to ensure that the implementation of IGRT fulfilled these criteria. It was also important to address issues that were of use to the wider wider international radiotherapy community's knowledge on IGRT in lung cancer.

The calculation of set-up errors at our centre, to facilitate all further investigation into IGRT is obviously the first step in this thesis. This was required to ensure the safety of any IGRT process. With a view to implementing 4DCT, there was an obvious paucity of papers discussing how to define the target in node-positive patients, so further work was required prior to use of 4DCT to ensure the method suggested of using the MIP image was safe. MV-cine offer a simple, method of verification, without additional radiation exposure, that is available to on all modern LinAcs and therefore of interest due to the safety and lack of impact on resource. Investigation into whether these fulfil a role in radiotherapy verification is of interest. AMTD is a topic that many centres around the UK have discussed implementing, and the VUMC have already implemented however, further studies are required to assess the robustness of this technique.

2. THE CALCULATION OF AN SITE SPECIFIC MARGIN FROM INTERNAL TARGET VOLUME (ITV) TO PLANNED TARGET VOLUME (PTV)

2.1 Introduction

Currently in The Beatson West of Scotland Cancer Centre, as discussed in the introduction during 3-D CT based radiotherapy of lung cancer, a combined margin from GTV to PTV of 15mm anteriorly, posteriorly and in both directions laterally and 20mm superiorly and inferiorly is used. This margin is to encompass microscopic disease, a population based margin for intra-fraction respiration induced tumour motion, and the set-up margin from ITV to PTV as suggested by the ICRU guidelines [19,20]. However, only the GTV to CTV margin for microscopic disease is quantified. Although Giraud et al. quantified a microscopic margin of 6-8mm, when this is used in combination with other margins in clinical practise, 5mm is most commonly used. As discussed in section 1.2.5, margins are not added linearly and it is up to the local centre how to combine the different margins. The general consensus worldwide is that when in combination with other margins, this margin should be 5mm. Neither the population based margin for intra-fraction respiratory induced tumour motion nor the set-up margin from ITV to PTV have ever been quantified in our centre. As a result, the amount of the combined margin that is allocated to each specific margin is unknown.

There are three main reasons why calculating the ITV to PTV set-up error is vital, especially in any study of IGRT.

1) Even without the study of IGRT, set-up errors vary from centre to centre. The verification techniques differ in the types of images used, how they are acquired and analysed, and the acceptance thresholds. . As a result set-up errors should be calculated on a centre-specific basis so that they are accurate and they are neither too small resulting in geographical miss, nor too big resulting in unnecessary irradiation of normal tissue.

2) As discussed above, one of the imaging technologies used in IGRT is 4DCT for planning, which allows the intrafraction respiration-induced tumour motion to be visualised so that the margin for this motion can be individualised. In 4DCT scans, the volumes delineated begin with GITV, which is grown to CITV for microscopic disease followed by a further margin for set-up error to create the PTV, as discussed in section 1.3.2. If the set-up margin from CITV to PTV is currently unknown, this needs to be calculated so that once a GITV has been delineated on a 4DCT scan, and the 5mm has been added for microscopic disease, an accurate set-up margin can be added to create the PTV.

3) As a result of different verification protocols and the corrections applied, the set-up error varies between centres. Online imaging with CBCT and kV imaging can be used to minimise the set-up error so that target coverage is improved and margins can potentially be reduced to spare more normal tissue. In order to implement CBCT and kV imaging, and to confirm these new imaging technologies are reducing the set-up errors from our current practice, it is necessary to estimate a baseline set-up error using our current off-line verification technique.

There are two margin recipes that are used widely. McKenzie et al. wrote extensively in a British Institute of Radiology publication on how to calculate the standard deviation of the systematic and random set up errors from iso-images. He derived an equation to calculate the set-up margin [23]. Van Herk et al. also published a margin recipe [22]. The McKenzie paper was used to calculated the standard deviation of the systematic and random errors in our department, and then used both the McKenzie and van Herk margin equations to calculate our site specific CITV to PTV margin.

2.2 Method

- McKenzie Publication

McKenzie discusses two aspects of the margin he has published. The first stage called the "treatment preparation" is to determine a volume large enough to contain the CTV in the majority of cases so that the defined volume will encompass the mean position in 90% of cases. This stage of delineation is primarily concerned with the intra-fraction tumour motion as a result of respiration. However, as 4DCT enables the GITV to be individually visualised and delineated it is not necessary to include this potential error in our margin and hence, this stage is not required. We therefore concentrated on the second stage of defining treatment margins which is to calculate an uncertainty of position as a result of set-up errors only. As there can be movement in three dimensions, the calculation has to be performed separately for lateral movement, superior/inferior movement, and anterior/posterior motion.

The McKenzie et al. equation to calculate CTV to PTV margin:

$$2.5 \, \Sigma + a + b + \beta(\sigma - \sigma p)$$

Symbol	Explanation
Σ	Standard deviation of the systematic error.
a	The photon beam algorithm error.
b	Motion of the target caused by breathing.
β	This depends upon the detailed beam configuration and is given in the publication.
σ	Standard deviation of the random error.
σp	The unblurred photon beam penumbra width.

How each parameter was calculated will be discussed in turn.

1) The Standard Deviation of the Systematic Error (Σ)

Σ represents the systematic errors that are incorporated into the margin in a Gaussian fashion. A number of potential systematic errors make up Σ and the value is calculated by adding these together in a quadratic fashion. Of these errors, the most significant one is the standard deviation of the systematic set-up error. The majority of the other errors mentioned such as a phantom transfer error, treatment planning system error and LinAC geometry error, are so insignificant that in the face of larger errors being added in a quadratic nature, they would have had no effect on the final value and were therefore not calculated. The only other systematic error that has the potential to be large and may have some effect on the final value is the interclinician variation error which will be discussed in some detail later.

To calculate the standard deviation of the systematic set-up error, a research radiographer reviewed pairs of AP and lateral MV orthogonal iso-images of 100 patients retrospectively. Each patient had between 2 and 10 iso-images each taken on different fractions for off-line verification. There were 412 images analysed in total. Reference landmarks were delineated on the DRR created from the planning CT and then on the iso-images. These reference landmarks were highlighted on the iso-images and compared to the same landmarks on the DRR produced at planning. The iso-image was shifted to match the DRR image as closely as possible. It is important to use reference landmarks that are immobile, or do not exhibit any interfraction patient motion, such as the paraspinal line, clavicle, trachea, thoracic wall and apex of lung [109,110]. The deviation from the iso-image position to the DRR position in all three directions, superior/inferior, laterally and anterior/posteriorly was noted. The above analysis was performed by the research radiographer, the accumulation of this data and all further analysis was performed by myself. All the deviation data was recorded in Microsoft Office XL Professional 2007, one page for each direction. To calculate the standard deviation of the systematic set up error, the following equation was used:

$$\Sigma \text{ set-up} = \sqrt{\left[\frac{P}{N(P-1)} \ \Sigma\, np\,(mp - m\text{ overall})^2 \right]}$$

Symbol	Explanation
Σ set-up	Standard deviation of the systematic treatment set-up error for all patients P in a given direction.
P	Total number of patients for which images were acquired.
N	Total number of images in study
np	Number of images taken for patient p.
mp	Mean set up deviation for patient P.
moverall	Overall mean population error. This is the mean systematic set-up error.

- The anterior / posterior standard deviation of systematic set-up error was calculated as: 3.0mm

- The superior / inferior standard deviation of systematic set-up error was calculated as: 3.0mm

- The lateral standard deviation of systematic set-up error was calculated as:

  2.9mm

The inter-clinician variation, which is the difference between GTVs drawn by clinicians, has been calculated in a number of papers and the figures vary widely [39,40]. There was an attempt to ask clinicians at our own centre to delineate the same patients so to enable site-specific inter-clinician variation to be calculated, but due to time constraints on our clinicians and the volume of additional delineation required to achieve any sort of meaningful figure, this was not possible. It became apparent after a few delineations that in lung cancer, the large inter-clinician errors do not occur as a result of discrepancies at the edges around the same agreed high density area or lymph node, but in deciding whether or not to include a lymph node in the volume or a blood vessel in the volume, or an area of opacified lung in the volume. This variation cannot easily quantified and added to a margin, as clinicians can identify gross tumour that lies centimetres away from the primary tumour in any direction and incorporating this would likely involve large margins in some directions that bear no relevance to the majority of patients. In order to assess whether this made a significant difference to the margin we calculated a margin with and without incorporating the error to enable us to decide whether it was feasible to incorporate this into the margin recipe.

To identify a figure for interclinician variation, as it proved impossible to calculate one at our centre, we conducted a literature search for an appropriate value. A literature search for "interclinician variation" and "delineation variation" was undertaken on "PubMed" and "ScienceDirect" for any papers regarding interclinician discrepancies within the last ten years. Steenbakkers et al. calculated the standard deviation of the interclinician discrepancies [24]. This paper was chosen as it had the largest number of

patients and radiation oncologists and it also had a wide range of tumour positions and stages. Eleven radiation oncologists were asked to delineate 22 patients. The radiation oncologists were given all the clinical information, all available pathology and the diagnostic scans and asked to delineate the GTV. The observer variation was computed in three dimensions by measuring the distance between the median GTV surface and each individual GTV. The inter-clinician discrepancy error, as described by Steenbakkers et al. was 4.2mm. This was with the use of PET/CT in planning as most patients are planned with the assistance of PET/CT scans at The Beatson, West of Scotland Cancer Centre.

The margins in all three directions were initially calculated without the inter-clinician error for the reasons given above. In this equation, the sole error to be incorporated into Σ was the standard deviation of the systematic set-up error. However in addition, the figure of 4.2mm was then incorporated in a further calculation to see whether incorporating this error would make a large difference to the final set up error.

2) Treatment planning system (TPS) beam algorithm error (a)

This is an error incorporated to allow for any error in the planning algorithm calculation. This would result in a systematic under dosing of the target by the linear accelerator beams therefore the margin for this error is added linearly. The 90% dose level is used to determine the correction. The TPS beam algorithm error when calculated on different systems falls between -2 to 2mm. 2mm was used in the equation as it is the maximum error that could occur and using 2mm would mean all potential error would be included in the margin.

3) Breathing positional error (b)

This is the amplitude of motion of the CTV caused by respiratory induced motion. As discussed above, we plan to address this error by using 4DCT where the GITV already encompasses an individualised margin for respiration induced tumour motion and hysteresis. We therefore used 0mm in the equation as this is already incorporated in the volume.

4) Planning Parameter (ß)

The value of ß depends on the different beam combinations. A table providing the different values for the planning parameter error is present in the document. The value chosen depends on the number of beams in use and gives different values for the error in transverse and superior / inferior directions.

- For a 3 field plan, as is routinely used for radical lung treatments, the value for (ß) in the superior / inferior direction is 1.64.
- For a 3 field plan, the value for (ß) in a transverse plane with beams not parallel and opposed is 1.04.

5) Treatment execution errors (σ)

The main two parameters that need to be combined in quadrature to give σ are the standard deviation of random set-up error and the penumbra width (σp)

To calculate the standard deviation of random set-up error, the same iso-images and deviations noted in the calculation of the systematic set-up error were used with the following equation to calculate the standard deviation of the random set-up error.

The McKenzie et al. equation for the standard deviation of the random set-up error is:

$$\sigma \text{ set-up} = \surd \left[\ \underline{\ \ \ 1\ \ \ }\ \Sigma\ \sigma_2 \text{ inter } (np - 1) \right]$$

$$N - P$$

Symbol	Explanation
σ set-up	Standard deviation of the random treatment set-up error for all patients P in a given direction.
P	Total number of patients for which images were acquired.
N	Total number of images in study
np	Number of images taken for patient p.
σ2inter	Standard deviation of the inter-fractional random treatment set-up error for patient p in a given direction.

- The anterior / posterior standard deviation of the random set-up error was calculated as: 0.8mm

- The superior / inferior standard deviation of the random set-up error was calculated as: 3.6mm

- The lateral standard deviation of the random set-up error was calculated as:

        2.7mm

6) Photon Penumbra Width (σp)

The penumbra is the area on the edge of the beam that can receive radiation from some parts of the source but not from the whole source. This depends on the diameter of the source, the source-skin distance and the collimated length. This was calculated by the on site Dosimetry Physicists using appropriate parameters for lung cancer plans. The penumbra width for a 10cm x 10cm field at 5cm depth was calculated as 8.5mm.

- <u>Van Herk Publication</u>

In order to validate the margin given by the McKenzie equation, a further margin was calculated using the van Herk equation:

$$2.5 \Sigma + 0.7 \sigma$$

2.3 Results

- <u>McKenzie Equation</u>

The results of the calculations using the McKenzie equation to calculate the CITV to PTV margin without adding the interclinician variation are:

In the anterior/posterior position:

Margin =   2.5 Σ + a + b + ß(σ – σp)

Margin =   (2.5 x 3.0) + 2 + 0 + 1.04 [√(8.52 + 0.82) – 8.5]

Margin =   9.5mm

In the superior/inferior position:

Margin =   2.5 Σ + a + b + ß(σ – σp)

Margin =   (2.5 x 3.0) + 2 + 0 + 1.64 [√(8.52 + 3.62) – 8.5]

Margin =   10.7mm

In the each lateral direction:

Margin =   2.5 Σ + a + b + ß(σ – σp)

Margin =   (2.5 x 2.9) + 2 + 0 + 1.04 [√(8.52 + 2.72) – 8.5]

Margin =   9.7mm

The same McKenzie equation was performed but this time incorporating 4.2mm as the value for inter-clinician variability as discussed above. The results of the further calculation are:

In the superior/inferior position:

Margin =   2.5 Σ + a + b + ß(σ – σp)

Margin =   (2.5 x √3.02+4.22) + 2 + 0 + 1.64 [√(8.52 + 3.62) – 8.5]

Margin =   16.1mm

- Van Herk Equation

The results of the calculations using the van Herk equation to calculate the CITV to PTV margin are:

In the anterior/posterior position:

Margin = 2.5 Σ + 0.7 σ

Margin = 8.1mm

In the superior/inferior position:

Margin = 2.5 Σ + 0.7 σ

Margin = 10.0mm

In the each lateral direction:

Margin = 2.5 Σ + 0.7 σ

Margin = 9.1mm

2.4 Discussion

These two equations are different and either can be used taking into account certain caveats. The Van Herk equation was calculated so that 90% of patients receive at least

95% to the CTV. In the McKenzie equation, the objective was to have a large enough margin between the edge of the incident radiation beam and the CITV that over the course of the fractionated schedule the accumulated dose is >95%. Both equations imagined the penumbra to be blurred. This blurring occurs due to the motion between the target and the beam, both due to day-to-day differences over the treatment course and target motion during a fraction. As a result both equations are only applicable to fractionated treatments and cannot be used in hypofractionated treatments such as SBRT. The main problem with the Van Herk equation is that it is calculated presuming the tumour is a perfect sphere, and treatment is entirely conformal. This results in a "fringe dose" where there is a background dose because of the penumbras of multiple other beams. McKenzie et al. address this by removing this fringe dose so that it can be applied with less beams and less conformal treatment hence calculation for an onsite penumbra. Despite these slight differences, it is reassuring to note the similar results obtained in both calculations.

The addition of the inter-clinician error resulted in a significant increase the margins. However, whether or not to use this larger margin has to be considered. One has to ask whether the incorporation of inter-clinician value will increase the likelihood of covering 90% of patients with a minimum dose of 95% as the two margins are designed to do. The inter-clinician variation in lung cancer tends to be whether or not to include a structure, rather than a delineation line falling a few millimetres symmetrically round an agreed structure. To incorporate this error would increase the margin by around 6mm however as different clinicians identify different areas of gross tumour that are usually more than 6mm from the primary GTV this addition is unlikely to improve tumour coverage. A true interclinician variation would be the estimate of the error drawing lines around agreed structures, these would be very small and added together in quadrature, would likely not influence the margin. We therefore plan to use the margin calculated without the incorporation of an inter-clinician variation error.

This work highlighted the need to improve interclinician variation within the department. Since this work was carried out there has been a planning meeting introduced where volumes are assessed by all clinicians. There is a radiologist and

nuclear medicine physician present to assist with the interpretation of images. There are also proposals being put together to import the PET images into the delineation system to reduce this further.

As most centres have improved their set up with online imaging, or use shrinking action protocol or the no-action level protocol, it is difficult to find papers using a similar off-line verification technique from recent years. However in 2001, Hurkmans et al. published a review of set up errors in the thoracic region. These were with different immobilisation techniques but prior to the advent of online imaging. The standard deviation of the systematic error ranged from 1.8mm to 5.1mm and the SD of the random error ranged between 2.2mm and 5.4mm. Our set up errors are on the better end of these figures, probably as a result of improved immobilisation and the vague, subjective off-line review technique that we use [111].

As most of the values calculated were 10mm +/- 2mm, and the fact it is easier in a large institution to have one value for all directions, consequently a margin of 10mm is recommended for set-up margin for further investigation.

3. THE USE OF THE MAXIMUM INTENSITY PROJECTION (MIP) FOR TARGET OUTLINING IN 4DCT RADIOTHERAPY PLANNING.

3.1 Introduction

As discussed in the introduction, the intra-fraction movement of lung tumours for radical radiotherapy is currently encompassed within the margin between the CTV and the ITV. With the traditional method of Helical CT scans for conformal planning, the intra-fraction movement, due primarily to respiration, cannot be quantified accurately, therefore a standard "population-based margin" is applied. The margin applied is crudely assessed for each individual patient in turn using fluoroscopy at the radiotherapy simulator and altered only if the tumour is obviously moving out with the PTV.

The system to create 4DCT's used in both centres where this work was carried out is discussed in detail in section 1.3.2 (page 20). Figure 3-1 illustrates this further. As is discussed, there are a few different images created; the phase bins of the different respiratory cycles, the MIP, the MinIP and the Ave-IP as seen in Figure 1-4.

Figure 3-1 An illustration of how the 4DCT scan is captured. The respiratory cycle is the motion of an external surrogate on the xiphisternum. During each respiratory cycle, 20mm of chest is imaged 10 consecutive times. Each image captured, taken at a different phase of respiration is demonstrated by the image-set names 0%, 10%, 20%.. to ..90%. During sorting of the images, all the images corresponding to a specific phase of the respiratory cycle (eg. maximum inspiration or 0%) are put on top of one another, to create an image-set of maximum inspiration that is in fact the combination of a large number of images taken over a large number of respiratory cycles. Ten different image-sets are created in this way representing different phases of the respiratory cycle.

One Respiratory Cycle
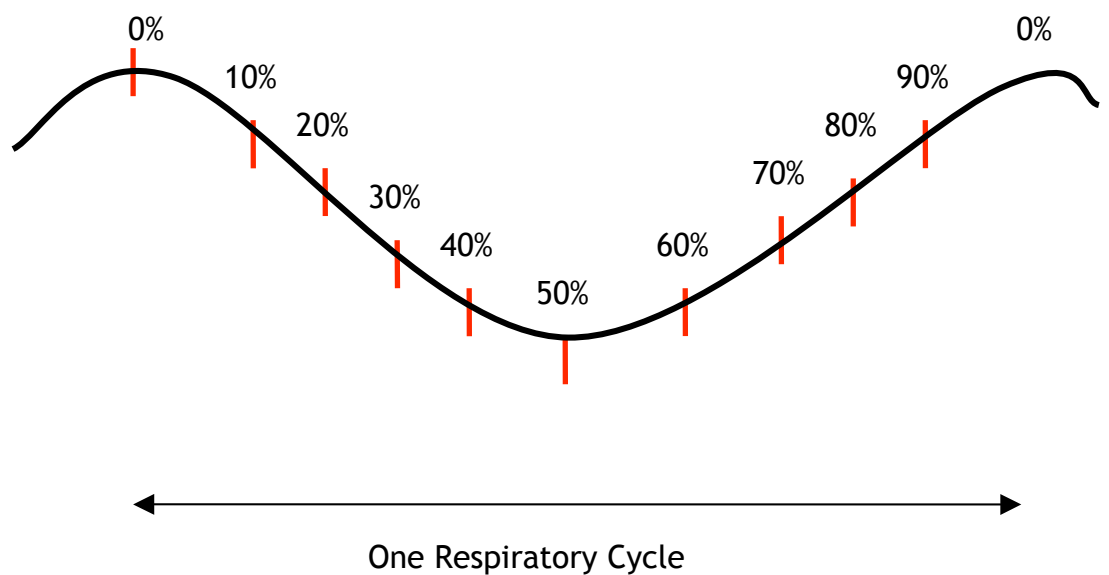
There have been various methods of creating a GITV or CITV from a 4DCT dataset reported. Whether it is a GITV or CITV depends on whether the clinician is delineating the gross tumour or the gross tumour with a margin for microscopic disease on the 4DCT. The first, most robust, but time consuming method, is to create a GTV or CTV on each of the 10 image-sets representing 10 phases of the respiratory cycle from the 4DCT dataset and combine these to create the GITV or CITV.

As radiotherapy centres implement 4DCT into planning, a limiting factor to clinical use is the time taken to delineate 10 scans for each patient. An alternative delineating method might be to use the MIP image set to create the GITV or CITV. One of the first questions that will be asked by centres implementing 4DCT is whether the GITV created using the MIP image, accurately represents the GITV or CITV. The advantage of this method is that once the MIP image set is produced, it comprises just one CT scan that should take no longer to volume than the current 3D helical scans. In a stretched radiotherapy centre such as the Beatson, this would obviously the ideal, we therefore elected to investigate the safety of this method further.

There is conflicting evidence in the literature regarding the use of MIPs for delineation. For Stage I lung tumours, Underberg et al. compared GITV_MIP (a GITV created using the MIP image) with GITV_10phase (a GITV created by making a composite of GTVs delineated on each of the 10 bins in turn) which is the gold standard method of delineation, in 12 patients [112]. They concluded that contouring of MIP scans was a reliable and fast clinical tool for generating GITVs. In the discussion, concerns were raised regarding the use of MIP in more advanced tumours. For node positive tumours, Ezhil et al. compared GITV_MIP to GITV_10phase in 27 patients with Stage I – III NSCLC [113]. They concluded that for all stages of disease, the GITV_MIP was significantly smaller in volume than the GITV_10phase.

As MIP is the most efficient method reported, we felt there was a lack of a comprehensive study to ascertain whether it is safe to delineate using the MIP, especially in node positive patients. Although the Ezhil et al. suggested the GITV_MIP is

smaller than the true GITV seen with GITV_10phase, this required additional confirmation. Consequently, it was elected to investigate whether the MIP image can be used in node-positive patients who constitute the majority of patients receiving radical radiotherapy.

3.2 Methods

CT image acquisition

All patients were routinely immobilised using a Sinmed Posirest Thoracic Board (Sinmed BV, The Netherlands) and a knee support prior to scanning on a GE Lightspeed RT 16 Multi-slice CT scanner (GE Healthcare, UK). Fifty millilitres of Omnipaque 300 intravenous contrast was administered by Stellant Contrast Injector. A helical scan was acquired followed immediately by a 4DCT taking a total <3minutes. Patients were asked to breathe freely throughout and scans covered the whole chest cavity.

4DCT scanning was performed using the Varian Real-Time Positioning Management System as described in detail in section 1.3.2 (page 20). Scanning parameters were set at 120 kV, 20mA with a slice thickness of 2.5mm. A block containing infrared-reflecting markers was placed on the patients' xiphisternum to monitor respiration. The motion of the block was captured by a camera fixed to the end of the treatment couch and a respiratory signal was displayed in the control room. For each patient the respiratory cycle was assessed. The cine-duration, which is the period of time for which the couch is static and images are acquired, was set as the mean respiratory cycle length for that patient plus 0.5 seconds. The X-ray tube rotation was set to 1/10th of the respiratory cycle length. In each static couch position, 8 contiguous slices of 2.5mm were acquired. The couch position was indexed by 20mm and the process repeated. Mean respiratory cycle lengths ranged from 2.9s to 7.9s. The helical scan acquisition time was about 18 seconds and the 4DCT acquisition time was about 90 seconds.

The 4DCT dataset was transferred to an Advantage 4D workstation (GE Healthcare, UK) where a software package was used to create 10 different scan sets relating to 10 sequential phases of the respiratory cycle, using the amplitude of the respiratory trace. These are labelled 0%, 10%, …. , 90%. The 4D software was also used to create a scan MIP from the raw data as described in section 1.3.2.

Patient Selection

This was a retrospective analysis for patients who had undergone both Helical and 4DCT for their radical radiotherapy planning. Fourteen consecutive patients, presenting to one consultant with radically treatable NSCLC, over a 4 month period, were studied.

Generating Target Volumes

The target outlining in all 14 patients was completed by the author. Helical scans were transferred directly from the scanner to the Varian Eclipse Treatment Planning System, software version 6.5 (Varian Medical Systems, Palo Alto, CA). The 4DCT was sent initially to ADW and once the creation of the respiratory bins had occurred, they were also transferred to the Varian Eclipse Treatment Planning System. The scans were viewed and outlined in the Beatson's standard mediastinal and lung window settings (-130HU to 200HU and -1000HU to -200HU, respectively). The CTV's of the primary tumour included all gross disease, with a margin added manually of approximately 3mm. Lymph nodes were included if they measured >1cm in diameter and were also given a margin of around 2-3mm to account for microscopic disease.

On the MIP image set, the gross tumour was delineated with a margin of ~3mm for microscopic disease. This created a CITV and was labelled CITV_MIP.

To create the composite volume from all 10 phases (CITV_10phase), each of the 10 phase image sets was contoured individually to create 10 CTVs. The images were all registered to a reference image, and CTVs from each phase were copied onto the reference image. Algebraic operators were used to create the CITV_10phase.

The MIP image was also registered with the reference image and the CITV_MIP was copied across so that it could be compared directly with the CITV_10phase.

Analysis of Target Volumes

The volumes of the two CITVs were compared by calculating the ratio between them. The regions on the scan where the volumes most differed were noted. Algebraic operators were used on the Varian Eclipse system to determine the volume of tissue enclosed by the CITV_10phase but not by CITV_MIP and, likewise, the volume of tissue enclosed by the CITV_MIP but not the CITV_10phase. The centre of mass co-ordinates (COM co-ordinates) of both volumes were recorded and compared.

Statistical Analysis

Wilcoxon signed-rank test, calculated on SPSS 15.0 for Windows, was used to compare volumes. A $p \leq 0.05$ was considered statistically significant.

3.3 Results

Tumour stages varied from Stage IB to Stage IIIB (Table 3-1).

Comparison of CITV_10phase to CITV_MIP

These results are presented in Table 3-2. In all patients the CITV_10phase was equal to or larger than the CITV_MIP. The mean ratio (+ S.D.) of CITV_10phase /CITV_MIP was 1.23 ± 0.17. The 95% confidence interval was between 1.13 and 1.32. The Wilcoxon Signed-Rank test showed there was a statistically significant difference between the two volumes ($p= 0.001$).

Table 3-1. Tumour Characteristics

Patient	TNM stage	Stage	Position
Patient A	T2 N0	Stage IB	LLL
Patient B	T2 N0	Stage IB	LUL
Patient C	T2 N2	Stage IIIA	RML. Partial collapse of RML
Patient D	T4 N0	Stage IIIB	Rt pancoast tumour
Patient E	T4 N2	Stage IIIB	Rt pancoast tumour
Patient F	T2 N1	Stage IIB	RUL. Collapsed RUL.
Patient G	T2 N2	Stage IIIA	RML. Adjacent to hilum
Patient H	T4 N2	Stage IIIB	LLL. Infiltrating pulmonary artery
Patient I	T1 N2	Stage IIIA	LUL. Adjacent to hilum
Patient J	T2 N2	Stage IIIA	RLL. Adherent to diaphram
Patient K	T2 N1	Stage IIB	RML. Adjacent to hilum
Patient L	T0 N2	Stage IIIA	Mediastinal recurrence following lobectomy
Patient M	T2 N1	Stage IIB	RUL
Patient N	T2 N1	Stage IIB	RML. Adjacent to hilum

LUL – left upper lobe. LLL – left lower lobe. RUL – right upper lobe. RML – right mid lobe. RLL – right lower lobe.

Table 3-2. Comparison of CITV_10phase to CITV_MIP

	CITV_10phase (cm3)	CITV_MIP (cm3)	Difference in Volumes (cm3)	CITV_10phase/ CITV_MIP
Patient A	37.0	36.8	0.2	1.01
Patient B	26.0	24.9	1.1	1.04
Patient C	140.1	116.2	23.9	1.21
Patient D	96.2	80.4	15.8	1.20
Patient E	67.2	52.2	15.0	1.29
Patient F	120.1	94.3	25.8	1.27
Patient G	111.4	91.5	19.9	1.22
Patient H	99.4	87.5	11.9	1.14
Patient I	112.5	87.3	25.2	1.29
Patient J	215.8	138.9	76.9	1.55
Patient K	71.2	63.2	8.0	1.13
Patient L	40.4	26.2	14.2	1.54
Patient M	51.7	39.0	12.7	1.33
Patient N	37.2	37.0	0.2	1.01
Mean +/- S.D				1.23 +/-0.17
Median				1.22
P-value				0.001

The median percentage of CITV_10phase, or potentially tumour tissue, which was not covered by the CITV_MIP, was 19.0% (range 5.5% – 35.4%) (Table 3-3). There was good agreement in delineation in areas where the higher density tumour adjoined lower density lung tissue. However, significant differences in delineation occurred where tumour adjoined the mediastinum or diaphragm i.e. where the tissue has a similar density to tumour. This is demonstrated in Figure 3-2. The median percentage of CITV_MIP that was not covered by CITV_10phase was 2.3% (range 0.4% - 9.8%) (Table 3-4). These areas were randomly distributed around the circumference of the volume and relate to very small displacements of the contour lines.

In the two patients with Stage I disease (Patients A and B), the CITV_MIP and CITV_10phase volumes were very similar with the ratios of 1.01 and 1.04 (Table 3-2). Only 6.8% and 5.5% of CITV_10phase was not enclosed by MIP (Table 3-3). These tumours were entirely surrounded by low density lung tissue and contour lines were again displaced by very small distances.

Comparison of COM co-ordinates

The COM co-ordinates and calculated displacement of centres are shown in Table 3-5. In the superior/inferior axis, medio-lateral axis and anterior/posterior axis the mean distance between co-ordinates was 0.15cm, 0.13cm and 0.07cm respectively. The mean (+ S.D.) displacement of the centres was calculated as 0.34cm (±0.31). There were 5 patients with a displacement of COM of ≥0.4cm. This level of displacement would cause a significant systematic error affecting ITV to PTV margin.

Table 3-3. The percentage volume covered by CITV_10phase that remained uncovered by CITV_MIP.

	Volume of CITV_10phase not encompassed by ITV_MIP (cm3)	Volume of CITV_10phase (cm3)	% of CITV_10phase not encompassed by ITV_MIP
Patient A	2.5	37.0	6.8
Patient B	1.4	26.0	5.5
Patient C	30.9	140.1	22.1
Patient D	11.6	96.2	12.1
Patient E	15.0	67.2	22.3
Patient F	23.1	120.1	19.2
Patient G	17.2	111.4	15.4
Patient H	18.0	99.4	18.1
Patient I	25.1	112.5	22.3
Patient J	76.4	215.8	35.4
Patient K	13.4	71.2	18.8
Patient L	13.0	40.4	32.2
Patient M	11.4	51.7	22.1
Patient N	2.5	37.2	6.6
Mean +/- S.D			18.5 +/- 8.5
Median			19.0

Table 3-4. The percentage volume covered by CITV_MIP that is uncovered by CITV_10phase.

	Volume of CITV_MIP not encompassed by CITV_10phase (cm3)	Volume of CITV_MIP (cm3)	% of CITV_MIP not encompassed by CITV_10phase
Patient A	1.3	36.8	3.6
Patient B	0.2	24.9	0.9
Patient C	2.0	116.2	1.7
Patient D	0.3	80.4	0.4
Patient E	2.5	52.2	4.9
Patient F	0.5	94.3	0.6
Patient G	0.5	91.5	0.5
Patient H	7.5	87.5	8.6
Patient I	1.9	87.3	2.2
Patient J	3.5	138.9	2.6
Patient K	6.2	63.2	9.8
Patient L	0.6	26.2	2.4
Patient M	0.7	39.0	1.7
Patient N	2.7	37.0	7.4
Mean +/- S.D			3.4 +/- 3.0
Median			2.3

Table 3-5. The COM Co-ordinates in the two different volumes (cm).

x= left/right axis, y= anterior/posterior axis, z= superior/inferior axis.

	CITV_10phase	CITV_MIP	Distance between centres
	x, y, z	x, y, z	(cm)
Patient A	3.5,1.5,1.3	3.9, 1.8, 1.3	0.45
Patient B	6.9, 8.1, -7.8	6.9, 8.1, -7.9	0.06
Patient C	-6.0,-4.2, 1.0	-6.2, -4.2, 1.0	0.23
Patient D	-6.7, 5.0, 11.7	-6.7, 5.0, 11.8	0.10
Patient E	-5.0, 1.5, 7.6	-5.5, 1.7, 8.5	1.05
Patient F	-3.7, -0.2, 6.2	-3.7, 0.0, 6.3	0.11
Patient G	-2.7, -0.1, 1.0	-2.7, 0.0, 1.1	0.13
Patient H	8.6, 5.5, -3.3	8.6, 5.5, -3.3	0.04
Patient I	5.2, 0.5, -0.1	5.5, 0.4, 0.2	0.45
Patient J	-7.0, -0.3, -2.2	-6.3, -0.1, -1.6	0.96
Patient K	-8.3, 3.0, 0.8	-8.7, 3.3, 1.0	0.53
Patient L	-0.9, -1.4, 4.8	-0.9, -1.5, 4.6	0.21
Patient M	-4.6, 1.5, 7.0	-4.8, 1.7, 7.0	0.25
Patient N	-5.8, -0.4, -3.6	-5.7, -0.4, -3.5	0.16
Mean ± S.D.			0.34 ± 0.31
Median			0.22

Figure 3-3. A coronal view of a planning 4DCT with CITV's created using different methods. The CITV_10phase is in cyan and the CITV_MIP in red. This demonstrates the high density areas missed by the CITV_MIP.
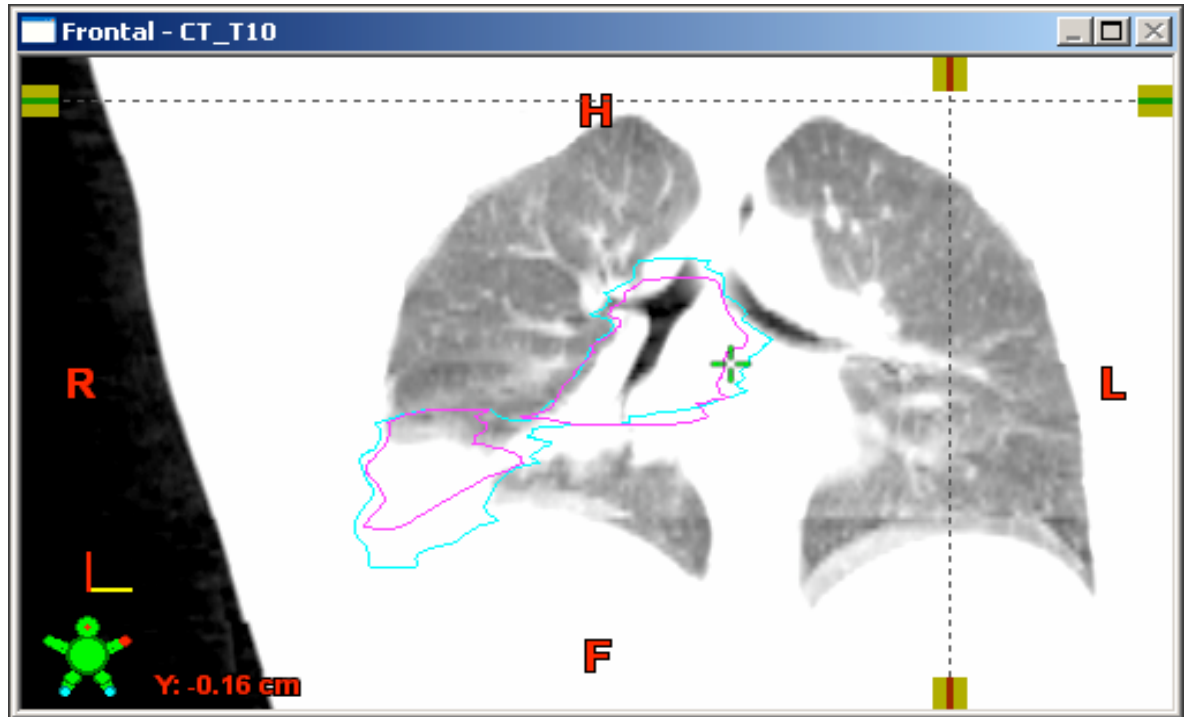
3.4 Discussion

This study suggests that CITV_MIP cannot be used for accurate delineation of Stage II-III tumours as there are significant volumes of tumour tissue, identified by the CITV_10phase, that are not encompassed by the CITV_MIP. In contrast, CITV_MIP could be used for Stage I tumours, but this is based on data from only two patients.

Although we have only limited data, and hence statistical findings may not be robust, 18.5% of uncovered tumour is sufficient to raise concerns regarding this method. Allowing for the fact there were only two Stage I patients it is reassuring to find the results in these patients are in keeping with the findings of Underberg et al., that an ITV created using a MIP image is reliable. The concerns regarding locally advanced tumours mentioned in that discussion are corroborated by this study. Figure 3-3, used to illustrate the problems with MIP in locally advanced tumours, resembles the image used in the discussion of the Underberg paper. It is reassuring to note that even given the different observers and patient group, the conclusion remains the same.

For those with experience in the use of 4DCT datasets, this is not a surprising finding. For most patients with Stage 1 NSCLC, a discrete tumour mass moves within much lower density lung tissue, allowing large differences in density providing obvious contour lines. In patients with Stage II-III, the tumour mass will be adjacent, at least on some boundaries, to tissue of equal density, such as mediastinum, chest wall or diaphragm. A boundary between tumour and normal tissue may be clearly visible on any individual phase scan. On the MIP image, boundaries become blurred. There is a natural tendency towards presuming that tissue is 'normal' unless there is evidence otherwise and so the extent of disease tends to be underestimated on the MIP. It is possible that individual nodes may not be identified. This is an important point to highlight to those beginning to use 4DCT, and a further discussion regarding alternative techniques will take place in more detail below.

The information from a diagnostic PET/CT was not available for this group of patients as it was not in routine use at the time of the planning scans. Although the use of PET/CT has a significant effect on inter-clinician variability, it should not impact on intra-clinician variability. As there is no consensus on what level of SUV, or percentage of SUV, constitutes the tumour edge [39,114] PET/CT should be used for localisation purposes rather than delineation. Although it may have highlighted different nodal groups, hence increasing the CITVs, the intra-observer variation would be the same, hence generating the same outcome.

The intra-observer variation goes some way to explain why in all cases the CITV_10phase is bigger than CITV_MIP. Intra-observer variations in PTV are reported to vary from $3.9cm^3$ to $95.8cm^3$ [115]. The algebraic method of adding volumes means that small drawing variations in different bins always forms a larger composite volume than if one volume alone was delineated as in CITV_MIP. As a result, small differences in CITVs such as $0.2cm^3$ or $1.1 cm^3$, as in the Stage I tumours, are likely due only to intra-observer variation, rather than a difficulty in delineating the tumour.

The creation of the CITV in the above manner with gross tumour and an additional margin of approximately 3mm, was adopted as a standard throughout all patients. For a more accurate addition of 5mm for microscopic disease, a GITV would be created with any of the below methods, and thereafter a margin of 5mm would be added to create the CITV. Although, for some, the method used in this study would not be standard delineation margins, what is important in the validity of the study is that the method used is consistent. As it is widely accepted that interclinician discrepancies remain high, there would be disagreement from some whichever method was used. The study remains valid as there was a consistent method used throughout all the delineation. The window levels were not according to EORTC guidelines however the same values were used throughout the study [116].

The major practical drawback to the use of ITV_10phase is the long operator time required. Delineation of 10 scans and creation of composite volumes takes on average

2.5 hours per patient and it is very desirable to reduce this time requirement. A number of alternative methods have been reported in the literature:

1) Ezhil et.al. [108] described the creation of a structure labelled ITV_MIP_Modified. The ITV was delineated on the MIP image and this volume was superimposed onto each of the 10 phases in turn, where it was modified by only enlarging boundaries when appropriate. The ITV_MIP_Modified was in close agreement with ITV_10phase. This could offer some time savings but remains a work intensive method.

2) A number of studies created an ITV from a composite of the two scans with the tumour in the most superior and inferior position [51,117]. There are a number of concerns with this method. This does not take into account lateral or anterior/posterior motion of the tumour nor hysteresis. There is also evidence describing the lack of correlation between the primary tumour and lymph node movement [118,119]. When selecting the two scans for delineation it may be that the primary tumour and involved lymph nodes are at their craniocaudal extreme positions in different scans. Care must also be taken to review the 4DCT cinescan in all planes. The method can be used if careful review of the 4D window cinescan takes place, in all planes, noting any areas of significant movement in other directions. A margin could be added to the ITV to PTV margin for the additional movement and hysteresis that takes place as above. Unless used with care and experience, this technique could lead to geographical miss of disease.

3) Wolthaus et.al. [120] reported a method for constructing a single CT scan from the 4D dataset which represents the tumour in its time-averaged position over the respiratory cycle (mid-ventilation scan). Whilst diaphragm movement could be used to quickly identify the mid-ventilation scan for Stage I tumours, for Stage II and III disease, delineation of all 10 phases was required, which is the time-consuming process we are trying to avoid.

4) Bosmans et al. [121] described a method where the 4D cinescan is used to identify the scan where the tumour is in its central position and measure the motion of the tumour in all three orthogonal directions. After delineating a CTV on the half ventilation scan individual margins are added which are calculated using

the motion seen on the 4D cinescan. The volumes created in this method are comparable in the above paper.

5) There are a number of other methods reported, using different imaging techniques for individualising margins including; slow CT [122], end-tidal breath-hold CTs [123], composite of 2 different helical scans in maximal inhale and exhale [124] and breath-hold CT [125], however each of these have their drawbacks and as software and systems have moved on, the 4DCT dataset is now regarded as the gold standard.

Although there is evidence that normal tissue irradiation is reduced and target localization improves with the use of individualized margins, it has to be noted there is a lack of clinical outcome data. As with the introduction of conformal radiotherapy, there is a general consensus within clinical circles that this constitutes an improvement from current techniques and a randomised control trial of 3D versus 4D planning scans may be difficult to recruit to on ethical grounds. Clinicians may feel 3D planning scan may constitute sub-optimal treatment. Hence a comparative study with outcome data and cost effectiveness data is unlikely to occur.

For Stage II and III disease, with the planning system Eclipse Version 8.4 (Varian Medical Systems, Palo Alto, CA) that was in use during this study, using a 4DCT was not possible in routine patients due to time limitations involved in delineating ITV_MIP_Modified or ITV_10phase. This was primarily because the different image-sets were not automatically registered and volumes could not be combined easily between different image-sets. However since the study was completed, there has been an upgrade to Version 8.6. This version has undergone significant improvements to software and permits automatic matching and registration across multiple image sets where they are already DICOM matched i.e. they have been acquired in the same scan process. In addition, it allows blending of different image-sets so volumes delineated on one image-set can be manipulated while viewing a different image-set. Since the implementation of Version 8.6 we have put together a protocol for delineation of Stage

II-III NSCLC which is very similar to ITV_MIP_Modified which we know from the literature is comparable to the gold standard of delineating all 10 phases.

The steps involved in delineation of a node positive tumour are as follows:

1) The 4DCT movie, created by running all 10 respiratory phases together, is reviewed on Eclipse 8.6.

2) The phases where the tumour is in the most extreme position in all 6 directions are identified. These often fall within the same 2 phases, representing expiration and inspiration but any number can be selected to ensure the extreme of position is captured.

3) All the delineating is saved onto the Ave-IP, as this is the image-set that will be used for calculation, although this image-set is never visualised.

4) The first image-set that was selected in step 2 is blended with Ave-IP, so that although the volume is being saved on Ave-IP, only the image-set selected is being seen, and a GITV is delineated.

4) In turn, all the image-sets selected in step 2 are blended with Ave-IP and the GITV is enlarged with each image-set to encompass all gross tumour in all phases of the respiratory cycle.

5) It is vital to remember that the GITV can only ever be enlarged. Although the gross tumour may not appear on the image-set being visualised, it has been present on a previously reviewed image-set as it has been included in the volume.

In conclusion, in the meantime, in our centre, in Stage 1 disease, if the tumour does not sit adjacent to high density structures, we propose the use of target delineation on the MIP image-set target. In Stage II-III disease, we will use the method described above.

4. FEASIBILITY OF MV-CINE FOR VERIFICATION OF INTRAFRACTION TUMOUR MOTION.

4.1 Introduction

In the past, small irregularities in intrafraction tumour motion were not so clinically relevant due to the fact offline verification protocols resulted in large margins and 3D conformal therapy plans lacked the conformality of IMRT plans. However recent changes in radical radiotherapy in lung cancer have resulted in the assessment and verification of intrafraction respiration induced tumour motion becoming increasingly important:

1) New, sophisticated planning and delivery techniques such as IMRT [126], stereotactic radiation therapy (SRT) [14] and Tomotherapy [127] can produce increasingly conformal treatment plans.

2) It is also known that these technologies are labour-intensive and can lead an increase in treatment times [128] which in turn increases the risk of intrafraction shifts in tumour position [68].

3) Due to the complexities of these delivery techniques concerns have been raised that therapy may be more error-prone [129].

The issue of verification of the intrafraction respiration induced tumour motion on treatment remains one for which there is no consensus. The relatively short duration of acquisition of 4DCT contrasts with the far longer duration of treatment delivery. All these factors have led to calls for the development of methods of independent verification of treatment delivery, in order to pick up the minority of patients with significant errors during treatment delivery [124].

Quality assurance in radiotherapy would improve if IGRT allowed for repeated verification of tumour position during treatment delivery, either directly or via other internal surrogates, during the delivery of the radiation. The position of the carina can

be used as an internal surrogate as previous work had shown a good correlation with total lung volumes [130] and recent studies have confirmed the correlation between the carina and 3D tumour position [131]. Real time tumour tracking using fiducial markers is not commonly performed, as insertion can be technically difficult, there is a significant risk of pneumothorax [81] and there are high drop-out rates after bronchoscopic placement [82]. Electronic portal imaging device (EPID) images have been used previously for off-line set up assessment as they enable the internal structures during treatment delivery to be visualized [132]. These MV images involve no extra dose to the patient and require no prolongation of radiation delivery. However, the limited image quality with MV imaging was previously considered a drawback. With recent advances in this imaging technology, megavoltage planar images have been re-evaluated using phantom studies. In their current form, megavoltage planar, kilovoltage (kV) planar, and cone beam computed tomography imaging systems, on a Varian linear accelerator, have been reported to be of sufficient quality as to allow for image-guidance approaches [133]. The possibility of using an MV cine-image, which refers to a number of consecutive MV image frames run together to create a movie, has been used together with and without implanted fiducial markers for quality assurance of gated treatment delivery [134,135].

The hypothesis was that if internal structures could be visualized on MV-cine without use of fiducial markers, review of these images could potentially provide off-line information on both intrafractional and interfractional motion, with no increase in treatment time or radiation dose. Preliminary data from patients supported this hypothesis [136]. The aim of the present study was three-fold: firstly to identify intrathoracic structures which could be visualized consistently during thoracic radiotherapy in stage III NSCLC; secondly, to identify factors which impaired the quality of MV-cine; and finally, to assess the residual motion of the same structure (internal surrogates) relative to motion observed on the planning 4DCT.

4.2 Materials and Methods

Radiation Planning and Delivery

This was a single-centre retrospective analysis of consecutive patients who had recently undergone radical conformal external beam radiotherapy for non-small cell lung cancer at the VU Medical Centre (VUMC). All such patients routinely underwent a 4DCT scan, performed on a GE Lightspeed RT 16 Multi-slice CT scanner (GE Healthcare, UK) with the use of a Varian Real-Time Positioning Management System (RPM; Varian Medical Systems, Palo Alto, CA) as described in section 1.3.2. In order to select patients the 4DCT was reviewed on the Advantage 4D workstation (GE Healthcare, UK) by a clinician. The maximum 2D movement of the tumour was measured in the coronal view of the movie with the straight line measuring device. Motion measurements were taken for the apex of the tumour, the inferior border of the tumour, the lateral edge of the tumour and the carina. The maximum tumour movement was noted as the largest of the three tumour vectors. Six consecutive patients with tumour movement of over 2.5mm were included in the analysis.

All patients had treatment plans, consisting of 5-10 fields using 6 or 15 MV photons. Routine daily patient positioning was performed using laser beams and On Board Imaging. Radiotherapy was delivered on a Varian 2300 C/D linear accelerator equipped with a 120 multileaf collimator, (Varian Medical Systems, Palo Alto, CA) to total doses of between 45Gy to 66Gy in fractions of 2-3Gy.

The key aspect of treatment is that it was delivered using 'Amplitude Monitored Treatment Delivery' (AMTD), an approach discussed in section 1.3.3, where the RPM trace is continuously monitored throughout treatment. Any increase in amplitude over the amplitude threshold set at the planning 4DCT causes the radiation beam to temporarily stop. AMTD delivery minimizes the likelihood of a systematic difference between intra-fraction tumour motion, at 4DCT and during treatment delivery.

MV-cine were collected from all gantry angles unless two fields had the same gantry angle, in which case the field with the largest dimensions was selected on the EPID system. The EPID system consists of an image detection unit (IDU) featuring detector and accessory electronics, an image acquisition unit containing drive, acquisition

electronics and interfacing hardware, and a dedicated workstation for off-line image review (Portal Vision 6.5, Varian Medical systems). The IDU matrix consist 1024 x 768 pixels (pixel size: 0.39x0.39mm) enabling a 40 x 30 cm2 sensitive area at 145 cm source detector distance, i.e. 27.5 x 20.7 cm2 with typical 100 cm isocenter-based radiation techniques. During all MV cine acquisition procedures clinical beam parameter settings were used (6 MV photon energy; dose rate setting 600 MU/Min.). MV cine imaging supports fast image capture of 7-8 image frames per second. Figure 4-1 demonstrates an MV cine-image with the tumour highlighted.

Retrospective assessment of MV images

From each of the first 6 patients selected for review, MV-cine of four consecutive fractions were analyzed. To create the MV-cine, initially they were exported, in DICOM format from the patient data base system (ARIA Version 8.5, Varian Medical Systems, Palo Alto, CA) to the station's hard-drive. Software developed in-house for the ImageJ program was used to resolve the time order for DICOM-based images in exported stacks. ImageJ is a Java-based image processing package (http://rsb.info.nih.gov/ij/) that was run under the Windows XP operating system on a Pentium 4 processor with 2 GB on board access memory.

- AIM 1: Identification of intrathoracic structures in treatment fields

Two independent observers, the author and one research physicist, reviewed one fraction of radiation belonging to each patient. They were asked if they could identify the carina, the hilum and the tumour mass respectively in each field. Only if both parties where confident the structure could be identified was the structure noted as identifiable. The Beams Eye View (BEV) of the treatment plan with the different structures highlighted was available for assistance in identifying structures.

- AIM 2: Factors which impaired the quality of MV cines images

To identify characteristics of MV-cine that limited their use, when structures could not be identified, the observers were asked to document the reasons for this. To assess the minimum number of MU's necessary to encompass a whole breathing cycle, MV-cine

were also assessed to see whether a complete respiration cycle had occurred during the movie and compared to the MU's used. Without an entire breathing cycle, internal structure movement would be underestimated, and therefore there is limited value in analyzing these images.

- AIM 3: Comparison of motion of a structure on MV cine-image versus motion on 4DCT.

Finally, the two-dimensional (2D) motion path for several thoracic structures on MV-cine images, were measured offline using experimental research software (RPM-Fluoro tool kit version 0.7.5, Varian Medical Systems, Palo Alto, CA). The 2D motion path is calculated by highlighting the internal structure on the first frame of the MV cine-image with a reference box and using the markerless tracking tool. The reported 2D distance the internal structure moved is the beam's eye view 2D displacement of markers from their expected home position. See Figure 4-2 for a flow chart on creation of MV cine-image and analysis of movement.

Figure 4-1. Megavoltage image with tumour mass highlighted.
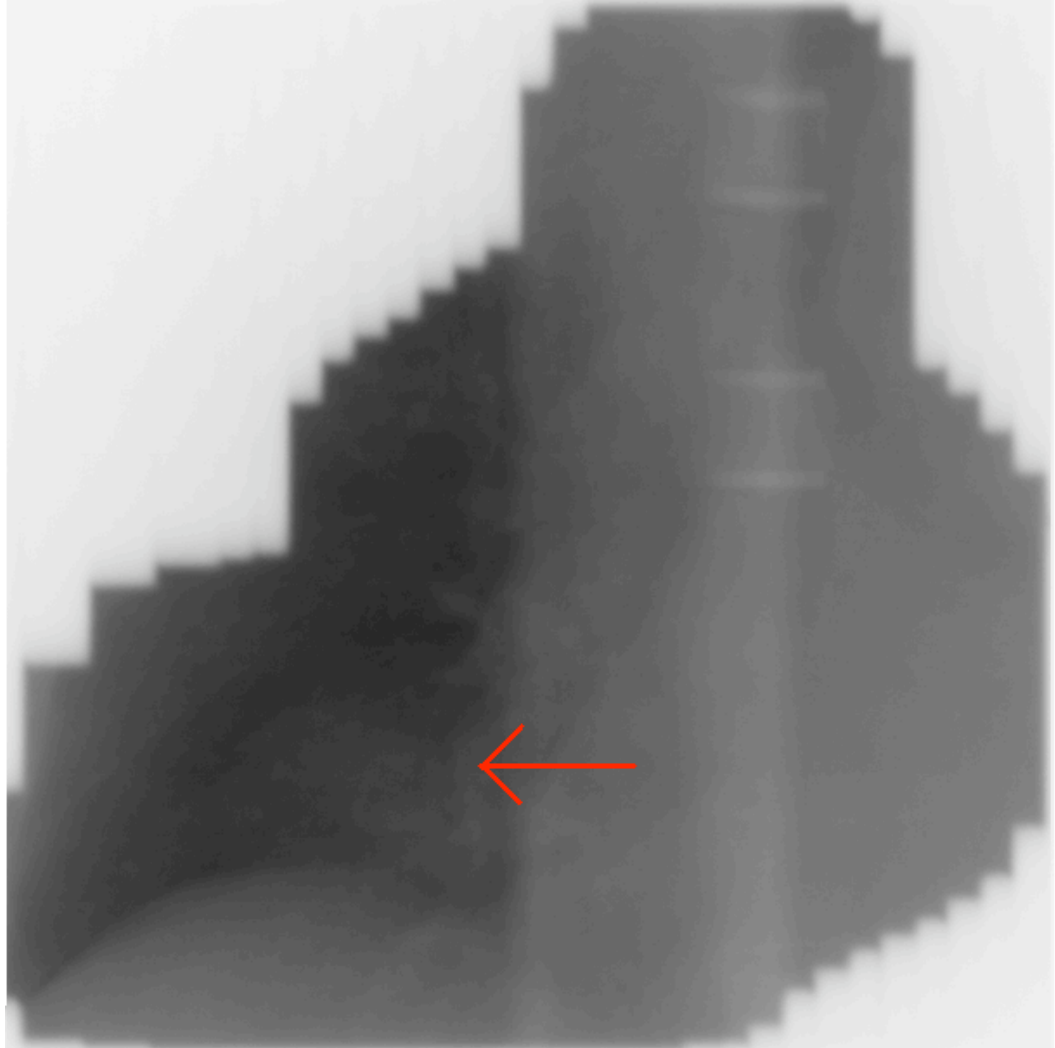
The RPM-Fluoro Tool

A research software tool, the RPM-Fluoro Tool (Varian Medical Systems, Palo Alto, Ca) was used to quantitatively assess the motion of all three internal structures. The RPM-Fluoro Tool was installed on same independent station hard-drive as the MV-cine. To review a MV cine-image and to calculate motion, the relevant MV cine-image file was selected from hard-drive. This toolkit is able to track obvious soft-tissue targets without the need for implanted marker seeds. The markerless registration and tracking method is based on spatial template matching. Because the target appearance in radiographic images is often quite different at different breathing phases, reference images should generally capture target motion over the whole breathing cycle. For each incoming frame the registration algorithm goes through a subset of reference images to find a best spatial match. Figure 4-3 demonstrates screen-shots of the RPM-Fluoro Tool with each of the internal structures highlighted with a reference box.

Two short assessments were made of the RPM Fluoro-Tool. Firstly there was a phantom assessment to validate the measurements it produced, then an assessment for an operator difference.

1. Phantom assessment

An initial assessment of the RPM Fluoro-Tool was performed to validate measurement, using a QUASAR TM programmable respiratory motion phantom (Modus Medical Devices, London, ON, Canada). QUASARTM phantom consists of a programmable stepper motor with a stage, an acrylic body oval, and a cylinder insert that moves in superior-inferior directions in the body oval. Motion of the insert is manually set using visualization of a gauge and synchronized with the vertical movements of the stage that surrogates chest wall motion with 1cm default amplitude. Tumour motion was simulated with 20mm peak-to-peak amplitude with cycle duration times of 4 sec, and MV-cine were acquired using 100 MU with the same EPID system as described above using clinical settings. The MV-cine collected 2.5 respiratory cycles of the moving insert. Motion was assessed using the RPM-Fluoro Tool as described above and repeated ten times in order to assess measurement accuracy of toolkit with respect to mechanics of the phantom and the used MV-cine imaging procedure. An identical storage system to that used with clinical

Figure 4-2. Flowchart of steps required to produce an MV cine-image.

MV-cine exported from Aria Version 8.5 to computer hard drive.

MV-cine imported into ImageJ for sorting into chronological order on computer hard drive.

MV-cine opened in RPM Fluoro Tool.

Reference Box placed around internal structures using RPM Fluoro Tool and motion calculated.
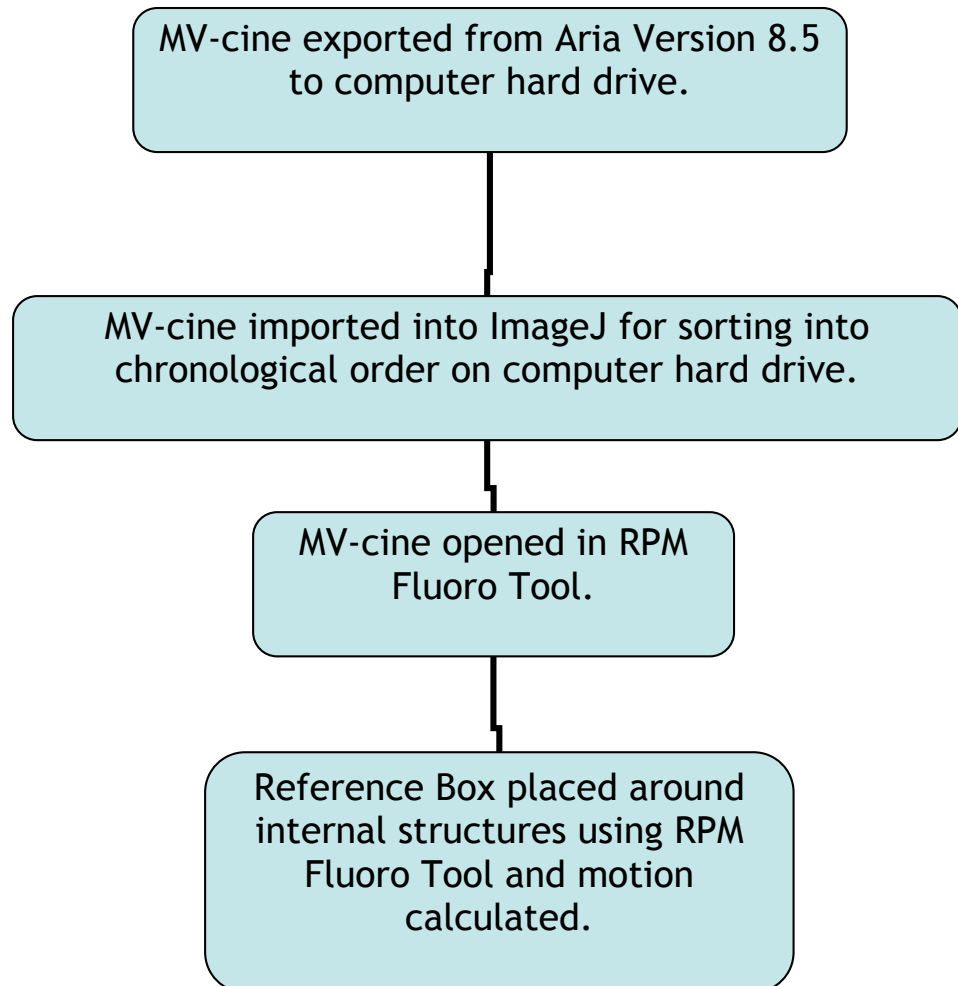
Figure 4-3. Screen-shots of the RPM-Fluoro Tool with each of the internal structures highlighted with a reference box. From the top; primary tumour, carina and hilar structure respectively.
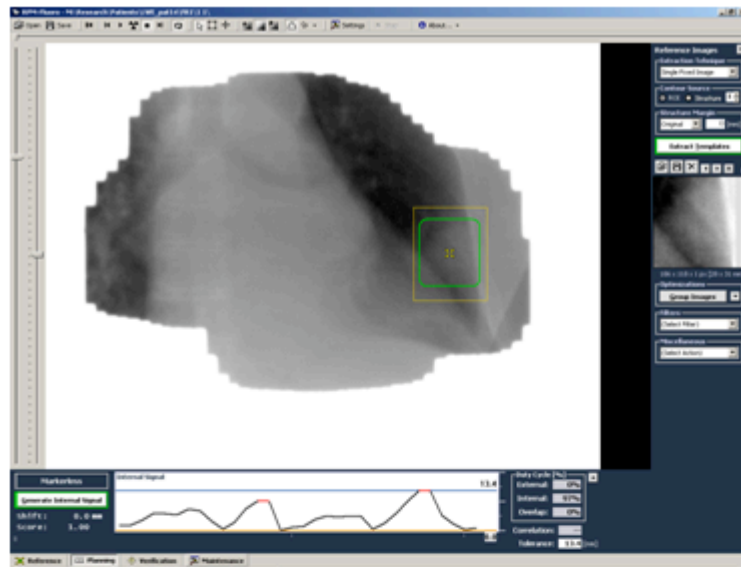
(a)
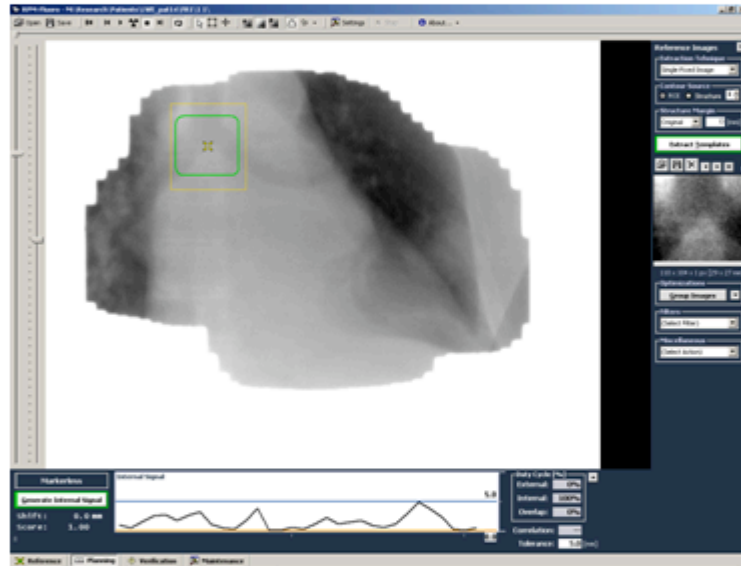
(b)
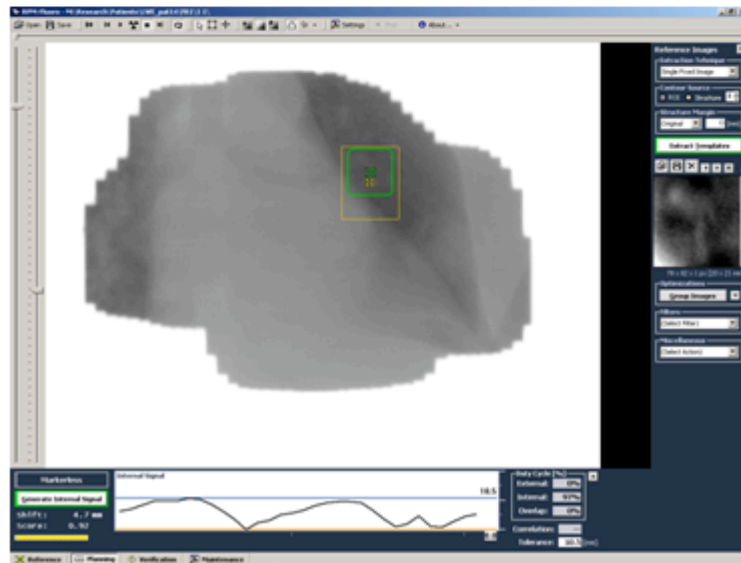
(c)

cine-images was used with an average image of every two frames (image pairs) making up the MV cine-image.

2. Assessment of interclinician variability in motion calculation.

The results derived using the tool with two different users were assessed. The motion of the primary tumour, hilum and carina were assessed in 6 MV-cine by two independent observers. A patient with significant motion was selected so that the potential for differences in motion would be larger. The two different motion measurements for each structure in each cine-image were compared to ensure the tool was not user dependent.

4.3 Results

RPM-Fluoro Tool Analysis

The mean peak-to-peak amplitude of the phantom measured from 20 imaged full respiratory cycles was 19.5 mm (range 19.3 to 19.7mm). There are a number of factors which may affect this result. As discussed above the predefined motion of the phantom was manually set using a gauge that will introduce a small offset value. In addition the standard deviation of 0.16 mm is smaller than the pixel dimension 0.26mm at 100cm isocenter level. The range in measurements are likely introduced due to measuring object position from averaged image pairs, as depending on the velocity of object, the average image will show slightly variable blurring. Taking all these effects into account we felt confident the RPM-Fluoro Tool accurately measured the motion of object on MV-cine.

The mean difference in tumour, hilar structure and carina motion between the two observers was 0.4mm (range 0.0 to 0.9mm), 0.6mm (0.1 to 1.0mm), 0.3mm (range 0.1 to 0.8mm) respectively. None of the analyses demonstrated a difference in structure motion between observers larger than 1mm.

The Clinical MV-cine Analysis

Six patients with either stages IIIA or IIIB lung cancer were identified for the analysis, and tumour characteristics are summarized in Table 4-1.

- AIM 1: Identification of intrathoracic structures in treatment fields

Each treatment plan consisted of between 5 – 10 fields. In the six patients there were a total of 25 fields. These 25 fields were assessed on 4 consecutive days, so in total 100 MV-cine were assessed.

The most commonly recognizable structure was the carina, which was situated within 96 of the fields. With the guidance from the corresponding digitally reconstructed radiograph (DRR), the carina was identifiable in 80 of the 96 MV-cine (83%). The primary tumour mass could be identified in 68 of the 100 cine-images (68%). The hilum

was situated in 88 fields and could be identified in 64 (73%). It is important to highlight that in this group of patients, 4 of the 6 patients had hilar tumours, which may have resulted in the hilum being more readily visible. There were 60 oblique fields. In these fields, the carina was visible in 80%, the tumour mass in 32% and the hilar mass in 50% of the fields it was situated in.

Table 4-1. Patient Characteristics

	Tumour Stage	Nodal Stage	Primary Tumour maximum diameter (cm)	Location	Total Dose (cGy)	Dose per fraction	No of Fields
Patient 1	T4	N3	7.2	RMZ	4500	300	5
Patient 2	T3	N2	4.2	RMZ	6000	200	10
Patient 3	T3	N2	7	RMZ	6600	200	5
Patient 4	T4	N2	11	RMZ / RLZ	6000	200	7
Patient 5	T3	N2	5.8	RMZ	5775	275	5
Patient 6	T3	N2	7.5	LMZ	4500	300	5

LMZ – left mid zone. RMZ – right mid zone. RLZ – right lower zone.

- AIM 2: Factors which impaired the quality of MV cines images

Among the factors which limited the ability to visualize the carina were a dense mediastinal shadow of similar density, MLC obliterating almost the entire field and a 60 degree dynamic wedge obliterating the field before any structures could be visualized. Although the placement of a treatment bed bar over a structure did not inhibit identification, it prevented the assessment of structure movement. The RPM Fluoro Kit follows the densest object in the reference box and with an immobile treatment bed bar, it continuously registered no movement.

Of the 100 cine-images, the number of breathing cycles visualized using the RPM fluoro tool could be assessed in 91. Respiratory motion could not be visualized in five cine recordings due to all the visible movement being due to heartbeat and in four cine-images of the same field, due to the MLC taking up almost the entire field. Of these 91 fields, 70 included at least one complete respiratory cycle (77%). The median number of intra-fraction respiratory cycles observed was 2 (range, 1-6). Of the 21 fields that did not include a whole breathing cycle, 16 had <30MU in the field, in 4 although there were 40MU, a 60 degree wedge obliterated the field before any assessment could be made. In summary, without a wedge present, any field with >30MU's is likely to include an entire breathing cycle.

- AIM 3: Comparison of motion of a structure on MV cine-image versus motion on 4DCT.

The median 2D movement of the primary tumour was 5mm (range, 1 – 15mm) [Table 4-2] in comparison to the median movement of the primary tumour on the 4DCT of 10mm (range, 7 – 15mm). The median 2D motion of the carina in all assessable fields during AMTD was 3mm (range, 1 – 10mm) [Table 4-3] in comparison to the median 2D motion measured on the 4DCT's of the same patients, which moved 7mm (range, 4- 10mm).

Table 4-2. Two-dimensional intra-fraction tumour motion (mm) during delivery of Amplitude Monitored Treatment Delivery.

		Intra-fraction Tumour Motion during Amplitude Monitored Treatment Delivery (mm)							
		Fraction 1		Fraction 2		Fraction 3		Fraction 4	
	4DCT motion	Mean	S.D.	Mean	S.D.	Mean	S.D.	Mean	S.D.
Patient 1	6.9	6.6	1.8	4.6	1.0	4.6	0.8	4.4	0.8
Patient 2	6.5	1.6	0.6	2.2	0.9	2.6	0.2	2.0	0.3
Patient 3	7.8	9.4	3.7	6.2	2.3	9.1	0.8	7.3	2.9
Patient 4	9.8	11.0	3.9	5.3	0.3	5.2	1.3	9.9	2.4
Patient 5	15.0	8.7	1.6	10.0	1.4	8.9	0.1	7.4	1.0
Patient 6	10.5	5.7	1.1	3.8	0.3	7.0	2.3	7.6	1.4

Table 4-3. Two-dimensional intra-fraction carina motion during delivery of Amplitude Monitored Treatment Delivery.

- 95 -

| | | Intra-fraction Carina Motion during Treatment Delivery | | | | | | | |
| | | Fraction 1 | | Fraction 2 | | Fraction 3 | | Fraction 4 | |
	4DCT motion	Mean	S.D.	Mean	S.D.	Mean	S.D.	Mean	S.D.
Patient 1	3.7	2.3	0.9	2.4	1.2	2.2	0.5	1.9	0.9
Patient 2	6.9	1.9	0.7	2.3	0.3	2.5	0.8	1.6	0.4
Patient 3	10	6.8	2.1	5.4	1.5	6.4	1.9	4.2	1.9
Patient 4	7.8	3.4	0.9	3.0	0.4	4.1	1.1	2.8	0.1
Patient 5	7	3.8	3.1	3.9	0.4	2.5	0.9	4.0	3.1
Patient 6	5.6	1.3	0.0	1.6	0.8	1.9	0.9	1.5	0.6

4.3 Discussion

This study shows that intrathoracic structures can be visualized in MV-cine for a significant proportion of patients undergoing radiotherapy for stage III lung cancer, both in AP and oblique fields. The frequency with which structures were identified was higher than is generally expected. This may be due to the images being cine-images rather than single frames as both observers noted that the identification of structures was significantly easier with the cine-image rather than single frames. The use of the BEV also contributed to a higher identification rate. This is similar to having the structures superimposed onto the cine-image which is routine practice in other verification images.

Factors which impair the ability to identify structures on MV images were identified and these included selection of dynamic wedge angles above 60°, fields with large quantities of MLC, and delivery of ≤30MU. The position of the treatment bed bar limited the assessment of internal structure movement. We are continuing to collect data on MV-cine; these guidelines have enabled us to only image fields that will allow motion assessment.

The use of the RPM fluoroscopy tool permits calculation of intrafraction motion of these internal structures. In order for MV-cine to be used as an independent verification tool, other motion must be assessed such as interfraction motion and set-up error. This can currently be assessed by superimposing structures from the planning scan onto the MV cine-image and making manual measurements, however it is a time-consuming, complicated process. In order for MV-cine to be used routinely as an independent verification tool, assessing inter and intra fraction motion as well as set-up variation, significant software development would be required to streamline this process. As this was only an explorative study, only observations can be made on the analysis of internal structure movement. 4DCT remains a snap shot of tumour motion and it is therefore reassuring to see that the majority of intrafraction motion on treatment was less than the motion visualized in the 4DCT. This is reassuring because if the 4DCT over

estimates intrafraction motion, and as a result a larger margin and more adverse effects occur, at least there is no geographical miss of the tumour due to underestimation of tumour motion at 4DCT. One can speculate as to why intrafraction motion is less on treatment than during 4DCT. It is possible that patients are more anxious during the 4DCT as it is their first visit to the department and they are unsure of proceedings. This may result in a slightly increased tidal volume, increasing tumour motion. As they attend daily, their anxiety disappears and as a result their tidal volume and tumour motion. These are speculations however the reason for this fall in motion requires further investigation. It must be noted that in this study, AMTD may have prevented unusually large respiration cycles from being treated. In centres where AMTD is not routinely used, this verification tool would highlight those patients with unusually shallow breathing at 4DCT scanning, resulting in a systematic error due to underestimation of tumour movement. It is also of interest to note that different fields provided different amounts of movement, indicating that analysis of motion on MV-cine from one field alone is not necessarily representative of all the treatment. With the knowledge of the factors that allow a good MV cine-image, the VUMC are continuing to collect data in a larger group of the lung cancer patients in order to draw some conclusions on intra-fraction motion.

Although the use of techniques such as IMRT do not support acquisition of MV-cine, such plans can be adapted to include at least one non-IMRT AP field which would allow the capture of MV images as a verification tool [137].

In conclusion, internal anatomy can be reliably identified using MV-cine of the thorax. This allows for residual motion to be measured during the delivery of image-guided radiotherapy. Our analysis highlights the potential of these images for use as an independent verification tool but in order for quick-step assessment of the tumour intrafraction and interfraction motion, as well as setup variation, significant software development is required.

5. AMPLITUDE MONITORED TREATMENT DELIVERY (AMTD): A RESPIRATORY-MOTION MANAGEMENT TECHNIQUE AIMED TO LIMIT VARIATIONS IN INTRA-FRACTION MOTION BETWEEN PLANNING AND TREATMENT DELIVERY.

5.1 Introduction

In patients whose tumours show significant respiration-induced motion, 4DCT identifies those who may benefit from respiratory-gated radiotherapy (RGRT) by identifying potential windows within the respiratory cycle, for gated-delivery [87,138]. However, this form of RGRT is not suitable for all patients. There is a clinical benefit in only a minority of patients, whose tumours show significant motion [139]. In addition a regular respiratory cycle is required and although the reproducibility can be improved on with respiratory coaching [140], it remains unachievable for some patients.

In order to exclude the possibility of acquiring non-representative motion data on the 4DCT, as well as to overcome limitations of traditional forms of RGRT, the VUMC implemented a novel form of respiratory management 'Amplitude Monitored Treatment Delivery' (AMTD) which is illustrated in Figure 1-7. This approach is essentially respiratory gating with a larger duty-cycle, where the radiation is delivered while the intra-fraction surrogate motion is equal, or less, to what was recorded at 4DCT and automatically withheld when the intra-fraction motion exceeds that seen at 4DCT. AMTD aims to limit the possibility of a geographic miss arising when a larger tumour amplitude occurs during treatment delivery, than what was observed in the planning 4DCT.

In the feasibility study of MV-cine, the MV-cine images demonstrated that in the majority of patients there was more motion on the 4DCT than on the MV-cine, which is preferable as it prevents geographical miss. As we have now confirmed that MV-cine can be used to monitor motion, and have identified the limiting factors so they can be avoided, we embarked on a project to verify the use of AMTD using MV-cine images.

The implementation of the AMTD technique is described and MV-cine images were collected and analysed to verify the AMTD treatment.

5.2 Materials and Methods

Patient selection, image acquisition and target definition

Data from twenty consecutive patients who completed AMTD treatment for node-positive, non-small cell lung cancer at the VUMC, Amsterdam, The Netherlands, were retrospectively analyzed. Patients are eligible for AMTD if their primary lung tumours showed limited motion (generally ≤10 mm) on 4DCT scan, or if the tumour motion exceeds 1cm but they are unable to maintain a regular respiratory cycle despite respiratory coaching. For those patients with tumour motion ≥1.0 cm and/or when a reduction in the volume of lung tissue receiving threshold doses of 20 Gy (V20) is expected with phase gating at end-inspiration lung volume, phase-based gated delivery is employed. In three of the 20 patients, the maximum motion of the primary tumour exceeded 11 mm (13.2-13.8 mm), but the patients were unable to maintain a regular respiratory cycle hence AMTD treatment was chosen. Patient characteristics are summarized in Table 5-1.

All patients undergoing high dose thoracic radiotherapy at the VUMC undergo a single 4DCT scan on a GE Lightspeed RT 16 Multi-slice CT scanner (GE Healthcare, UK) during quiet uncoached respiration as previously described in Chapter 4.2. The respiratory waveform is co-registered using the Varian Real-Time Positioning Management System (RPM; Varian Medical Systems, Palo Alto, CA). The 10 phases of the 4DCT were created and reviewed on the Advantage 4D workstation (GE Healthcare, UK). All phases where the tumour or lymph nodes lie in the extremes of motion were identified and used to create a gross tumour volume encompassing the tumour in all phases of the respiratory cycle on Eclipse Planning System (Varian Medical Systems, Palo Alto, CA). Subsequently, a margin of 5mm was added for microscopic disease and 5mm for set-up error was

Table 5-1. Patient characteristics.

	Tumour Stage	Nodal Stage	Tumour Size (max. diameter in cm)	Location	Total Dose (cGy)	Dose per fraction	No of Fields
Patient 1	T4	N3	7.2	RMZ	4500	300	5
Patient 2	T3	N2	4.2	RMZ	6000	200	10
Patient 3	T3	N2	7	RMZ	6600	200	5
Patient 4	T4	N2	11	RMZ / RLZ	6000	200	7
Patient 5	T3	N2	5.8	RMZ	5775	275	5
Patient 6	T3	N2	7.5	LMZ	4500	300	5
Patient 7	T4	N1	7.8	LMZ	6600	200	5
Patient 8	T4	N2	10.35	LMZ	5000	200	6
Patient 9	T4	N2	11.8	LMZ	4500	300	6
Patient 10	T2	N2	2.8	RMZ	6000	200	7
Patient 11	T2	N2	5.75	RMZ	6000	200	6
Patient 12	T2	N2	4.3	LMZ	6000	200	6
Patient 13	T4	N3	5.7	RLZ	6000	200	5
Patient 14	T4	N3	9.15	mediastinal	4600	200	5
Patient 15	T3	N2	9.15	RUL	6600	200	7
Patient 16	T3	N2	5.3	LLL	6600	200	6
Patient 17	T4	N3	5.19	LMZ	5000	200	5
Patient 18	T1	N2	1.8	RMZ	5000	200	7
Patient 19	T3	N1	8.5	RUL	5000	200	4
Patient 20	T4	N1	7.3	RUZ	6600	200	4

added to create the planned target volume (PTV). All patients have treatment plans consisting of 5-10 fields using 6 or 15 MV photons.

Treatment delivery

Radiotherapy was delivered on a Varian 2300 C/D linear accelerator equipped with a 120 multileaf collimator, (Varian Medical Systems, Palo Alto, CA) to total doses of between 45Gy in pre-operative cases to 66Gy in radical cases, in fractions of 2-3Gy.

During treatment delivery, no form of respiratory coaching was undertaken as a regular wavelength and amplitude are not required for AMTD treatment. Patient positioning was performed using laser beams and either an orthogonal pair of kV images, taken in the anterior-posterior and lateral position, or kV cone-beam CT (CBCT) images. An online bony match was performed followed by a shift to eliminate the disparities. The original volumes are superimposed on the images and a visual check was made to ensure the tumour lay within the GTV. The RPM system was used to record a respiratory waveform. On each treatment day, the end-expiration position of the respiratory trace was programmed as the baseline for the amplitude threshold. The maximum amplitude of the respiratory trace observed at the time of 4DCT was specified as the maximum acceptable respiratory trace amplitude during treatment. During delivery, if the respiratory trace amplitude exceeded the maximum acceptable amplitude, the linac was programmed to automatically turn off. Once the respiratory trace fell back between these points, irradiation was resumed.

Intra-fractional image acquisition

The acquisition of MV-cine is identical to that described in section 4.2 with a step by step illustration of the steps involved in the production of MV-cine in Figure 4-2.

During all clinical MV-cine acquisition procedures, clinical beam parameter settings were used (6 MV photon energy; dose rate setting 600 MU/min). MV-cine imaging supports fast image capture of 7-8 image frames per second. The beams that would give the best image quality were selected by using fields closest to gantry angles 0 or

180 degrees, with large dimensions, large numbers of monitor units and minimal wedges. For storage purposes every two frames were saved as an average frame. This prevented overload of the hard drive on which the images were saved.

Six MV-cine from different fractions were randomly selected and analysed for each patient. Initially they were exported, in DICOM format from the patient data base system (ARIA Version 8.5, Varian Medical Systems, Palo Alto, CA) to an independent station's hard-drive. Software developed in-house for the ImageJ program was used to resolve the time order for DICOM-based images in exported stacks. ImageJ is a Java-based image processing package (http://rsb.info.nih.gov/ij/) that was run under the Windows XP operating system on a Pentium 4 processor with 2 GB on board access memory.

The number of available respiratory cycles captured in each MV cine-study was noted.

Assessment of 4DCT Motion

For the purposes of this study, the 4DCT motion of the tumour, hilum and carina was measured at an Advantage 4D workstation (GE Healthcare, UK) by a clinician. The maximum 2D movement of all three internal structures was measured in the coronal view of the movie with the straight line measuring device. When assessing tumour and hilar structures, the motion measurements were taken for the apex, the inferior border and the lateral edge of the structures. The maximum movement was noted as the largest of the three measurements.

Assessment of motion during AMTD

Each MV cine-image was reviewed using the RPM-Fluoro Tool as described above. Following the calculation of motion of each internal structure, the MV cine-image was reviewed with the reference box moving in tandem with the internal structure, to ensure the reference box encompassed the internal structure throughout the respiratory cycle. If the reference box did not follow the internal structure well, the process was repeated. The motion was noted when the internal structure and the reference box moved together coherently.

5.3 Results

Clinical Analysis

Tumour characteristics of all 20 patients are summarized in Table 5-1. Six MV-cine were analyzed for each patient. Both observers identified images of the primary tumour in 95% of cases, although it must be noted that 12/20 patients (60%) had primary hilar tumours. Separate hilar structures were identified in the other 40% of patients with a primary tumour located elsewhere. Of these, only 88% had hilar structures that were consistently identifiable by both observers. The carina was visible in 95% of MV-cine. The mean number of respiratory cycles in all 120 MV-cine was 2.45 cycles (range 1 to 6), as assessed by peak-to-peak amplitudes, allowing for tumour amplitude assessment in all the MV-cine.

In 19 patients, the 2D superior-inferior primary tumour movement was calculated on the 4DCT. Motion of the primary tumour was not assessed for a primary mediastinal tumour. The mean motion of the primary tumour on 4DCT was at 7.3mm (range 2mm to 13.8mm). Of those 7 patients without hilar tumours, the mean movement of the hilar structure was 11.0mm (range 4.2mm to 15.1mm). The mean carina movement was calculated from measurements from all patients and was 6.8mm (range 1.8mm to 21.2mm).

Tables 5-2, 5-3 and 5-4 demonstrates the tumour, hilar structure and carina motion seen on the MV-cine of each patient respectively in comparison to the internal structure motion seen at 4DCT. A total of 6 MV-cine were studied per patient. Mean motion of primary tumour, carina and hilum on 4DCT was at 7.3mm (range 2-13.8mm); 6.8mm (1.8-21.2mm) and 11.0mm (4.2-15.1mm) respectively. Corresponding motion during AMTD was 4.1mm (0.6-13.6mm); 2.7mm (0-10mm) and 6.0mm (1.8-14.4mm), respectively.

The tumour and the hilar structures were tracked well by the RPM-Fluoro Tool. The carina often had areas of the treatment bed or a vertebrae in the field, all which make

tracking impossible as the reference box follows the immobile high dense structure, hence only 34%, (39 from 114) of the MV-cine with visible carina's could be tracked.

The number of studies in which the primary tumour motion on an MV cine-image exceeded that on the corresponding 4DCT was 16 of the 114 (14%) cine-images. Interestingly, nearly all were acquired from Patients 1 and 2, indicating a systematic error in 10% of patients. The remaining MV-cine demonstrating more motion than the 4DCT, were sporadically distributed between all the other patients and hence are likely to represent random errors.

Table 5-2. Primary tumour motion on 4DCT and during AMTD treatment.

	4DCT Tumour Motion (mm)	MV cine-image Tumour Motion (mm)			
		Mean	S.D.	Min	Max
Patient 1	5.9	8.2	3.2	4.5	12.8
Patient 2	2.0	3.9	1.5	2.0	6.3
Patient 3	6.9	3.8	0.9	2.9	5.1
Patient 4	10.5	6.9	1.6	5.0	8.9
Patient 5	9.8	7.6	2.8	4.6	12.6
Patient 6	7.8	2.1	0.3	1.7	2.4
Patient 7	6.4	2.5	0.4	2.0	2.9
Patient 8	4.9	2.6	0.6	1.7	3.3
Patient 9	5.4	0.9	0.2	0.6	1.1
Patient 10	7.6	4.7	2.1	2.0	7.8
Patient 11	3.0	1.9	0.8	1.2	3.5
Patient 12	13.2	9.0	3.7	5.0	13.6
Patient 13	Mediastinal tumour therefore analysis not undertaken				
Patient 14	13.4	4.2	1.2	2.3	5.8
Patient 15	8.3	3.4	1.3	2.0	5.1
Patient 16	4.9	4.3	1.5	2.2	6.4
Patient 17	13.8	5.1	1.1	3.5	6.5
Patient 18	5.9	2.7	0.9	1.7	4.3
Patient 19	3.4	0.8	0.2	0.6	1.0
Patient 20	6.9	2.6	1.0	1.6	4.4

Table 5-3. Hilar Structure motion on 4DCT and during AMTD treatment.

	4DCT Hilar Motion (mm)	MV cine-image Hilar Structure Motion (mm)			
		Mean	S.D.	Min	Max
Patient 1	15.1	10.9	2.8	6.1	14.4
Patient 2	15.0	7.8	2.3	5.2	11.5
Patient 10	8.1	8.1	3.0	4.7	11.7
Patient 11	12.8	2.1	0.2	1.8	2.3
Patient 12	9.9	6.3	3.3	2.3	10.5
Patient 15	11.8	4.6	1.5	3.2	7.3
Patient 19	4.2	2.4	0.5	1.8	2.8

Table 5-4. Carina motion on 4DCT and during AMTD treatment.

	4DCT Carina Motion (mm)	MV cine-image Carina Motion (mm)			
		Mean	S.D.	Min	Max
Patient 1	7.0	2.2	0.5	1.5	2.6
Patient 2	10.0	5.7	1.6	4.0	8.3
Patient 3	5.6	Cannot see carina			
Patient 4	3.7	0.9	0.3	0.6	1.2
Patient 5	7.8	2.9	1.0	2.0	4.4
Patient 6	6.9	2.0	0.8	1.4	3.1
Patient 7	7.3	2.0	0.0	2.0	2.0
Patient 8	5.4	1.2	0.5	0.6	2.0
Patient 9	4.2	1.1	0.0	1.1	1.1
Patient 10	6.0	3.1	1.3	2.2	4.0
Patient 11	4.4	2.4	1.5	0.6	4.5
Patient 12	4.9	2.6	2.1	0.0	5.1
Patient 13	4.4	4.2	1.7	2.2	7.2
Patient 14	4.7	2.0	0.9	1.0	3.5
Patient 15	8.9	5.8	2.7	1.6	9.1
Patient 16	6.9	RPM-Fluoro Tool failed to track carina			
Patient 17	8.6	5.1	4.3	2.3	10.0
Patient 18	6.9	2.3	2.5	1.0	7.5
Patient 19	1.8	1.2	0.6	0.6	2.0
Patient 20	21.2	RPM-Fluoro Tool failed to track carina			

5.4 Discussion

Our study highlights the importance of independently verifying novel radiotherapy techniques. We used MV-cine to study intra-fraction motion; an approach has been reported to be a feasible and clinically effective method of independent verification [141,142,143]. The quality of MV-cines is supported by the fact that tumour and carina were visualized in 95% of all analyzed images, and the hilum in 88%. In cases where the primary tumour is not visualized, the carina and the hilar structure can act as surrogates for tumour motion [126]. In 34% of MV-cines, difficulties were observed in tracking the carina, mainly due to the bed frame in the field. The latter was solved by repositioning the former out with the field for future fractions. Use of MV-cines were not possible using conventional IMRT plans, but hybrid IMRT plans that use at least one non-IMRT anterior field would allow an MV cine-image for independent verification [144].

The motion demonstrated in this group of locally advanced tumours can be compared to that of Liu et al [145]. Liu et al assessed the motion of 166 locally advanced tumours and found that the population averages of tumour motion were 0.50cm in the superior-inferior in comparison to our mean motion of 0.74cm on 4DCT. They noted the percentage of patients with >0.5cm of motion as 39.2% and >1.0cm of motion as 10.8% respectively. In our series the tumours moved more with motion >0.5cm and >1.0cm in 74% and 21%. The slightly larger motion seen in our series, may be in part due to a smaller sample size however despite this, it is unexpected, as those with large motion who were suitable for RGRT were excluded.

AMTD appears to be a suitable approach for the majority of patients who are not candidates for traditional RGRT due to limited tumour motion, irregular breathing or intolerance of coaching. It does not require mandatory respiratory coaching, as maintaining a reproducible wavelength and amplitude is not integral to delivery, and is more efficient than traditional RGRT as the duty-cycle is larger. With AMTD delivery,

only 10% of patients have consistently more intra-fraction tumour motion on treatment than at 4DCT.

The AMTD technique is not without limitations. Although correlation coefficients between tumour and external surrogates have been reported to be as high as 87% in the superior-inferior direction [85] and 81% in all directions [88], little or no correlation is seen in a minority of patients. It requires further study to investigate whether the 10% of patients with consistently larger intra-fraction tumour motion on during treatment are those with little or no correlation. If a lack of correlation is the cause of the larger intra-fraction motion, new software tools are available to assess the correlation between external surrogate and internal motion prior to treatment to identify those in whom AMTD is not applicable [146]. If there is an alternative explanation this study offers a simple, radiation free method of identifying them with use of MV-cines, although improved software would be required as the current process is time-consuming and not feasible for routine clinical use. The alternative imaging techniques that can be used on-line to assess intra-fraction motion are fluoroscopy [49,147] or 4D-CBCT [65], however the disadvantages of these include the additional radiation dose and treatment time. Also, the intra-fraction motion seen during online imaging does not necessarily represent the motion during treatment, only prior to treatment, at which time the patient may be breathing differently for a variety of reasons including anxiety due to the gantry rotating or additional noise.

A further limitation of AMTD is the lack of assessment of baseline shifts. Our current technique of online CBCT, utilizes the fact a CBCT is taken over a number of respiratory cycles, hence creating an image demonstrating the tumour in the mean position. The visual check comparing the tumour on the CBCT to the planning gross tumour throughout the respiratory cycle highlights any obvious baseline shift in mean position of the tumour. The MV-cine could potentially be used to make a comment on baseline position however due to lack of integration into the planning and delivery system, software limitations make it is impossible to confidently comment on baseline shift at present. 4D-CBCT is currently the gold standard for online assessment of baseline shift, however the limitations are noted above.

There may be concerns that AMTD requires additional time for treatment delivery due to steps such as placement of an infrared marker box, assessment of the respiratory waveform, and the intermittent treatment beam. However our treatment slots have not increased with the introduction of AMTD and the 15 minute treatment slots are identical to non-AMTD thoracic treatments.

AMTD offers a novel method of limiting variation in intra-fraction motion and is applicable to the majority who are not suitable for traditional forms of RGRT. Our findings also add to the growing body of data showing the potential of MV-cine as a verification tool in the delivery of thoracic radiotherapy.

6. INVESTIGATION OF THE CLINICAL BENEFIT OF RESPIRATORY GATED RADIOTHERAPY (RGRT) IN LOCALLY ADVANCED NON-SMALL CELL LUNG CANCER (NSCLC).

6.1 Introduction

Traditional forms of RGRT such as phase-based or amplitude-based RGRT, have been shown to reduce the size of the PTV when compared to the standard 4D PTV [91]. The theoretical advantages are: reduction in toxicity; potential for dose escalation; and fewer patients having radical treatment withheld on account of large volumes or unacceptable toxicity parameters.

Despite the enthusiasm regarding this new technique, it is essential to be aware of the potential disadvantages which are discussed in detail in section 1.3.4.1.

In view of these concerns and controversies, it is imperative to quantify the clinical benefit to patients that RGRT provides, when compared to continuous (non-gated) 4DCT treatment to save embarking unnecessarily on complex and costly techniques. As yet, there are no randomised clinical trials and only one paper suggesting there is a reduction in lung V20 with RGRT [91]. There is no consensus on which parameters can predict an improvement in clinical outcome when comparing RGRT to continuous irradiation of 4DCT; however the toxicity parameters that are routinely used in clinical practice can be used as surrogates. These include the volume of lung receiving 20Gy (V20 lung); volume of lung receiving 5 Gy (V5 lung); mean lung dose (MLD); and volume of oesophagus receiving 50Gy (V50 oes). As there is no consensus on the best lung parameters, a number of different parameters were used that have all been demonstrated to correlate with radiation pneumonitis [148,149,150]. There is no consensus on the toxicity parameter to be used with the oesophagous, some use the length of oesphagous irradiated others the V50 or V55. V50 was selected as a recent

study of 100 patients assessing different dosimetric parameters that identified this as the one that best correlated with toxicity [151]. If the toxicity parameters are reduced with RGRT in comparison to continuous (non-gated) 4DCT treatment, three theoretical benefits of RGRT could be achieved: toxicity will decrease; there is potential for dose escalation; and more patients would have toxicity parameters within the acceptable levels to proceed to radical radiotherapy.

There were four aims of this study (1) quantify the improvement in clinical outcome of RGRT in comparison to continuous (non-gated) 4DCT irradiation, by using toxicity parameters as surrogates for clinical outcome; (2) assess the correlation between tumour motion and benefit of RGRT with a view to identifying a threshold of tumour motion where RGRT should be considered; (3) compare the benefit of inspiration RGRT to expiration RGRT; (4) assess the benefit of RGRT when smaller set-up margins (CITV to PTV margin) are used.

6.2 Materials and Methods

Patient Data Acquisition.

CT image datasets of consecutive node-positive lung cancer patients were reviewed retrospectively. These patients had previously undergone 4DCT for treatment planning and completed routine radical radiation to a dose of 55Gy in 20 fractions with continuous (non-gated) 4DCT treatment. In order to select patients for the study, an assessment of tumour motion was undertaken using the cine-movie facility on an Advantage 4D workstation (GE Healthcare, UK). The maximum distance the apex and inferior border of the primary tumour moved during the respiration cycle was measured using the straight line measuring device. Any patient with >5mm craniocaudal tumour movement at either of these points was eligible. Fifteen consecutive patients were selected.

The 4DCT image acquisition has been reported in detail in Section 2-2. In brief, patients were scanned on a GE Lightspeed RT 16 Multi-slice CT scanner (GE Healthcare, UK) with scanning parameters set at 120 kV, 20mA with a slice thickness of 2.5mm. Patients were audio-coached, with the rate of respiration set at their initially recorded respiratory rate. The RPM System is used to record a trace of the patient's respiratory cycle during acquisition of the scan. In each couch position, the scanner acquired 10 consecutive scans over the course of one breathing cycle. These scans were sorted using the Advantage 4D workstation into 10 phase-bins representing the 10 phases of the respiratory cycle.

Delineation of Targets.

The author delineated 3 different GITVs for each patient using Varian Eclipse Treatment Planning System, software version 8.6 (Varian Medical Systems, Palo Alto, CA). The different GITVs were created to represent, the full extent of respiratory motion, end-inspiration and end-expiration.

To delineate the GITV for gating in end-expiration, Exp_GITV, the cine movie of all phase-bins was reviewed. The Exp_GITV was delineated using the phase-bin with the tumour in the most superior position. The Exp_GITV was then reviewed in the surrounding 2 phase-bins and enlarged to encompass any additional tumour visualised. This additional tumour visualised represents tumour movement during the imaging of the 3 expiratory "bins". The GITV for gating in end-inspiration, Insp_GITV, was created in the same way however this time identifying the phase-bin with the tumour in the most inferior position and the surrounding 2 phase-bins. A composite of Exp_GITV and Insp_GITV was created to represent the positional variation of the tumour throughout all phases of respiration (4D_GITV). A margin of 5mm was added to encompass microscopic invasion to each of these GITVs and then two different planned target volumes (PTV) for each GITV were created using set-up margins of 5mm and 10mm respectively. This created 6 different PTVs:

- 4D_PTV (10mm margin) – 4D_GITV with a 5mm for microscopic spread and 10mm set-up margin.

- Insp_PTV (10mm margin) – Insp_GITV with a 5mm for microscopic spread and 10mm set-up margin.

- Exp_PTV (10mm margin) - Exp_GITV with a 5mm for microscopic spread and 10mm set-up margin.

- 4D_PTV (5mm margin) - 4D_GITV with a 5mm for microscopic spread and 5mm set-up margin.

- Insp_PTV (5mm margin) Insp_GITV with a 5mm for microscopic spread and 5mm set-up margin.

- Exp_PTV (5mm margin) - Exp_GITV with a 5mm for microscopic spread and 5mm set-up margin.

Organs at Risk Delineation and Treatment planning.

The two 4D_PTVs had the dose calculation undertaken on an Average Intensity Projection (Ave-IP) data-set, created using all ten phase-bins. The two Insp_PTVs were calculated on an Ave-IP data-set created using the three phase-bins representing end-inspiration and the two Exp_PTVs were calculated on an Ave-IP data-set created using the three end-expiration phase-bins. The whole lung was delineated on each of the different Ave-IPs using automatic segmentation followed by manual editing if required. To calculate the lung toxicity parameters the whole lung of the appropriate Ave-IP minus the relevant PTV was used in each plan. The oesophagus was delineated from the oropharynx to the oesophageo-gastic junction.

Six treatment plans were generated for each patient by the author. All plans consisted of 55Gy in 20 fractions delivered using 3-5, 6MV photon beams with 100% prescribed to isocentre. For each patient, an initial plan was created for the 4D_PTV. Most treatments used beams at gantry angles of 0, 60-70 and 120-130 degrees from the vertical. Additional boost fields were used to boost the periphery of the PTV where necessary. The plan was optimized to cover as much of the PTV as possible with between 95% and 107% of the prescribed dose, maintaining the dose to spinal cord

below 42Gy and the V20 as low as possible, as is routine in our clinical practice. The same beams were then applied to the other 5 PTVs. Small adjustments were made to beam size, gantry angle, wedge and beam weight where necessary to optimise these plans to the same standards.

Data Analysis

Cranio-caudal tumour motion was set as the cranio-caudal difference between geometric centre positions of the GTVs in the single phase-bins representing the most superior and most inferior tumour positions.

The volumes of the PTVs and the toxicity parameters V20 lung, V5 lung, MLD and V50 oes were noted in all six plans for each patient. The reductions in volumes and toxicity parameters between the 4DCT and the two RGRT plans with corresponding set-up margins were calculated. The correlation coefficient between the reduction in toxicity parameters and tumour movement was calculated using Pearson's product correlation coefficient on Microsoft Excel 2002. The two-tailed t-test was used to check for statistical significance.

6.3 Results

Fifteen patients, with node positive lung cancer were identified with >5mm of movement on the 4DCT planning scan. Tumour staging, location, cranio-caudal movement for all patients along with PTV, V20 and MLD from 4D_PTV (10mm margin) are presented in Table 6-1. In the pre-selection cine-movie process all patients demonstrated >5mm of movement in the primary tumour, but some of the cranio-caudal movements noted using the geometric centre of the entire gross tumour were <5mm. This is mostly due to the incorporation in the GITV of the lymph nodes which move less than the primary tumour.

Dose and volume statistics are presented in Table 6-2. In the plans created using the margin of 10mm, the PTV delineated for inspiration RGRT [Insp_PTV (10mm margin)] and expiration RGRT [Exp_PTV (10mm margin)] were compared to the plan created using all phases of the respiration cycle [4D_PTV (10mm margin)]. The median reduction in V20 with inspiratory gating and expiratory gating was 2.0% (range 0.7% – 3.9%) and 0.6% (range -1.1% to 4.7%) respectively; the reduction in V5 was 3.8% (range 1.3% to 8.0%) and 1.0% (range -2.6% to 6.4%) respectively and the reduction in MLD was 0.9Gy (range 0.2Gy to 3.2Gy) and 0.7Gy (range -0.1Gy to 2.7Gy) respectively.

Similarly, with only a 5mm set-up margin, median reduction in V20 with inspiratory gating and expiratory gating was 2.4% (range 0.5% to 4.4%) and 0.5% (range -0.7% to 3.6%) respectively; the reduction in V5 was 4.9% (range 1.2% to 8.7%) and 1.3% (range -0.9% to 6.2%) respectively and the MLD reduction was 0.9Gy (range -0.1Gy to 3.9Gy) and 0.7Gy (range -0.5Gy to 3.2Gy) respectively.

Figure 6-1 allows easy visualisation in scatter plots of the lack of correlation between the cranio-caudal tumour movement and both V20 and MLD. Table 6-3 shows the correlation coefficients between tumour motion and each toxicity parameter. The only toxicity parameter that showed a statistically significant correlation was between tumour motion and V5 in both the inspiration plans. All the other toxicity parameters of the lung showed no correlation.

The V50 oes is reduced by a mean of 2.1% (range 0% - 9.33%), 1.4% (range 0% - 9.0%) with inspiration and expiration RGRT using 10mm margins respectively. With the margins of 5mm the inspiration and expiration margin reduction was 1.6% (range 0% - 6.6%), 1.0% (range 0% - 4.6%) respectively. The correlation between motion and reduction in V50 oes is a statistically significantly negative correlation in both the inspiration and expiration plans with the smaller margin, and fails to demonstrate any correlation in both 10mm margin plans, indicating that it is not the case that increased motion results in larger reduction in oesophageal toxicity.

Figure 6-1. Correlations between reduction in lung toxicity parameters and tumour motion in: (a) Insp PTV (10mm margin) (b) Exp PTV (10mm margin) (c) Insp PTV (5mm margin) (d) Exp PTV (5mm margin).
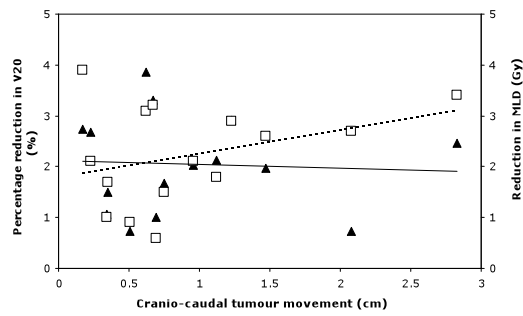
(a)
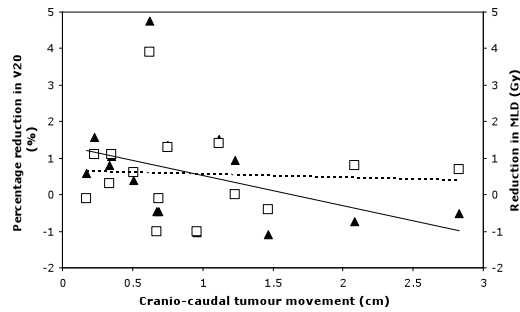
(b)
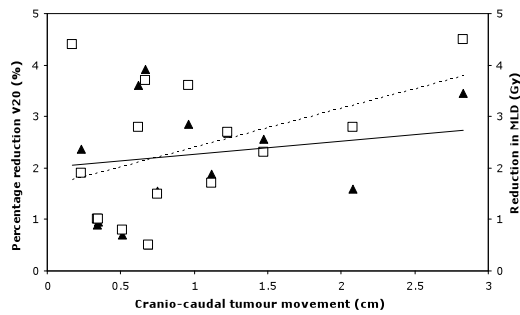
(c)
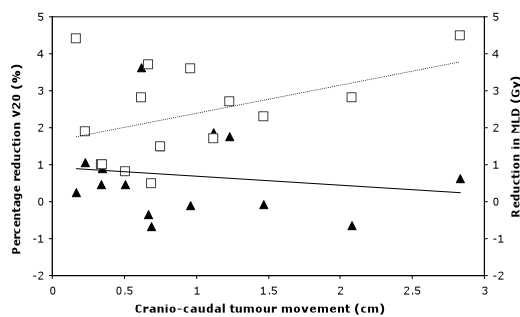
(d)
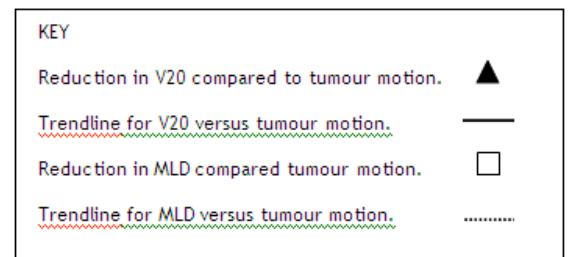
An additional observation of our study was that the reduction in toxicity parameters achieved by reducing the set-up margin, from 10mm to 5mm, during continuous (non-gated) 4DCT treatment was actually larger than that seen with the addition of RGRT. This suggests that if a centre wished to reduce toxicities, there is more benefit to be gained by improved online verification which can reduce margins from 10mm to 5mm than introducing RGRT which is a complicated, work intensive technique that is only suitable for a minority of patients. Table 6-4 demonstrates the reduction of toxicity parameters when the margin is reduced versus the reduction when end-inspiration RGRT is used.

Table 6-1. Patient characteristics

	Tumour Stage	Tumour Position	Tumour Motion (cm)	4D PTV [10mm margin] (cm3)	V20 lung (%)	MLD(Gy)
Patient 1	T4 N2	LLL	0.62	664.56	41.8	21.7
Patient 2	T2 N1	RML	1.47	359.10	18.0	10.2
Patient 3	T2 N1	RUL	0.34	331.09	16.7	10.8
Patient 4	T2 N1	RML	0.75	230.99	20.1	11.6
Patient 5	T2 N1	RML	0.17	588.92	48.0	25.0
Patient 6	T1 N2	LUL	0.69	615.54	28.3	14.8
Patient 7	T2 N1	RLL	2.08	1323.71	28.0	18.0
Patient 8	T4 N1	RLL	0.67	425.97	21.5	11.8
Patient 9	T2 N2	RUL	2.83	770.88	31.7	17.4
Patient 10	T2 N2	RLL	0.23	527.85	42.4	21.6
Patient 11	T3 N2	RUL	0.51	163.48	13.3	7.1
Patient 12	T2 N1	RML	1.12	197.01	22.9	12.4
Patient 13	T2 N1	RLL	1.23	818.79	20.9	12.6
Patient 14	T3 N1	RLL	0.35	573.28	31.3	16.8
Patient 15	T4 N2	RML	0.96	903.00	43.7	23.6

Abbreviations: R, right; L, left; LL, lower lobe; UL, upper lobe; ML, middle lobe; PTV, planned target volume; V20, volume of lung receiving >20Gy; MLD, mean lung dose.

Table 6-2. Reductions of volume and toxicity parameters using RGRT compared with continuous (non-gated) 4DCT treatment.

		PTV (cm^3)	V20 Lung (%)	V5 Lung (%)	MLD (Gy)	V50 oesophagus (%)
Insp PTV (10mm margin)	Mean	86.40	2.05	3.95	1.09	2.09
	SD	65.60	0.92	1.84	0.71	2.84
	Range	16.58 - 242.15	0.72 - 3.86	1.29 - 8.00	0.22 - 3.20	0 - 9.33
Exp PTV (10mm margin)	Mean	106.04	0.58	1.25	0.87	1.36
	SD	111.61	1.43	2.11	0.68	2.42
	Range	26.78 - 460.62	-1.1 - 4.74	-2.59 - 6.44	-0.1 – 2.7	0 - 9.03
Insp PTV (5mm margin)	Mean	69.39	2.26	4.25	1.17	1.61
	SD	56.07	1.20	2.16	0.95	2.22
	Range	11.61 - 213.21	0.5 - 4.4	1.21 - 8.73	0.1 – 3.9	0 - 6.6
Exp PTV (5mm margin)	Mean	83.21	0.70	1.63	0.97	1.03
	SD	92.34	1.10	1.83	0.53	1.38
	Range	17.71 - 384.43	-0.68 - 3.61	-0.9 - 6.23	-0.1 – 2.3	0 - 4.6

Abbreviations: SD, standard deviation; MLD, mean lung dose; PTV, planned target volume; Insp PTV, PTV created at Inspiration RGRT; Exp PTV, PTV created at Expiration RGRT.

Table 6-3. The correlation between tumour motion and toxicity parameters.

	V20 Lung (%)	V5 Lung (%)	MLD (Gy)	V50 oesophagus (%)
Correlation between tumour motion and Insp PTV (10mm margin)	-0.06	0.60*	0.34	-0.37
Correlation between tumour motion and Exp PTV (10mm margin)	-0.41	0.29	-0.06	-0.39
Correlation between tumour motion and Insp PTV (5mm margin)	0.15	0.59*	0.43	-0.57*
Correlation between tumour motion and Exp PTV (5mm margin)	-0.15	0.44	0.12	-0.57*

* Indicates correlation is statistically significant with p = <0.05

Abbreviations: V20, volume of lung receiving >20Gy; V5, volume of lung receiving >5Gy; MLD, mean lung dose; PTV, planned target volume; Insp PTV, PTV created at Inspiration RGRT; Exp PTV, PTV created at Expiration RGRT.

Table 6-4. Reductions of volume and toxicity parameters with the use of RGRT versus the reduction of set-up margins.

		PTV (cm^3)	V20 Lung (%)	V5 Lung (%)	MLD (Gy)	V50 oesophagous (%)
Reduction in toxicity parameters from: 4D_PTV (10mm margin) to 4D_PTV (5mm margin)	Mean	171.93	2.81	4.95	1.59	4.05
	SD	78.79	1.83	1.71	0.63	3.83
	Range	73.9 - 357.8	-0.1 - 6.3	1.1 - 7.8	0.8 – 3.0	0.0 - 12.6
Reduction in toxicity parameters from: 4D_PTV (10mm margin) to Insp_PTV (10mm margin)	Mean	86.40	2.05	3.95	1.09	2.09
	SD	65.60	0.92	1.84	0.71	2.84
	Range	16.6 - 242.2	0.72 - 3.86	1.29 - 8.00	0.22 – 3.20	0.00 - 9.33

6.3 Discussion

With all the interest there is in RGRT and its implementation, it is a significant finding that we have demonstrated a very limited improvement of lung and oesophageal toxicity parameters with the use of RGRT in node positive lung tumours. There are numerous papers addressing the likelihood of radiation pneumonitis and thereafter long term lung damage, and equally as many papers calculating methods of predicting these, however there remains no consensus on what reduction of lung toxicity parameters, provides what reduction in likelihood of radiation pneumonitis [143,144,145]. To quantify the reduction in risk, we would need to select a paper at random and calculate this risk reduction using their NTCP models, for each individual patient, using each different plan. However there are widely felt concerns regarding the use of these models for an individual patient and therefore they must be used with caution [152]. Due to the lack of consensus on which model should be used, the concerns regarding these models in individual patients and the large quantities of further work required to calculate a model driven reduction of risk of radiation pneumonitis for each patient, this analysis was not carried out. Some might argue that any improvement in toxicity parameters is a step in the right direction. For example, in our centre, radical radiotherapy is withheld for patients with a lung V20 of 35% however individual clinicians may have different limiting parameters both in our centre and in other centres. In some patients, a small reduction from above to below the believed cut off may render a patient radically treatable within the strict confines of a protocol. However, out with the rigid limitations of protocols, one has to be sceptical whether a reduction in V20 of around 2% will reflect in a better clinical outcome for any patient. We feel that this is outweighed by additional potential errors and the significant additional time involved in implementation and treatment with RGRT. In view of the limited reduction in toxicity parameters, it is unlikely any of the three theoretical advantages of RGRT will be achieved.

The challenge is to identify the minority of patients who would receive the most benefit from RGRT. Only one of the 15 patients (6%) had a reduction of V50 lung of >4%

and MLD of >4Gy. However we found no convincing correlation between tumour motion and toxicity parameters indicating that tumour motion cannot be used as a method of identification. This suggests that there is a complex combination of factors which determines treatment toxicity parameters e.g. tumour size, tumour location (extension into lung or solid tissue), tumour motion, treatment beam configuration and relative dose weighting per beam. Further investigation is required, to see whether it is possible to pre-select patients for RGRT. Failing that, comparative planning will be required on a patient by patient basis.

There are two papers investigating this issue. Starkschall et al. found that only in small tumours (volume of GTV <100cm3) was there a correlation between tumour motion and improvement in V20 [91]. Direct comparison with our results is difficult for a variety of reasons: they reported the V20 reduction only as a ratio, and not with any absolute values; they only investigated end-expiration RGRT, which we found to be of less benefit; they used the same free-breathing scan for dose calculation of all plans; thirteen of their 20 patients had GTVs of <100cm3, which are likely to represent Stage I tumours, of which we had none due to deliberately omitting them, the reasons for which are discussed below. An additional difference is the planning techniques. Starkschall et al. based their analysis on a prescription of 60Gy to the 93% isodose. Treatment was with a 4 field technique. AP-PA fields were weighted to deliver 44Gy and lateral or lateral-oblique opposing fields delivered 16Gy. This creates a very different dose distribution than our 3-field technique. In their technique, lung tissue which lies only within the lateral fields cannot reach a dose of 20Gy whereas all lung tissue which lies within the AP-PA fields must inevitably receive in excess of 20Gy. The impact on V20 of treatment field size adjustment to account for target motion in the 3 principal axes would be quite different in the 2 techniques. Underberg et al. performed a similar study looking at the benefit of gating in 15, Stage III NSCLC patients [92]. The PTV sizes were comparable to ours however the motion of the tumour in our study was marginally more as we specifically selected patients with more motion. They compared a number of different plans, but those of interest for comparison are the plans created from the volumes encompassing all motion versus an end-expiration gate. It is

reassuring they demonstrated similar small reductions in toxicity parameters with an absolute reduction in MLD and V20 of 0.9Gy and 1.9% respectively.

There is some suggestion in the literature that RGRT can be used in Stage I tumours with stereotactic radiotherapy [153], however the three theoretical benefits of RGRT have already been achieved by the development of standard stereotactic radiotherapy [12,13,14]. This technique has limited toxicity, can deliver biological equivalent doses of 180Gy with excellent local control rates, and all patients are eligible as the volumes in Stage I tumours tend to be small. Consequently, reducing the volumes and hence the toxicity parameters in Stage I tumours may not be a worthwhile exercise hence, our study concentrated on node-positive lung cancers where the theoretical benefits of RGRT have not yet been achieved by other technologies.

There was an additional observation that reducing the set-up margin from 10mm to 5mm provides a larger reduction in the V20 than RGRT. This raises the question as to whether the emphasis in radiotherapy departments should be to improve set-up errors using on-board imaging rather than implementing RGRT. Both techniques involve increase in work intensity however, online verification techniques can be used for all patients where as RGRT is only useful in a minority of patients. Therefore if a centre is to implement a technique to decrease toxicity, an online verification technique would provide a bigger decrease.

Comparing the benefit of Expiration RGRT versus Inspiration RGRT, we have shown that gating has a greater effect on toxicity parameters at end-inspiration. This would be consistent with the assumption that the lung volume is expanded and greater sparing is possible. Table 6-2 highlights the very marginal improvements at end-expiration. The authors feel that should RGRT be applied, end-inspiration is recommended, with an awareness of its problems. However this cannot be applied indiscriminately to all patients and it may be appropriate to assess the possible improvements on a patient by patient basis with computer comparison of gating versus continuous (non-gated) 4DCT treatment.

In conclusion, there is a great deal of interest in RGRT and its development in radiotherapy centres worldwide, however this study demonstrates that the vast majority of patients are unlikely to have a better clinical outcome with RGRT treatment. Due to the additional potential errors involved in RGRT, we feel that until further investigation identifies a good method of selecting patients for RGRT, it should only be performed if comparative planning of RGRT plans and continuous (non-gated) 4DCT plans has been undertaken and a likely clinical benefit has been confirmed.

7. CONCLUSIONS.

The conclusions to each individual study have been discussed in each chapter in turn. There are a number of issues that the thesis as a whole highlights which will be discussed below.

This thesis demonstrates how IGRT involves the integration of imaging techniques in all three of the stages of radiotherapy; delineation, verification and treatment delivery. In addition, the thesis also highlights that each stage has many different imaging techniques that could be used, usually in combination. For example, in verification, it is apparent that each imaging technique is more suited to identifying and limiting different types of potential error; MV cine-images are useful for intrafraction tumour motion, while CBCT is the best imaging modality to highlight any significant interfraction tumour motion over the treatment course. The ideal would therefore be to use the different imaging techniques in combination. The challenge in future investigations of IGRT is to identify the combination and timing of different images to maximize tumour coverage and minimise irradiation of normal tissues. One of the hypothetical aims of this thesis was to ensure IGRT could be implemented into a busy clinical department. As a result, investigation into the minimal number of each imaging technique would be a useful research avenue to minimise the impact on clinical departments.

It is apparent that for most technologies used within IGRT, other than SBRT, that there is no clinical outcome data. In IGRT, surrogates such as improved target coverage or decreased toxicity parameters are used. Primarily, this is because these newer imaging techniques address potential errors we were not capable of visualising or quantifying before. Trials comparing current IGRT techniques with previous methods would be considered unethical by many, as we would be treating patients while aware there are preventable errors. As a result, once a centre has confirmed improved target coverage and reduced normal tissue toxicity, departments are happy to implement them into clinical care without clinical outcome data. In addition, without implementing IGRT it

is impossible to begin to use other radiotherapy technologies, such as IMRT or SBRT which do have good published outcome data. We hope that with the implementation, auditing and continuous improving of appropriate IGRT technologies, we will see an improvement in local control and overall survival over the coming years.

The different outcomes of the different chapters emphasise the need to critically analyse any new technique. RGRT and AMTD are two different techniques that are implemented and studied. The study in chapter 6 examining AMTD is an initial report confirming there are only a small number of patients whose tumours occasionally move out with the PTV delineated. It requires further investigation, initially to compare the technique to standard delivery of radiation throughout the respiratory cycle and laterally to assess the potential clinical benefit. As discussed above, the outcomes of these studies will likely be surrogates of clinical outcome, due to the difficulties of using clinical outcome as an endpoint. The RGRT study, suggested there was a minimal reduction in toxicity parameters and therefore had limited clinical benefit to the majority of patients. Both of these studies affirm the need to study and publish results on new techniques once they have been implemented to confirm they offer some improvement on current techniques.

Lastly, during these investigations, it is evident that radical radiotherapy for lung cancer should be tailored to each patient. It is not appropriate to have one method of treatment for all. The gating study highlights that although RGRT can offer a reduction in toxicity for a few patients, it is not clinically relevant for a vast majority. The delineation study is in accordance with this finding as it finds the MIP image from the 4DCT scan can be used in those with Stage I tumours but is not appropriate for those with node positive disease. A further avenue for research in IGRT is how to tailor our new techniques to patients those who stand to gain the most from them. New techniques must be investigated in specific homogenous patient groups so that conclusions identify whether or not they are applicable in that patient group.

In summary, the era of IGRT is in the early stages. There is so much new technology available, but significant careful further study is required to ascertain more regarding the role of some techniques and how to implement them into clinical care. Further to that, the challenge is to identify the most appropriate combination of imaging techniques for each individual, in order to achieve the best clinical outcome for every patient.

[1] http://info.cancerresearchuk.org/cancerstats/types/lung/

[2] Parkin DM, Whelan SL, Ferlay J, et al. Cancer Incidence in Five Continents Volume VIII. *IARC Scientific Publications, International Agency for Research on Cancer, Lyon, France*. 2002;155

[3] Scottish Executive Health Department. Cancer Scenarios: An aid to planning cancer services in Scotland in the next decade. *Edinburgh: The Scottish Executive*, 2001.

[4] Pearce J, Boyle P Is the urban excess in lung cancer in Scotland explained by patterns of smoking? *Soc Sci Med* 2005;60:2833-43

[5] De Vos Irvine, H., et al. Asbestos and lung cancer in Glasgow and the west of Scotland. *Brit Med J*, 1993;306:1503-6

[6] ISD Online. Cancer Incidence, Mortality and Survival data. Accessed 2009

[7] Scottish Intercollegiate Guidelines Network SIGN guidelines, February 2005. Royal College of Physicians, Edinburgh. *Available from www.sign.ac.uk*

[8] National collaborating Centre for Acute Care, February 2005. Diagnosis and treatment of lung cancer. National Collaborating Centre for Acute Care, London. *Available from www.rcsseng.ac.uk*

[9] Rami-Port R, Crowley JJ, Goldstraw P. The Revised TNM Staging System for Lung Cancer. *Ann Thorac Cardiovasc Surg* 2009;15:4-9

[10] Fry WA, Menck HR, Winchester DP. The National Cancer Data Base report on lung cancer. *Cancer* 1996;77:1947-55

[11] Rowell NP, Williams CJ. Radical radiotherapy for stage I/II non-small cell lung cancer in patients not sufficiently fit for or declining surgery (medicallyinoperable): a systematic review. *Thorax* 2001;56:628-638

[12] Onishi H, Tsutomu A, Shirato Y et al. Stereotactic Hypofractionated High-Dose Irradiation for Stage I Non-small Cell Lung Carcinoma: clinical outcomes in 245 subjects in a Japanese multiinstitutional study. *Cancer* 2004;101:1623-1631

[13] Timmerman R, McGarry R, Yiannoutsos C, et al. Excessive Toxicity When Treating Central Tumours in a Phase II Study of Stereotactic Body Radiation Therapy for Medically Inoperable Early-Stage lung Cancer *J Clin Onc* 2006;24:4833-38

[14] Lagerwaard FJ, Haasbeek CJA, Smit EF, et al. Outcomes of risk-adapted fractionated stereotactic radiotherapy for stage I non-small cell lung cancer. *Int J Radia Oncol Biol Phys* 2008;70:685-692

[15] Auperin A, Le Pechoux C, Rolland E et al. Meta-analysis of concomitant versus sequential radiochemotherapy in locally advanced non-small-cell lung cancer. *J Clin Onc* 2010;28:2181-2190

[16] Saunders M, Dische S, Barrett A, et al. on behalf of the CHART Steering Committee. Continuous hyperfractionated accelerated radiotherapy (CHART) versus conventional radiotherapy in non-small cell lung cancer: a randomised multicentre trial. *Lancet* 1997;350:161-165

[17] Sause W, Scott C, Taylor S, et al. Radiation Therapy Oncology Group (RTOG) 88-08 and Eastern Cooperative Oncology Group (ECOG) 4588: Preliminary Results of a phase III trial in regionally advanced, unresected non-small cell lung cancer. *J Natl Cancer Inst* 1995;87(3):198-205

[18] Perez CA, Pajak TF, Rubin P, et al. Long-term observations of the patterns of failure in patients with unresectable non-oat cell carcinoma of the lung treated with definitive radiotherapy. Report by the Radiation Therapy Oncology Group. *Cancer* 1987;59(11):1874-1881

[19] Xiao J, Zhang H, Gong Y et al. Feasibility of using intravenous contrast-enhanced computed tomography (CT) scans in lung cancer treatment planning. *Radiother Oncol* 2010;96:73-77

[20] International Commission on Radiation Units and Measurements. Prescribing, recording and reporting photon beam therapy. Report 50, Bethesda, MD: ICRU;1993.

[21] International Commission on Radiation Units and measurements. Prescribing, recording and reporting photon beam therapy. Report 62 (Supplement to ICRU Report 50) Bethesda, MD: ICRU;1999

[22] De Ruysscher D, Faivre-Finn C, Nestle U et al. European Organisation for Research and Treatment of Cancer Recommendations for planning and delivery of high-dose, high-precision radiotherapy for lung cancer. *J Clin Onc* 2010;28:5301-5310

[23] Giraud P, Antoine M, Larrouy A, et al. Evaluation of microscopic tumour extension in non-small-cell lung cancer for three-dimensional conformal radiotherapy planning. *Int J Radiat Oncol Biol Phys* 2000;48:1015-24

[24] Van Herk M. The probability of correct target dosage: dose-population histograms for deriving treatment margins in radiotherapy. *Int J Radiat Oncol Biol Phys* 2000;47:1121-1135

[25] McKenzie A, Coffey M, Greener T., et al. *Geometrical Uncertainties in Radiotherapy*, London: British Institute of Radiology Working Party; 2003.

[26] Seppenwoolde Y, Lebesque JV. Partial irradiation of the lung. *Sem Radiat Oncol* 2001;11:247-258

[27] Valicenti RK, Michalsi JM, Bosch WR et al. Is weekly port filming adequate for verifying patient position in modern radiotherapy. I*nt J Radiat Oncol Biol Phys* 1994;30:431-438

[28] Bel A, van Herk M, Bartelink H et al. A verification procedure to improve patient set-up accuracy using portal images. *Radiother Oncol* 1993;29:253-260

[29] de Boer HCJ, Heijmen BJM. A protocol for the reduction of systematic patient setup errors with minimal portal imaging workload. *Int J Radiat Oncol Biol Phys* 2001;50(5):1350-1365

[30] Vorwerk H, Beckmann G, Bremer M et al. The delineation of target volumes for radiotherapy of lung cancer patients. *Radiother Oncol* 2009;91:455-460

[31] Rosenzweig KE, Sura S, Jackson A, et al. Involved-field radiation therapy for inoperable non-small-cell lung cancer. *J Clin Oncol* 2007;35:5557-5561

[32] Senan S, Burgers S, Samson MJ et al. Can elective nodal irradiation be omitted in stage III non-small cell lung cancer ? Analysis of recurrences in a phase II study of induction chemotherapy and involved field radiotherapy. *IJROBP* 2002;54:999-1006

[33] Kimura T, Togami T, Nishiyama Y, et al. Impact of incidental irradiation on clinically uninvolved nodal regions in patients with advanced non-small-cell lung cancer treated with involved-field radiation therapy: does incidental irradiation contribute to the low incidence of elective nodal failure? *Int J Radiat Oncol Biol Phys* 2009:77:337-343

[34] Stroom J, Blaauwgeers H, van Baardwijk A, et al. Feasibility of pathology-correlated lung imaging for accurate target definition of lung tumours. *Int J Radiat Oncol Biol Phys* 2007;69:267-275

[35] Stevens CW, Munden RF Forster KM, et al. Respiratory driven lung tumour motion is independent of tumour size, tumour location and pulmonary function. *Int J Radiat Oncol Biol Phys* 2001;51:62-68

[36] Van Sornsen de Koste JR, Lagerwaard FJ, Nijssen-Visser MR et al. Tumour location cannot predict the mobility of lung tumours: A 3D analysis of data generated from multiple CT scans. *Int J Radiat Oncol Biol Phys* 2003;56:348-354

[37] Plathow C, Ley S, Fink C et al. analysis of intrathoracic tumour mobility during whole breathing cycle by dynamic MRI. *Int J Radiat Oncol Biol Phys* 2004;59:952-959

[38] Gould MK, Maclean CC, Kuschner WG et al. Accuracy of positron emission tomography for diagnosis of pulmonary nodules and mass lesions: A meta-analysis. *JAMA* 2001;285:914-924

[39] Gould MK, Kuschner WG, Rydzak CE et al. Test performance of positron emission tomography and computed tomography for mediastinal staging in patients with non-small cell lung cancer: A meta-analysis. *Ann Intern Med* 2003;139:879-892

[40] Hellwig D, Ukena D, Paulsen F et al. Meta-analysis of the efficacy of positron emission tomography with F-18-fluorodeoxyglucose in lung tumours. Basis for discussion of the German Consensus Conference on PET in Oncology 2000 *Pneumologie* 2001;55:367-377

[41] MacManus MP, Hicks RJ, Matthews JP et al. Positron emission tomography is superior to CT scanning for response-assessment after radical radiotherapy/chemoradiothearpy in patient with non-small cell lung cancer. *J Clin Oncol* 2003;21:1285-1292

[42] Davies A, Tan C, Paschalides C, et al. FDG-PET maximum standardised uptake value is associated with variation in survival:Analysis of 498 lung cancer patients. *Lung Cancer* 2007;55:75-78

[43] Greco C, Rosenzweig K, Cascini GL, et al. Current status of PET/CT for tumour volume definition in radiotherapy treatment planning for non-small cell lung cancer (NSCLC). *Lung Cancer* 2007;57:125-134

[44] Steenbakkers RJHM, Duppen JC, Fitton I et al. Reduction of observer variation using matched CT-PET for lung cancer delineation: A three-dimensional analysis. *Int J Radiat Oncol Biol Phys* 2006;64:435-448

[45] Vanuytsel LJ, Vansteenkiste JF, Stroobants SG, et al. The impact of 18F-Fluoro-2-deoxy-D-glycose positron emission tomography (FDG-PET) lymph node staging on the radiation treatment volumes in patients with non-small cell lung cancer. *Radiother Oncol* 2000;55:317-324

[46] Bradly J, Thorstad WL, Mutic S, et al. Impact of FDG-PET on radiation therapy volume delineation in non-small cell lung cancer. *Int J Radiat Oncol Biol Phys* 2004;59:78-86

[47] Paulino AC, Johnstone PA. FDG-PET in radiotherapy treatment planning: Pandora's box? *Int J Radiat Oncol Biol Phys* 2004;59:4-5

[48] Aerts HJWL, Lambin P, De Ruysscher. FDG for dose painting: A rational choice. *Radiother Oncol* 2010;97:163-164

[49] Abramyuk A, Tokalov S, Zophel K, et al. Is pre-therapeutical FDG-PET/CT capable to detect high risk tumour subvolumes responsible for local failure in non-small lung cancer? *Radiother Oncol* 2009;91:399-404

[50] Gillham C, Zips D, Ponisch F, et al. Additional PET/CT in week 5-6 of radiotherapy for patients with stage III non-small cell lung cancer as a means of dose escalation planning? *Radiother Oncol* 2008;88:335-341

[51] Vedam SS, Keall PJ, Kini VR, et al. Acquiring a four-dimensional computed tomography dataset using an external respiratory signal. *Phys Med Biol* 2003;48:45-62.

[52] Ford EC, Mageras GS, Yorke E, et al. Respiration-correlated spiral CT: A method of measuring respiratory-induced anatomic motion for radiation treatment planning. *Med Phys* 2003;30:88-97.

[53] Van der Geld YG, Senan S, van Sornsen de Koste JR, et al. Evaluating mobility for radiotherapy planning of lung tumours: A comparison of virtual fluoroscopy and 4DCT. *Lung Cancer* 2006;53:31-37.

[54] Underberg RWM, Lagerwaard FJ, Cuijpers JP, et al. Four-dimensional CT scans for treatment planning in stereotactic radiotherapy for stage 1 lung cancer. *Int J Radiat Oncol Biol Phys* 2004;60:1283-1290.

[55] Rietzel E, Liu AK, Doppke KP, et al. Design of 4D treatment planning target volumes. *Int J Radiat Oncol Biol Phys* 2006;66:287-295

[56] Jiang SB. Technical aspects of image-guided respiration-gated radiation therapy. *Med Dosim* 2006;31:141-151

[57] Haasbeek CJA, Spoelstra FOB, Lagerwaard FJ, et al. Impact of audio-coaching on the position of lung tumours. *Int J. Radiat Oncol Biol Phys* 2008;71:1118-1123

[58] Persson GF, Nygaard DE, Olsen M, et al. Can audio coached 4DCT emulate free breathing during the treatment course. *Phys Med Biol* 2006;51:617-636

[59] Bissonnette J-P, Purdie TG, Higgins JA, et al. Cone-beam computed tomographic image guidance for lung cancer radiation therapy. *Int J Radiat Oncol Biol Phys* 2009;73:927-934

[60] Muirhead R, van Sornsen de Koste JR, Munro P, et al. A novel approach for independent verification of lung radiotherapy. *J Thorac Oncol* 2009;4:S530

[61] Borst GR, Sonke JJ, Betgen A, et al. Kilo-voltage cone-beam computed tomography setup measurements for lung cancer patients; first clinical results and comparison with electronic portal-imaging device. *Int J Radiat Oncol Biol Phys* 2007;68:555-561

[62] Li H, Zhu XR, Zhang L, et al. Comparison of 2D radiographic images and 3D cone beam computed tomography for positioning head and neck radiotherapy patients. *Int J Radiat Oncol Biol Phys* 2008;71:916-925

[63] Higgins JA, Bezjak A, Hope A, et al. Effect of Image-Guidance Frequency on Geometric Accuracy and setup margins in radiotherapy for locally advanced lung cancer. Int J Radiat Oncol Biol Phys 2010; [Epub ahead of print]

[64] Sonke J-J, Lebesque J, van Herk M. Variability of four-dimensional computed tomography patient models. *Int J Radiat Oncol Biol Phys* 2008;70:590-598

[65] Britton KR, Starkschall G, Tucker SL, et al. Assessment of gross tumour volume regression and motion changes during radiotherapy for non-small cell lung cancer as measured by four-dimensional computed tomography. *Int J Radiat Oncol Biol Phys* 2007;68:1036-1046

[66] Erridge SC, Seppenwoolde Y, Muller SH et al. Portal imaging to asses set-up errors, tumour motion and tumour shrinkage during conformal radiotherapy of non-small cell lung cancer. *Radiother Oncol* 2003;66:75-85

[67] Bosmans G, van Baardwijk A, Dekker A, et al. Intra-patients variability of tumour volume and tumour motion during conventionally fractionated radiotherapy for locally advanced non-small cell lung cancer: A prospective clinical study. *Int J Radiat Oncol Biol Phys* 2006;66:748-753

[68] Underberg RW, Lagerwaard FJ, van Tinteren H et al. Time trends in target volumes for stage I non-small-cell lung cancer after stereotactic radiotherapy *Int J Radiat Oncol Biol Phys* 2006;64:1221-1228

[69] Sonke J-J, Rossi M, Wolthaus J, van Herk M, et al. Frameless stereotactic body radiotherapy for lung cancer using four-dimensional cone beam CT guidance. *Int J Radiat Oncol Biol Phys* 2009;74:567-574

[70] Sonke J-J, Zijp L, Remeijer P, et al. Respiration correlated cone beam CT. *Med Phys* 2005;32:1176-1186

[71] Grills I, Hugo G, Kestin LL, et al. Image-Guided radiotherapy via daily online cone-beam CT substantially reduces margin requirements for stereotactic lung radiotherapy *Int J Radiat Oncol Biol Phys* 2008;70:1045-1056

[72] Purdie TG, Bissonnette J-P, Franks K, et al. Cone-beam computed tomography for on-line image guidance of lung stereotactic radiotherapy: localization, verification, and intrafraction tumour position. *Int J Radiat Oncol Biol Phys* 2007;68(1):243-252

[73] Higgins J, Bezjak A, Franks K, et al. Comparison of spine, carina and tumour as registration landmarks for volumetric image-guided lung radiotherapy. *Int J Radiat Oncol Biol Phys* 2009;73:1404-1413

[74] Britton K.R, Starkschall G, Liu H, et al. Consequences of anatomic changes and respiratory motion on radiation dose distributions in conformal radiotherapy for locally advanced non-small cell lung cancer. *Int J Radiat Oncol Biol Phys* 2009;73(1):94-102

[75] Harsolia A, Hugo G.D, Kestin L.L, et al. Dosimetric advantages of four-dimensional adaptive image-guided radiotherapy for lung tumours using online cone-beam computed tomography. *Int J Radiat Oncol Biol Phys* 2008;70(2):582-589

[76] Parikh S.D, Levina V, Wang T, et al. Radioresistance of Non-small cell Lung Cancer Stem Cells. Int J Radiat Oncol Biol Phys 2009;75:S542-S543

[77] Hoogeman MS, Nuyttens JJ, Levendag PC, et al. Time dependence of intrafraction patient motion assessed by repeat stereoscopic imaging. *Int J Radiat Oncol Biol Phys* 2008;70:609-618

[78] Seppenwoolde Y, Shirato H, Kitamura K et al. Precise and real-time measurement of 3D tumor motion in lung due to breathing and heartbeat, measured during radiotherapy *IJROBP* 2002;53:822-834

[79] Heinzerling JH, Anderson JF, Papiez L, et al. Four-dimensional computed tomography scan analysis of tumour and organ motion at varying levels of abdominal compression during stereotactic treatment of lung and liver. *Int Radiat Oncol Biol Phys* 2008;70(5):1571-1578

[80] Negoro Y, Nagata Y, Aoki T et al. The effectiveness of an immobilization device in conformal radiotherapy for lung tumour: Reduction of respiratory tumour movement and evaluation of the daily setup accuracy. *Int J Radiat Oncol Biol Phys* 2001;50:889-898

[81] Bissonnette J-P, Franks FN, Purdie TG, et al. Quantifying interfraction and intrafraction tumour motion in lung stereotactic body radiotherapy using respiration-correlated cone beam computed tomography. *Int J Radiat Oncol Biol Phys* 2009;75:688-695

[82] Mah D, Hanley J, Rosenzweig KE, et al. Technical aspects of the deep inspiration breath-hold technique in the treatment of thoracic cancer. *Int J Radiat Oncol Biol Phys* 2000;48(4):1175-1185

[83] Kimura T, Hirokawa Y, Murakami Y, et al. Reproducibility of organ position using voluntary breath-hold method with spirometer for extracranial stereotactic radiotherapy. *Int J Radiat Oncol Biol Phys* 2004;60(4):1307-1313

[84] Michalski D, Sontag M, Li F, et al. Four-dimensional computed tomography-based interfractional reproducibility study of lung tumour intrafractional motion. *Int J Radiat Oncol Biol Phys* 2008;71:714-724

[85] Guckenberger M, Wilbert J, Meyer J et al. Is a single respiratory correlated 4D-CT study sufficient for evaluation of breathing motion? *Int J Radiat Oncol Biol Phys* 2007;67:1352-1359

[86] Kothary N, Heit JJ, Louie JD, et al. Safety and Efficacy of Percutaneous Fiducial Marker Implantation for Image-guided Radiation Therapy. *J Vasc Interven Radiol* 2009;20:235-239

[87] Nelson C, Starkschall G, Balter P, et al. Assessment of lung tumour motion and setup uncertainties using implanted fiducials. *Int J Radiat Oncol Biol Phys* 2007;67:915-923

[88] Poulson PR, Cho B, Keall PJ. A method to estimate mean position, motion magnitude, motion correlation and trajectory of a tumour from cone-beam CT projections for image-guided radiotherapy. *Int J Radiat Oncol Biol Phys* 2008;72(2):1587-1596

[89] Koch N, Liu HH, Starkschall G, et al. Evaluation of internal lung motion for respiratory-gated radiotherapy using IMR: Part I- Correlating internal lung motion with skin fiducial motion. *Int J Radiat Biol Phys* 2004;60(5):1459-1472

[90] Hoisak JDP, Sixel KE, Tirona R, et al. Correlation of lung tumour motion with external surrogate indicators of respiration. *Int J Radiat Oncol Biol Phys* 2004;60(4):1298-1306

[91] Berbeco RI, Nishioka S, Shirato H, et al. Residual motion of lung tumours in gated radiotherapy with external respiratory surrogates. *Phys Med Biol* 2005;50(16);3655-67

[92] Spoelstra FOB, van Sornsen de Koste JR, Cuijpers JP, et al. Analysis of reproducibility of respiration-triggered gated radiotherapy for lung tumours. *Radiother Oncol* 2008;87:59-64

[93] Giraud P, Yorke E, Ford EC, et al. Reduction of organ motion in lung tumours with respiratory gating. *Lung Cancer* 2006;51:41-51

[94] Saito T, Sakamoto R, Oya N. Comparison of gating around end-expiration and end-inspiration in radiotherapy for lung cancer. *Radiother Oncol* 2009;93:430-435

[95] Wolthaus JWH, Sonke J-J, van Herk M, et al. Comparison of different strategies to use four-dimensional computed tomography in treatment planning for lung cancer patients. *Int J Radiat Oncol Biol Phys* 2008;70(4):1229-1238

[96] Starkschall G, Forster KM, Kitamura K, et al. Correlation of gross tumour volume excursion with potential benefits of respiratory gating. *Int J Radiat Oncol Biol Phys* 2004;60(4):1291-1297

[97] Underberg RWM, van Sornsen de Koste JR, Lagerwaard FJ, et al. A dosimetric analysis of respiration-gated radiotherapy in patients with stage III lung cancer. *Radiation Oncology* 2006;1:8

[98] Li XA, Keall PJ, Orton CG. Point/ counterpoint. Respiratory gating for radiation therapy is not ready for prime time. *Med Phys* 2007;34:867-870

[99] Mageras GS, Yorke E, Rosenzweig K, et al. Fluoroscopic evaluation of diaphragmatic motion reduction with a respiratory gated radiotherapy system. *J Appl Clin Med Phys* 2001;2:191-200

[100] Kubo HE, Wang L. Introduction of audio gating to further reduce organ motion in breathing synchronized radiotherapy. *Med Phys* 2002;29:345-350

[101] Korreman SS, Juhler-Nottrup T, Boyer AL. Respiratory gated beam delivery cannot facilitate margin reduction, unless combined with respiratory correlated image guidance. *Radiother Oncol* 2008;86:61-68

[102] Della Biancia C, Yorke E, Chui CS, et al. Comparison of end normal inspiration and expiration for gated intensity modulated radiation therapy (IMRT) of lung cancer. *Radiother Oncol* 2005;75:149-156

[103] Barnes EA, Murray BR, Robinson DM, et al. Dosimetric evaluation of lung tumour immobilization using breath hold at deep inspiration. *Int J Radiat Oncol Biol Phys* 2001;50:1091-1098

[104] Nakagawa K, Aoki Y, Akanuma A, et al. Real-time beam monitoring in dynamic conformation therapy. *Int J Radiat Oncol Biol Phys* 1994;30:1233-1238

[105] Murphy MJ, Balter J, Balter S, et al. The management of imaging dose during image-guided radiotherapy: Report of the AAPM Task Group 75. *Med Phys* 2007;34(10):4041-4063

[106] Potters L, Steinberg M, Rose C, et al. American society for the therapeutic radiology and oncology and American college of radiology practice guideline for the performace of stereotactic body radiation therapy. *Int J Radiat Oncol Biol Phys* 2004;60(4):1026-1032

[107] Grills IS, Hugo G, Kestin LL, et al. Image-guided radiotherapy via daily online cone-beam CT substantially reduces margin requirements for stereotactic lung radiotherapy *Int J Radiat Oncol Biol Phys* 2008;70(4):1045-1056

[108] Wang Z, Wu QJ, Marks LB, et al. Cone-beam CT localization of internal target volumes for stereotactic body radiotherapy of lung lesions. *Int J Radiat Oncol Biol Phys* 2007;69(5):1618-1624

[109] Samson MJ, van Sornsen de Koste JR, de Boer HCJ, et al. An analysis of anatomic landmark mobility and setup deviaitons in radiotherapy for lung cancer. I*nt J Radiat Oncol Biol Phys* 1999;43:827-832

[110] Van de Steene J, Van den Heuvel F, Bel A, et al. Electronic postal imaging with on-line correction of setup error in thoracic irradiation: clinical evaluation. *Int J Radiat Oncol Biol Phys* 1998;40:967-976

[111] Hurkmans CW, Remeijer P, Lebesque JV, et al. Set-up verification using portal imaging; review of current clinical practice. *Radiother Oncol* 2001;58:105-120

[112] Underberg RWM, Lagerwaard FJ, Slotman BJ, et al. Use of maximum intensity projections (MIP) for target volume generation in 4DCT scans for lung cancer. *Int J Radiat Oncol Biol Phys* 2005;63:253-260.

[113] Ezhil M, Vedam S, Choi B, et al. Determination of patient-specific internal gross tumour volumes for lung cancer using four-dimensional computed tomography. *Radiation Oncology* 2009;4:4

[114] Nestle U, Kremp S, Grosu A-L. Practical integration of [18F]-FDG-PET and PET-CT in the planning of radiotherapy for non-small cell lung cancer (NSCLC): The technical basis, ICRU-target volumes, problems, perspectives. *Radiother Oncol* 2006;81:209-225

[115] Senan S, van Sornsen de Koste J, Samson M et al. Evaluation of a target contouring protocol for 3D conformal radiotherapy in non-small cell lung cancer. *Radiother Oncol* 1999;53:247-55

[116] Senan S, De Ruysscher D, Giraud P et al. Literature-based recommendations for treatment planning and execution in high-dose radiotherapy for lung cancer. *Radiother Oncol* 2004;71:139-146

[117] Mageras GS, Pevsner A, York ED et al. Measurement of lung tumour motion using respiration-correlated CT. *Int J Radiat Oncol Biol Phys* 2004;60:933-941

[118] Donnelly ED, Parikh PJ, Lu W, et al. Assessement of intrafraction mediastinal and hilar lymph node movement and comparison to lung tumour motion using four-dimensional CT. *Int J Radiat Oncol Biol Phys* 2007;69:580-588.

[119] Pantarotto JR, Piet AHM, Senan S et al. Motion Analysis of 100 Mediastinal Lymph Nodes: Potential Pitfalls in Treatment Planning and Adaptive Strategies. *Int J Radiat Oncol Biol Phys* 2009;74:1092-1099

[120] Wolthaus JWH, Schneider C, Sonke JJ, et al. Mid-ventilation CT scan construction from four-dimensional respiration-correlated CT scans for radiotherapy planning of lung cancer patients. *Int J Radiat Oncol Biol Phys* 2006;65:1560-1571

[121] Bosmans G, Buijsen J, Dekker A, et al. An "in silico" clinical trial comparing free breathing slow and respiration correlated computed tomography in lung cancer patients. *Radiother Oncol* 2006;81:73-80

[122] Lagerwaard FJ, van Sornsen de Koste JR, Nijssen-Visser MR, et al. Multiple "slow" CT scans for incorporating lung tumour mobility in radiotherapy planning. *Int J Radiat Oncol Biol Phys* 2001;15:932-937

[123] Hughes S, McClelland J, Chandler A, et al. A comparison of internal target volume definition by limited four-dimensional computed tomography, the addition of patient-specific margins, or the addition of generic margins when planning radical radiotherapy for lymph node-positive non-small cell lung cancer. *Clin Oncol* 2008;20:293-300

[124] Allen AM, Siracuse KM, Hayman JA et al. Evaluation of the influence of breathing on the movement and modelling of lung tumours. *Int J Radiat Oncol Biol Phys* 2004;58:1251-1257

[125] Wong JW, Sharpe MB, Jaffray DA et al. The use of active breathing control (ABC) to reduce margin for breathing motion. *Int J Radiat Oncol Biol Phys* 2000;48:81-87

[126] Murshed H, Liu HH, Liao Z et al. Dose and volume reduction for normal lung using intensity-modulated radiotherapy for advanced staged non-small cell lung cancer. *Int J Radiat Oncol Biol Phys* 2004;58:1258-1267

[127] Scrimger RA, Tome WA, Olivera GH, et al. Reduction in radiation dose to lung and other normal tissues using helical tomotherapy to treat lung cancer, in comparison to conventional field arrangements. *Am J Clin Oncol* 2003;26:70-78

[128] Bijdekerke P, Verellen D, Tournel K, et al. TomoTherapy: Implications on daily workload and scheduling patients. *Radiother Oncol* 2008;86:224-230

[129] Van Herk M. Will IGRT live up to its promise? *Acta Oncologica* 2008;47:1186-1187

[130] Van der Weide L, van Sornsen de Koste JR, Lagerwaard FJ, et al. Analysis of Carina Position as Surrogate Marker for Delivering Phase-Gated Radiotherapy. *Int J Radiat Oncol Biol Phys* 2008;71:1111-1117

[131] Spoelstra FOB, van Sornsen de Koste JR, Vincent A, et al. An evaluation of two internal surrogates for determining the three-dimensional position of peripheral lung tumours. *Int J Radiat Oncol Biol Phys* 2009;74:623-629

[132] Berbeco RI, Neicu T, Rietzel E, et al. A technique for respiratory-gated radiotherapy treatment verification with an EPID in cine mode. *Phys Med Biol* 2005;50(16):3669-79.

[133] Ploquin N, Rangel A. Phantom evaluation of a commercially available three modality image guided radiation system. *Med Phys* 2008;35:5303-5311

[134] Arimura H, Egashira Y, Shioyama Y, et al. Computerized method for estimation of the location of a lung tumour on EPID cine images without implanted markers in stereotactic body radiotherapy. *Phys Med Biol* 2009;54(3):665-77.

[135] Berbeco RI, Hacker F, Zatwarnicki C, et al. A novel method for estimating SBRT delivered dose with beam's-eye-view images. *Med Phys* 2008;35:3225-3231

[136] Van Sornsen de Koste JR, Senan S, Haring B, et al. Verification of Intrafraction motion using Cine MV and Colour Intensity Projections. *Int J Radiat Oncol Biol Phys* 2008;72:S608

[137] Nelson C, Balter P, Morice RC, et al. A technique for reducing patient setup uncertainties by aligning and verifying daily positioning of a moving tumour using implanted fiducials. *J App Clin Med Phys* 2008;9:110-122

[138] Underberg RWM, Lagerwaard FJ, Slotman BJ, et al. Benefit of respiration-gated stereotactic radiotherapy for stage I lung cancer - An analysis of 4DCT datasets. *Int J Radiat Oncol Biol Phys* 2005;62:554-60

[139] Muirhead R, Featherstone C, Duffton A, et al. The potential clinical benefit of respiratory gated radiotherapy (RGRT) in non-small cell lung cancer (NSCLC). *Radiother Oncol* 2010;95:172-177

[140] George R, Chung TD, Vedam SS, et al. Audio-visual biofeedback for respiratory-gated radiotherapy: Impact of audio instruction and audio-visual biofeedback on respiratory-gated radiotherapy. *Int J Radiat Oncol Biol Phys* 2006;65:924-933

[141] Muirhead R, van Sornsen de Koste JR, Munro P, et al. A novel approach for independent verification of lung radiotherapy. *J Thorac Oncol* 2009;4:S530

[142] Tai A, Christensen JD, Gore E, et al. Gated treatment delivery verification with on-line megavoltage fluoroscopy. *Int J Radiat Oncol Biol Phys* 2010;76:1592-1598

[143] Richter A, Wilbert J, Baier K, et al. Feasibility for markerless tracking of lung tumours in stereotactic body radiotherapy. *Int J Radiat Oncol Biol Phys* 2010;78:618-627

[144] Mayo CS, Urie MM, Fitzgerald TJ, et al. Hybrid IMRT for treatment of cancers of the lung and esophagus. *Int J Radiat Oncol Biol Phys* 2008;71:1408-1418

[145] Liu HH, Balter P, Tutt T et al. Assessing respiration-induced tumor motion and internal target volume using four-dimensional computed tomography for radiotherapy of lung cancer. *Int J Radiat Oncol Biol Phys* 2007;68:531-540

[146] Muirhead R, van Sornsen JR, Haring B, et al. Evaluation of a software tool for verifying tumour motion and breathing patterns in patients undergoing stereotactic radiotherapy (SRT). *Int J Radiat Oncol Biol Phys* 2009;75:S450-S451

[147] Sixel KE, Ruschin M, Tirona R, et al. Digital fluoroscopy to quantify lung tumour motion : potential for patient-specific planning target volumes. *Int J Radiat Oncol Biol Phys* 2003;57:717-723

[148] Seppenwoolde Y, Lebesque JV, de Jaeger K et al. Comparing different NTCP models that predict the incidence of radiation pneumonitis. *Int J Radiat Oncol Biol Phys* 2003 ;55 :724-735

[149] Graham MV, Purdy JA, Emami B, et al. Clinical dose-volume histogram analysis for pneumonitis after 3D treatment for non-small cell lung cancer (NSCLC). *Int J Radiat Oncol Biol Phys* 1999;45:323-329

[150] Wang S, Liao Z, Wei X et al. Analysis of clinical and dosimetric factors associated with treatment-related pneumonitis (TRP) in patients with non-small-cell lung cancer (NSCLC) treated with concurrent chemotherapy and three-dimensional conformal radiotherapy (SBRT). *Int J Radiat Oncol Biol Phys* 2006;66:1399-1407

[151] Rodriguez N, Algara M, Foro P et al. Predictors of acute esophagitis in lung cancer patients treated with concurrent three-dimensional conformal radiotherapy and chemotherapy. *Int J Radiat Oncol Biol Phys* 2009;73:810-817

[152] Kocak Z, Evans ES, Zhou S-M et al. Challenges in defining radiation pneumonitis in patients with lung cancer. *Int J Radiat Oncol Biol Phys* 2005;62:635-638

[153] Guckenberger M, Krieger T, Richter A et al. Potential of image-guidance, gating and real-time tracking to improve accuracy in pulmonary stereotactic body radiotherapy. *Radiother Oncol* 2009;91:288-295